Field and Numerical Investigation to Determine the Impact of Environmental and Wheel Loads on Flexible Pavement

by

Alireza Bayat

A thesis
presented to the University of Waterloo
in fulfillment of the
thesis requirement for the degree of
Doctor of Philosophy
in
Civil Engineering

Waterloo, Ontario, Canada, 2009

AUTHOR'S DECLARATION

I hereby declare that I am the sole author of this thesis. This is a true copy of the thesis, including any required final revisions, as accepted by my examiners.

I understand that my thesis may be made electronically available to the public.

Abstract

There is a growing interest for the use of mechanistic procedures and analytical methods in the design and evaluation of pavement structure rather than empirical design procedures. The mechanistic procedures rely on predicting pavement response under traffic and environmental loading (i.e., stress, strain, and deflection) and relating these responses to pavement field performance.

A research program has been developed at the Center for Pavement and Transportation Technology (CPATT) test track to investigate the impact of traffic and environmental parameters on flexible pavement response. This unique facility, located in a climate with seasonal freeze/thaw events, is equipped with an internet accessible data acquisition system capable of reading and recording sensors using a high sampling rate. A series of controlled loading tests were performed to investigate pavement dynamic response due to various loading configurations. Environmental factors and pavement performance were monitored over a two-year period. Analyses were performed using the two dimensional program MichPave to predict pavement responses. The dynamic modulus test was chosen to determine viscoelastic properties of Hot Mix Asphalt (HMA) material. A three-step procedure was implemented to simplify the incorporation of laboratory determined viscoelastic properties of HMA into the finite element (FE) model. The FE model predictions were compared with field measured pavement response.

Field test results showed that pavement fully recovers after each wheel pass. Wheel wander and asphalt mid-depth temperature changes were found to have significant impact on asphalt longitudinal strain. Wheel wander of 16 cm reduced asphalt longitudinal strains by 36 percent and daily temperature fluctuations can double the asphalt longitudinal strain.

Results from laboratory dynamic modulus tests found that Hot Laid 3 (HL3) dynamic modulus is an exponential function of the test temperature when loading frequency is constant, and that the HL3 dynamic modulus is a non-linear function of the loading frequency when the test temperature is constant. Results from field controlled wheel load tests found that HL3 asphalt longitudinal strain is an exponential function of asphalt mid-depth temperature when the truck speed and wheel loading are constant. This indicated that the laboratory measured dynamic modulus is inversely proportional to the field measured asphalt longitudinal strain.

Results from MichPave finite element program demonstrated that a good agreement between field measured asphalt longitudinal strain and MichPave prediction exists when field represented dynamic modulus is used as HMA properties.

Results from environmental monitoring found that soil moisture content and subgrade resilient modulus changes in the pavement structure have a strong correlation and can be divided into three distinct Seasonal Zones. Temperature data showed that the pavement structure went through several freeze-thaw cycles during the winter months. Daily asphalt longitudinal strain fluctuations were found to be correlated with daily temperature changes and asphalt longitudinal strain fluctuations as high as 650μm/m were recorded. The accumulation of irrecoverable asphalt longitudinal strain was observed during spring and summer months and irrecoverable asphalt longitudinal strain as high as 2338μm/m was recorded.

Acknowledgments

I would like to express my sincere appreciation to my supervisor, Dr. Mark Knight, for all the patience, encouragement, and support I received during my study. I am very grateful to Dr. Knight who gave me complete freedom to explore on my own and at the same time provided watchful guidance whenever required. Thank you for all your support.

I would also like to thank my co-supervisor Dr. Leo Rothenburg for his invaluable advice excellent feedback and for sharing his experience. Special thanks to Dr. Ralph Haas for his help and support. I would also like to thank my examining committee members, Dr. Curtis Berthelot, Dr. Giovanni Cascante, Dr. Maurice Dusseault, and Dr. Carl Haas for reviewing this thesis and their advice.

This research would not have been possible without financial support from NSERC, CATT, CPATT, MTO, and the University of Waterloo. I appreciate the support of these institutions. I would also like to acknowledge the University of Waterloo technical staff, Mr. Ken Bowman and Mr. Terry Ridgway for their assistance. Also, I would like to express my appreciation to Ms. Alice Seviora for her help and assistance for finalizing the thesis manuscript. I thank my friends and colleagues in the Geotechnical laboratory Mr. Rizwan Younis, Mr. Rashid Rehan, and Dr. Ademola Adedapo for their friendship and help. Special thanks to Mr. Karl Lawrence and Ms. Colleen Ryan for their friendship and support and making my stay in Waterloo unforgettable.

Finally, I want to thank my wife and best friend, Fatemeh, my parents, my brother, and my sister for their love and persistent support in pursuing my educational goals.

Dedication

To my wife, Fatemeh, and my parents

Table of Contents

List of Tables

List of Figures

Chapter 1: Introduction

1.1 Problem Statement

The current empirical-based American Association of State Highway and Transportation Officials (AASHTO) Guide for Design of Pavement Structures, used by about 80 percent of transportation agencies in North America, is based on limited data gathered from the AASHO Road Test constructed in Ottawa, Illinois from 1958 to 1960 (AASHTO 1993). The conditions at the road test included one environmental condition, a limited number of axle weights, tire pressures and axle configurations and only 1.1 million axle load repetitions from which empirical design equations were developed. Currently, it is a common practice to design pavements for tens of millions of truck passes in varying climatic conditions (Huhtala et al. 1989). In addition, several vehicle characteristics (e.g., tire type, tire pressure, suspension system, axle configuration, axle loads and gross vehicle weights) have changed significantly since the AASHO Road Test was completed (Huhtala et al. 1989).

As a result of these limitations, there is a growing interest within the pavement engineering community for the use of mechanistic procedures and analytical methods for the design and evaluation of pavement structures rather than empirically-based design and analysis procedures. These design procedures rely on predicting pavement responses (i.e., stress, strain, deflection) under traffic and environmental loads and relating these responses to pavement performance. Therefore, the validity and accuracy of pavement response models in predicting pavement response under moving loads is of major importance.

Initially, mechanistic pavement analysis was limited to static loads resting on layered elastic systems. Over the years, studies have indicated a lack of agreement between field measured pavement responses and calculated pavement responses using layered elastic systems

(Hildebrand 2002; Ullidtz et al. 1994). Hildebrand (2002) has reported an overall deviation of 20 percent between observed and predicted strain and more than 35 percent deviation between observed and predicted vertical stress. One of the most important conclusions of AMADEUS (2000), a research project under European Union's 4^{th} framework, was that the vertical strain at the top of subgrade tends to be grossly underestimated by the response models, typically by a factor of two. Several finite element (FE) models, capable of modeling viscoelastic Hot Mix Asphalt (HMA) behavior and performing dynamic analysis, have been developed. However, the application of these programs requires considerable expertise from the user and demands a large amount of computation time (Loulizi et al. 2006). Thus, layered elastic models continue to be the state-of-the practice for most pavement design and analysis applications (Selvaraj 2007).

The most viable method of investigating the appropriateness of any analytical model is by comparing the model response to actual measured pavement response. Pavement instrumentation has recently become an important tool in monitoring and measuring pavement system response under various environmental and traffic loading conditions. Pavement instrumentation provides a valid and direct technique for measuring stresses and strains in pavement structure and validating existing analytical models.

Over the past three decades, several full-scale instrumented test sections have been constructed to monitor in situ material performance and measure pavement response. The Minnesota Road Research Project (Timm and Newcomb 2003; Tompkins et al. 2007; Worel et al. 2007), the Virginia Smart Road (Al-Qadi et al. 2004), the Ohio SHRP Test Pavement Sections (Sargand et al. 1997; Sargand et al. 2007), and the National Center for Asphalt Technology (NCAT) Test Track (Brown 2006; Priest et al. 2005; Timm et al. 2004) are some of the well known field

studies. These field studies are either in mild or cold climate with little seasonal variations. Currently, limited published literature is available for flexible pavements subject to freeze/thaw environment similar to southern Ontario, Canada.

1.2 Research Objectives

The primary focus of this research was to investigate the impact of traffic loading and environmental parameters on flexible pavement response. A two component research program involving a detailed field study and analytical investigations was developed at the Centre for Pavement and Transportation Technology (CPATT) test track facility. This unique facility, located in a climate with seasonal freeze/thaw events, was equipped with an internet accessible data acquisition system capable of reading and recording sensors using a high sampling rate.

The specific objectives of this research were to:

- Measure pavement response under a variety of dynamic wheel loads with the aid of a state-of-the-art pavement instrumentation and data acquisition system.

- Design, develop, and perform controlled wheel load testing to identify and study wheel load characteristics that influence flexible pavement response.

- Identify and study material properties that influence flexible pavement response.

- Numerically simulate flexible pavement response and compare the measured pavement field responses to predicted pavement response.

- Monitor daily and seasonal changes in environmental parameters that influence flexible pavement response and performance.

- Investigate and study flexible pavement response and performance due to changes in environmental parameters.

1.3 Thesis Organization

This thesis is prepared in an integrated-article format. Each chapter of the thesis presents separate but related studies. Chapter 2 presents the general background and a review of the pavement design methods, major wheel load and environmental factors impacting pavement responses, and pavement response models.

The reference project for this research is the CPATT test track located in Waterloo, Ontario, Canada. Chapter 3 provides a summary of the wheel load study including a description of the test site, field instrumentation program, and the state-of-the-art remote access data acquisition systems. It also describes the controlled wheel load test program and presents typical sensor data for asphalt strain gauges and total pressure cells. Field data is then used to determine the impact of wheel wander and temperature on measured asphalt longitudinal strains.

The current Mechanistic–Empirical Pavement Design Guide (MEPDG) proposes using the laboratory dynamic modulus test to determine the time-temperature dependent properties of HMA materials. Chapter 4 compares laboratory determined HMA dynamic modulus with the result of field measured asphalt longitudinal strains.

Chapter 5 presents a two dimensional FE model, developed using MichPave, to predict pavement responses and proposes a three-step procedure implemented to simplify the incorporation of

laboratory determined viscoelastic properties of HMA into the FE model. It also compares FE model predictions with field measured pavement response.

Chapter 6 provides an overview of the environmental data collection, processing, and analysis at the CPATT test track facility. It also presents and discusses two years of environmental data which includes several freeze-thaw cycles.

The seasonal variation of environmental factors and pavement performance in a climate subject to freeze/thaw is studied in Chapter 7. This chapter introduces the concept of three Seasonal Zones for climates subject to freeze/thaw events. It also presents and discusses soil moisture content and subgrade resilient modulus changes in each Seasonal Zone.

Chapter 8 explains the field study developed to quantify the flexible pavement response to thermal loading. It also presents and discusses the findings from over two years monitoring period.

Conclusions and recommendations for future work are presented in Chapter 9.

Chapter 2: Background and Literature Review

2.1 Pavement Design Methods

Flexible pavement design procedures involve the calculation of the required pavement structure thickness based on the structural characteristics of the materials used. Historical pavement design methods date back at least 80 years when empirical methods based on "rule-of-thumb" or engineering judgment were used to design pavements. Over the years, pavement engineers have attempted to replace empirical design methods with mechanistic based design procedures. The following sections provide an overview of AASHTO (1993) design procedure and will review the new design methods under evaluation for use by practitioners.

2.1.1 AASHTO Design Method

The empirically-based AASHTO flexible pavement design guide published in 1972, 1986, and 1993 uses empirical equations developed from AASHO road test, conducted near Ottawa, Illinois from 1958 to 1960 (AASHO 1962), to correlate pavement characteristics to pavement performance.

The 1993 AASHTO design guide requires the designer to input specific values for reliability, variability, subgrade modulus, change in serviceability, and predicted future traffic needs into Equation 2-1 to calculate the minimum required structural number:

$$\log(W_{18}) = Z_R * S_o + 9.36 * \log(SN+1) - 0.2 + \frac{\log\left[\frac{\Delta PSI}{4.2-1.5}\right]}{0.4 + \frac{1094}{(SN+1)^{5.19}}} + 2.32 * \log(M_R) - 8.07 \qquad (2\text{-}1)$$

where:

W_{18} = Predicted number of 80 kN single load applications

Z_R = Standard normal deviate corresponding to selected level of reliability

S_o = Overall standard deviation

SN = Structural number

ΔPSI = Design serviceability loss

M_R = Road bed Resilient Modulus

The required pavement thickness is determined using Equation 2-2:

$$SN = a_1 \cdot D_1 + a_2 \cdot D_2 \cdot m_2 + a_3 \cdot D_3 \cdot m_3 \qquad (2\text{-}2)$$

where :

a_i = i^{th} layer coefficient

D_i = i^{th} layer thickness

m_i = i^{th} layer drainage coefficient

The AASHTO design procedure is very simple and does not require extensive material characterization. However, the design equations are based on the specific pavement layer configuration, loading pattern, and environmental conditions present at AASHO Road Test and require many empirical parameters when applied to different conditions.

2.1.2 Mechanistic-Empirical (M-E) Design Method

The limited nature of AASHTO design procedure has forced pavement industry to move toward Mechanistic-Empirical (M-E) design methods. M-E procedures started gaining widespread attention as a method for pavement analysis and design in the early 60's. The rising costs of maintaining pavements have forced the pavement industry to move towards a design method which is based on the mechanical properties of materials. In M-E pavement design, pavement responses such as stress and strains are determined from the load, material properties, and climate, which are then empirically related to pavement performance. Fatigue cracking in asphalt layer and permanent deformation (rutting) in base and subgrade materials are two main types of distress used to evaluate pavement performance.

Figure 2-1 illustrates the typical M-E design procedure developed and used as part of COST 333, the new bituminous pavement design method for European Commission (COST 333, 1997). The climate and environmental conditions, pavement layer geometry, material properties, and traffic loading, are primary input variables used to analyze and predict critical pavement responses such as stress and strain due to traffic loading and environmental conditions for a selected trial or initial design. Once a response model is developed, the responses are input into distress models to determine pavement damage during a specified design period. Failure criteria are then evaluated, and an iterative process continues until a final acceptable design is achieved.

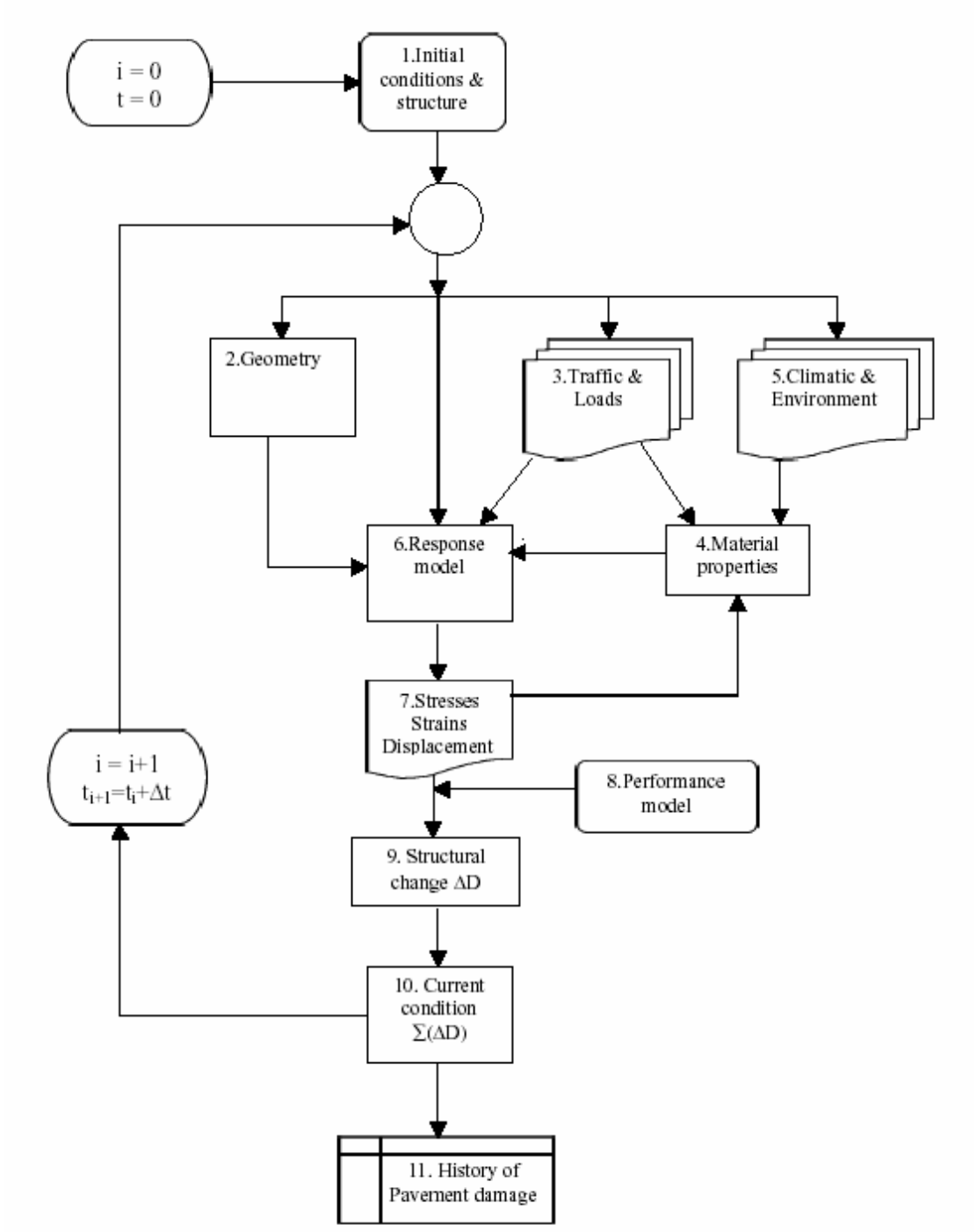

Figure 2-1:Mechanistic-Empirical Pavement Design Method (COST 333 1997)

2.2 Pavement Analysis Methods

The mechanistic model that computes pavement responses due to traffic loads and/or climatic factors is an essential part of the M-E design procedure and has been called "*the heart of a mechanistic–based design procedure*" (NCHRP 2004). Numerous mechanistic pavement response models have been developed over the years, ranging from Boussinesq's one-layer model to multi-layer elastic theories to dynamic finite element models. The following section provides a review of pavement response models.

2.2.1 Single Layer Model

Boussinesq (1885) formulated a simple formulation for determining stresses, strains and deflections of a homogeneous, isotropic, linear elastic half space, with modulus E and Poisson's ratio ν subjected to a static point load. A notation for Boussinesq's equations is presented in Figure 2-2, where z indicates depth and r is horizontal distance to the point of interest for the responses under the point load P. The equations for calculating normal stresses ($\sigma_z, \sigma_r, \sigma_t$), normal strains ($\varepsilon_z, \varepsilon_r, \varepsilon_t$), shear stress ($\tau_{rz}$) and shear strain ($\gamma_{rz}$) are given in Table 2-1.

Boussinesq's equations were originally developed for a static point load. Later, Boussinesq's equations were further extended by other researchers for a uniformly distributed load by integration (Newmark 1947; Sanborn and Yoder 1967).

Boussinesq's closed form solution is a very simple and useful approach to mechanistic pavement analysis; however it neglects practical aspects such as layered pavement structures, nonlinearity, non-homogeneity, and anisotropy of materials. The vertical stress and the major principal stresses are independent of elastic parameters, and modulus does not influence stresses.

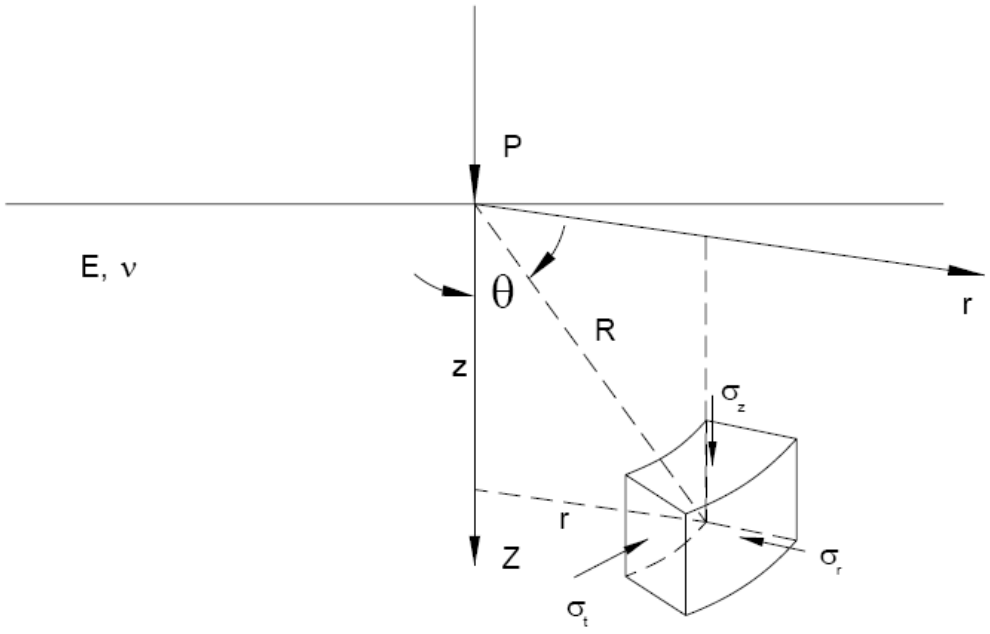

Figure 2-2: Notation for Boussinesq's Equation (Tu 2007)

Yoder and Witczak (1975) suggested that Boussinesq theory can be used to estimate subgrade stresses, strains, and deflections when base and the subgrade have similar stiffness.

Table 2-1: Boussinesq's Equations for a Point Load (after Ullidtz 1998)

$\sigma_r = \frac{P}{2 \cdot \pi \cdot R^2}\left[3 \cdot \cos\theta \cdot \sin^2\theta - \frac{1-2\nu}{1+\cos\theta}\right]$ $\sigma_t = \frac{(1-2\nu) \cdot P}{2 \cdot \pi \cdot R^2}\left[-\cos\theta + \frac{1}{1+\cos\theta}\right]$ $\sigma_z = \frac{3 \cdot P}{2 \cdot \pi \cdot R^2} \cdot \cos^3\theta$
$\varepsilon_r = \frac{(1+\nu) \cdot P}{2 \cdot \pi \cdot R^2 \cdot E}\left[-3 \cdot \cos^3\theta + (3-2\nu) \cdot \cos\theta - \frac{1-2\nu}{1+\cos\theta}\right]$ $\varepsilon_t = \frac{(1+\nu) \cdot P}{2 \cdot \pi \cdot R^2 \cdot E}\left[-\cos\theta + \frac{1-2\nu}{1+\cos\theta}\right]$ $\varepsilon_z = \frac{(1+\nu) \cdot P}{2 \cdot \pi \cdot R^2 \cdot E}\left[3 \cdot \cos^3\theta - 2 \cdot \nu \cdot \cos\theta\right]$
$\tau_{rz} = \frac{3 \cdot \pi}{2 \cdot \pi \cdot R^2} \cdot \cos^2\theta \cdot \sin\theta$
$\gamma_{rz} = \frac{(1+\nu) \cdot P}{\pi \cdot R^2} \cdot \cos^2\theta \cdot \sin\theta$

2.2.2 Layered Elastic Theory

Burmister (1945) developed a solution for two layers and subsequently for a three layers system. Several layered analytical elastic models have been developed which are generally based on Burmister (1945).

Acum and Fox (1951) used tabular format to determine normal and radial stresses in three-layer pavement systems using a circular loading area, two layers thickness, and elastic modulus of the layers. Schiffman (1962) developed a general solution for determining stresses and

displacements in a multi-layer elastic system subjected to non-uniform normal surface loads, tangential surface loads, rigid, semi-rigid, and slightly inclined plate bearing loads. Using Schiffman's solution, several computer programs (i.e. WESLEA, VESYS, KENLAYER, CIRCLY4, BISAR, VEROAD, ELSYM, PDMAP, CHEVRON, JULEA, ILLIPAVE, FENLAP) have been developed and used in pavement analysis and design to calculate stresses and strains in multi-layered elastic system (Monismith 2004).

The recently released Mechanistic Empirical Pavement Design Guide (MEPDG) recommends using the multilayer elastic program JULEA, which is a modified version of WESLEA, and linear models to compute flexible pavement responses (NCHRP 2004).

Pavement analysis procedures that are derived from the theory of elasticity are based on simplifications of the real condition. Major simplifications include considering HMA materials as pure elastic solids and the treatment of vehicular loads as static uniformly distributed circular area. In most cases, loading situation is dynamic not static. Furthermore, most pavement materials are neither homogenous nor isotropic, and most have viscoelastic behavior.

Immanuel and Timm (2006) used layered elastic analysis to compare predicted vertical stress in the base and subgrade layers to field measured vertical pressures obtained from the National Center for Asphalt Technology (NCAT) Test Track. The authors found that the predicted pressure was only a reasonable approximation up to vertical pressures of 82 kPa in the base and 48kPa in the subgrade.

Wu et al. (2006) calculated the vertical stress at the bottom of base layer using the multilayer elastic program ELSYM5 and compared it to data from the Louisiana ALF. The study found the calculated vertical stresses to be two to eight times higher than the measured field values.

2.2.3 Finite Element Analysis

Finite element analysis methods have been developed to model flexible pavement responses. Raad and Figueroaand (1980) developed ILLIPAVE, a 2-D finite element program, to simulate flexible pavement behavior. ILLIPAVE uses Mohr-Coulomb failure criterion for subgrade and non-linear constitutive relationship for pavement materials.

Harichandran et al. (1990) developed a non-linear mechanistic finite element program, MichPave, for the analysis of flexible pavements. The program was developed for the Michigan Department of Transportation and is in the public domain. MichPave computes displacements, stresses, and strains within the pavement due to a single circular wheel load and estimates fatigue life and rut depth through empirical equations.

Mamlouk and Mikhail (1998) developed a three-dimensional finite element nonlinear dynamic pavement model to compute dynamic pavement responses. This analysis considered the viscoelasticity of asphalt and non-linearity of granular and subgrade materials. The model also considered the truck-pavement interaction resulting from truck speed and dynamic loads imparted by truck bouncing. The predictions were not validated with field data.

Sargand and Beegle (2002) developed a three-dimensional finite element program, OUPAVE, at Ohio University to investigate flexible pavement responses subjected to static and dynamic loadings. Elastic and linear viscoelastic models were used for asphalt material. Calculated deflections correlated well with falling weight deflectometer (FWD) test data from the Ohio DEL-23 SHRP Test Road project. Stresses and strains were not investigated as part of this particular research.

Xu et al. (2002) and Park et al. (2005) assessed the condition of pavement layers using FWD data and the ABAQUS finite element program. This research stressed the importance of nonlinear behavior of the pavement system to accurately assess pavement deflections.

Hadi and Bodhinayake (2003) used ABAQUS/STANDARD, a three-dimensional finite element program, to investigate deflection predictions. Asphalt and granular material were considered as being linear and non-linear respectively. Static and cyclic loads were applied. The best correlation between field measured and computed deflections was obtained when the materials were considered non-linear and subjected to cyclic loading.

To characterize granular material using non-linear models, the MEPDG recommends using DSC2D, a two-dimensional finite element program. The program is recommended for use for research purposes only (NCHRP 2004).

2.3 Pavement Material Characterization

2.3.1 HMA Material

Two major factors are critical in the mechanistic analysis of pavements: (1) the material characterization method and its accuracy, and (2) the accuracy of mechanistic models to simulate pavement response (Sousa et al. 1991).

Traditionally, HMA materials have been considered to be purely elastic. However, the behavior of HMA materials is strongly dependent on temperature and loading frequency. Linear viscoelastic theory has been successfully used in recent years to describe the behavior of HMA materials. Elseifi et al. (2006) used finite element models to compare the elastic to linear

viscoelastic HMA behavior. The study found that incorporating the viscoelastic constitutive model improved the accuracy of the model and that elastic theory grossly underestimated the pavement response.

2.3.1.1 Dynamic Modulus Test

HMA is a composite material, whose mechanical behavior is primarily governed by the viscoelastic nature of the asphalt binder. The fundamental difficulty in the investigation of HMA viscoelastic property is establishing representative stress-strain relationships. For an unconfined or confined viscoelastic cylindrical test specimen under a continuous sinusoidal loading, the stress-strain relationship has been defined using a complex number called the complex modulus (E^*) (Bari and Witczak 2005; Tran and Hall 2003):

$$E^* = \frac{\sigma}{\varepsilon} = \frac{\sigma_0 \cdot e^{iwt}}{\varepsilon_0 \cdot e^{i\cdot(wt-\phi)}} \qquad (2\text{-}3)$$

where:

σ_o = Peak stress

ε_o = Peak strain

ω = Angular velocity

t = Time

ϕ = Phase angle

i = $\sqrt{-1}$

The dynamic modulus is defined as the absolute value of the complex modulus, which is represented by the ratio of peak stress to peak strain. Due to the nature of viscoelasticity, there is a time lag between the sinusoidal stress and sinusoidal strain, which is called the phase angle.

2.3.2 Unbound Material

Studies have shown that unbound material stress-strain response is non-linear and is a function of stress condition. Several non-linear constitutive equations have been developed to describe the stress-strain relation of unbound material as a function of the stress condition. The two most common models are $k-\sigma$ and $k-\theta$.

For fine grained materials, the $k-\sigma$ model is a non-linear relationship that relates the deviatoric stress (σ_d) to resilient modulus (M_R):

$$M_R = k_1 \cdot \sigma_d^{k_2} \qquad (2\text{-}4)$$

where

M_R = Resilient (elastic) modulus

σ_d = Deviatoric stress

k_1, k_2 = Constants

The deviatoric stress (σ_d) is defined as the difference between major (σ_1) and minor (σ_3) principal stress:

$$\sigma_d = \sigma_1 - \sigma_3 \qquad (2\text{-}5)$$

For coarse grained materials, the $k-\theta$ model is a non-linear relationship that relates the bulk stress to the resilient modulus (M_R):

$$M_R = k_1 \cdot \theta^{k_2} \tag{2-6}$$

where:

M_R = Resilient (elastic) modulus

θ = Bulk stress

k_1, k_2 = Constants

The bulk stress (θ) is defined as the summation of the principal stresses ($\sigma_1, \sigma_2, \sigma_3$):

$$\theta = \sigma_1 + \sigma_2 + \sigma_3 \tag{2-7}$$

Ullidtz (1985) carried out a finite element analysis and suggested a simple non-linear model for estimating the elastic modulus (E):

$$E = k_1 \cdot \left(\frac{\sigma_1}{p} \right)^{k_2} \tag{2-8}$$

where:

E = Elastic modulus

σ_1 = Major principle stress excluding any static stresses due to the weight of the material

p = Reference pressure-usually atmospheric (100kPa)

k_1, k_2 = Constants

Uzan (1985) suggested a nonlinear model for granular soils that considers both deviatoric stress (σ_d) and bulk stress(θ) :

$$M_R = k_1 \cdot \theta^{k_2} \cdot {\sigma_d}^{k_3} \tag{2-9}$$

where:

M_R = Resilient (elastic) modulus

θ = Bulk stress

σ_d = Deviatoric stress

k_1, k_2, k_3 = Constants

2.4 Full-Scale Instrumented Test Facilities

Over the past few decades considerable efforts have been made to enhance pavement design and analysis by measuring direct pavement responses under a variety of loading and environmental conditions and comparing them to calculated values from response models. Pavement instrumentation has recently become an important tool in measuring and quantifying pavement responses and the factors influencing the response parameters. Parameters that are measured in the field include strain, stress, deflection, moisture, and temperature. Measuring these parameters in the field also allows for accurate performance model development and mechanistic pavement analysis.

Several full-scale instrumented test sections have recently been constructed to monitor and measure in situ pavement response and performance under a variety of loading and environmental conditions. NCHRP Synthesis 235, published in 1996, indicates that 35 full-scale

and accelerated pavement testing facilities exist worldwide, of which 19 have active research programs (Metcalf 1996). Table 2-2 summarizes the facilities that have been active since 1962 and includes information about the year commissioned, cost of construction, and annual cost (Hamad 2007). The next section discusses some of the well known instrumented field test facilities.

2.4.1 Penn State Test Track

The Pennsylvania research program, sponsored by the FHWA, undertook a project to evaluate various pavement instrumentations (Sebaaly et al. 1991). An extensive literature review was carried out to identify the existing pavement instrumentation and to select the most promising types of gauges for a field-testing program. The response of selected gauges to dynamic loading applied by a tractor-semi-trailer at different levels of axle loading, tire pressure, and speed was investigated using two sections of flexible pavements, 152 and 254 mm HMA layer. The pavement response data collected in the field-testing program was used to evaluate methods for back-calculating pavement material properties. It was concluded that the back-calculated moduli were much more accurate if data from multiple sensors were used in the analysis rather than from a single sensor.

2.4.2 Minnesota Road (MnRoad)

The Minnesota Road Research Project (MnRoad) consists of approximately 40-160m pavement test sections totaling 9.6km in length. Twenty-three of these test sections have been loaded with freeway traffic, and the remainder sections have been loaded with calibrated trucks. Electronic transducers (4572) were embedded in the pavement (Baker et al. 1994). The main purpose of the

facility was to verify and improve existing pavement design models, investigate the factors affecting pavement response, and to develop new pavement models.

Table 2-2:Test Facilities Active since 1962 (Hamad 2007)

Acronym	Location	Year commissioned	Nr. Tests reported	In use 1995	Initial cost ($)	Annual cost ($)
TEST ROADS						
MnROAD	Minnesota	1993	40	yes	2,500,000	500,000
PWRI	Japan	1979		yes	500,000	200,000
CIRCULAR TEST TRACKS						
C-TIC	Saskatchewan	1978	3	no	400,000	
CAPTIP(1)	New Zealand	1987	20	yes	300,000	
ISETH	Switzerland	1979			750,000	
LCPC	France	1978	130	yes	5,000,000	800,000
PRT	Romania	1982	40	yes	420,000	100,000
UCF	Florida	1988		yes	250,000	
UNAM	Mexico	1970	100	yes	480,000	190,000
LINEAR TEST TRACKS						
ALF	Australia	1984	158	yes	1,000,000	600,000
FHWA-PIF	Washington	1986	25	yes	1,100,000	275,000
PRF-LA	Louisiana	1995	new	yes	1,800,000	200,000
DRTM	Denmark	1973		yes	200,000	100,000
CAL-APT	California	1994	new	yes	1,700,000	1,200,00
LINTRACK	Netherlands	1991	2	yes	1000,000	164,000
Minne-ALF	Minnesota	1990	new		200,000	
PTF	United	1984		yes	1,700,000	
INDOT-PURDUE	Indiana	1992	32	yes	140,000	49,000
Tx-MLX	Texas	1995	2	yes	2,500,000	
CEDEX	Spain	1987	new	yes	2,100,000	
OTHER						
MSU	Michigan	1990		no	100,000	
IN CANADA						
Brampton	Ontario	1965				
Ste. Anne	Manitoba	1967				
Lamont	Alberta	1991				
Laval	Quebec	1999				
CPATT/Waterloo	Ontario	2002				

2.4.3 Virginia Smart Road

The Virginia Smart Road is a 9.6-km connector highway with the first 3.2 km designated as a controlled test facility. The flexible pavement portion of the Virginia Smart Road includes 12 different flexible pavement designs (Loulizi et al. 2001). Each section is approximately 100m long. The sections are instrumented with pressure cells, strain gauges, time-domain reflectometry probes, thermocouples, and frost probes.

2.4.4 Ohio Test Track

The Ohio Department of Transportation, in cooperation with the Federal Highway Administration, constructed a 5-km-long test pavement to encompass four experiments identified in the Long Term Pavement Performance (LTPP) Specific Pavement Studies (SPS). The test sections were instrumented with various sensors, and response data were collected under various axle configurations, loads, speed, and tire types (Sargand et al. 1997). Environmental data was also collected periodically to investigate the impact of the ground temperature and moisture content on measured pavement response. The main objective of the Ohio Test Track was to investigate the interaction of load response to environmental parameters.

2.5 Validation of Response Models with Field Measured Pavement Response

A significant amount of work has been performed in investigating the influence of different load and environmental factors on pavement response and validating pavement response models.

Chatti et al. (1995) investigated the effects of truck speed and tire pressure on asphalt longitudinal response. The test section consisted of a 137mm thick surface layer over a 330mm thick crushed stone base layer and the subgrade was sandy clay. The author found that increasing

speed from 2.7 to 64km/hr reduced the asphalt longitudinal strain by approximately 35%. They also reported that tire pressure did not to have a significant impact on asphalt longitudinal strain when the speed was 64km/hr. However, when the truck speed decreased the tire pressure impact increased.

Huhtala et al. (1989) studied the impact of tires and tire pressures on asphalt longitudinal and transverse strains. Using fatigue performance models, the strain gauge responses showed that wide-base tires are 2.3 to 4 times more damaging than dual tires.

Huang et al. (2002) performed several numerical analyses with different structural models and included both static and transient loading. The calculated responses were compared to measured field values from the Louisiana Accelerated Loading Facility. The study showed that the predicted response correlated well with field measured pavement responses when the rate-dependent viscoplastic model for asphalt and elastoplastic models for the other layers were considered.

Siddharthan et al. (2002) developed a three-dimensional finite element code, 3D-MOVE, that considered vehicle speed, noncircular contact areas, and the complexity of the contact stress distributions. Asphalt and unbound materials were characterized as viscoelastic and elastic material respectively. The dynamic vehicle loading impact was accounted for using a dynamic load coefficient that is a function of vehicle speed, suspension system, and road roughness. The applicability of the program was verified using two well-documented full-scale field tests (Penn State University test track and Minnesota road tests). More than 25 percent deviation was observed between the predicted and measured strains when the truck was fully loaded. The

authors concluded that when the truck was fully loaded, the pavement response was expected to be significantly affected by the roughness of the road.

Wu and Hussain (2003) performed controlled wheel load tests and FWD tests at the Kansas Accelerated Testing Laboratory (K-ATL) to investigate pavement response. The authors used ELSYM5, a multi-layer elastic analysis program, to validate measured pavement responses. The measured vertical stresses on the top of the subgrade and the tensile strains at the bottom of the asphalt layer due to FWD loads were found to be very close to those calculated by ELSYM5. However, measured tensile strains and vertical stresses were higher than those predicted. The measured tensile strains under the wheel loads were found to increase with increasing number of wheel load repetitions.

Loulizi et al. (2006) compared measured pavement response with response calculated using elastic layer analysis performed with four software programs (Kenpave, Bisar 3.0, Elsym5, and Everstress 5.0) based on the layered elastic theory and two finite element models (ABAQUS and MichPave). Results indicated that all softwares that were based on elastic layered theory gave the same response to single and dual tire loading. It was found that the elastic layered theory underestimates pavement responses at high temperatures and overestimates at low and intermediate temperatures. As shown in Figure 2-3, at temperatures below 15°C, the measured asphalt transverse strain at a truck speed of 8km/hr is smaller than the strain calculated using the elastic layered theory. The measured strain at a truck speed of 8km/hr becomes increasingly higher than the calculated one at temperatures above 15°C. At temperatures below 28°C, the measured asphalt transverse strain at a truck speed of 72 km/hr is smaller than the strain calculated using the elastic layered theory. The measured strain at a truck speed of 72km/hr

becomes increasingly higher than the calculated one at temperatures above 28°C. The authors suggested more research is needed for on layer bonding, anisotropic material properties, and considering dynamic loading.

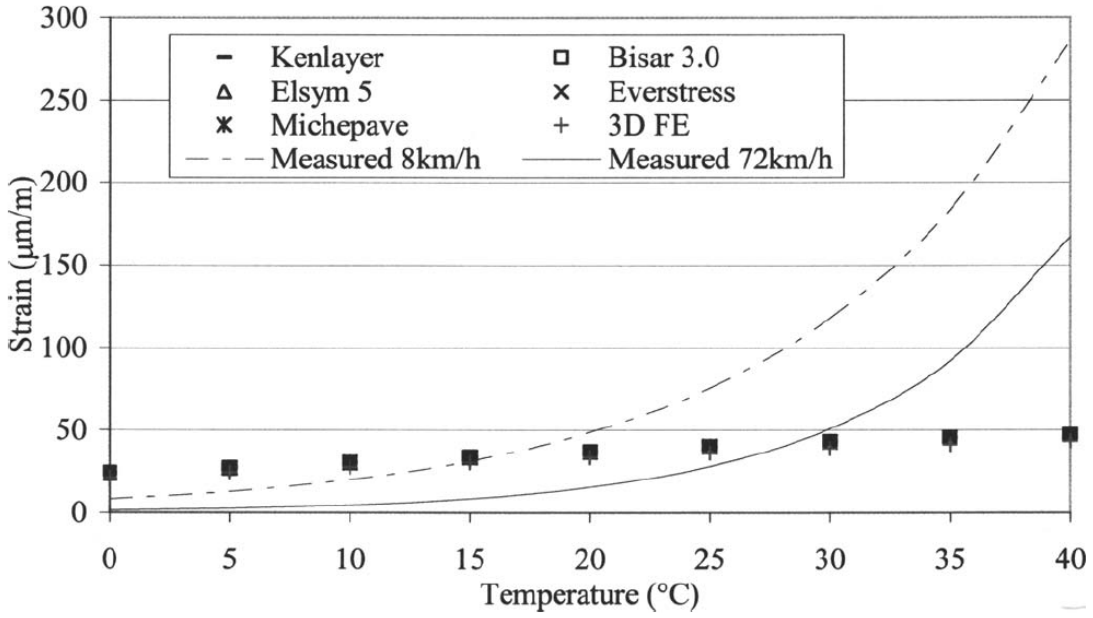

Figure 2-3: Measured and Calculated Asphalt Transverse Strain under HMA Layer for Single Load of 25.8kN (Loulizi et al. (2006))

Elseifi et al. (2006) incorporated a viscoelastic model, which used laboratory determined parameters, into a finite element model to predict horizontal tensile and vertical shear strains in the asphalt layers. The comparison of predicted responses with field measured pavement responses from Virginia Smart Road showed an average prediction error of 15 percent. The study showed that the calculated pavement responses using elastic models underestimate pavement response at intermediate and high temperatures.

Fernando et al. (2006) performed an extensive study to investigate the effect of tire contact stresses on pavement responses. A tire view program was developed by the authors to be used in

pavement responses analysis. The authors stated that the relevance of tire contact pressure distributions decreases as depth increases.

2.6 Environmental Impacts on Pavement Response and Performance

It is well known that environmental state play a major role in pavement response and consequent pavement performance (Salem 2004). The asphalt layer is sensitive to temperature variation and the unbound materials are sensitive to the moisture content changes. These two environmental factors, i.e., temperature and moisture content, impact flexible pavement responses and performance particularly in seasonal frost areas where pavements are susceptible to heave during winter and then lose their strength during spring thaw (Salem 2004).

Figure 2-4 illustrates the asphalt longitudinal strain for the Alberta Test Road under the standard axle load of 8165kg in July and October 1976 (Christison et al. 1978).

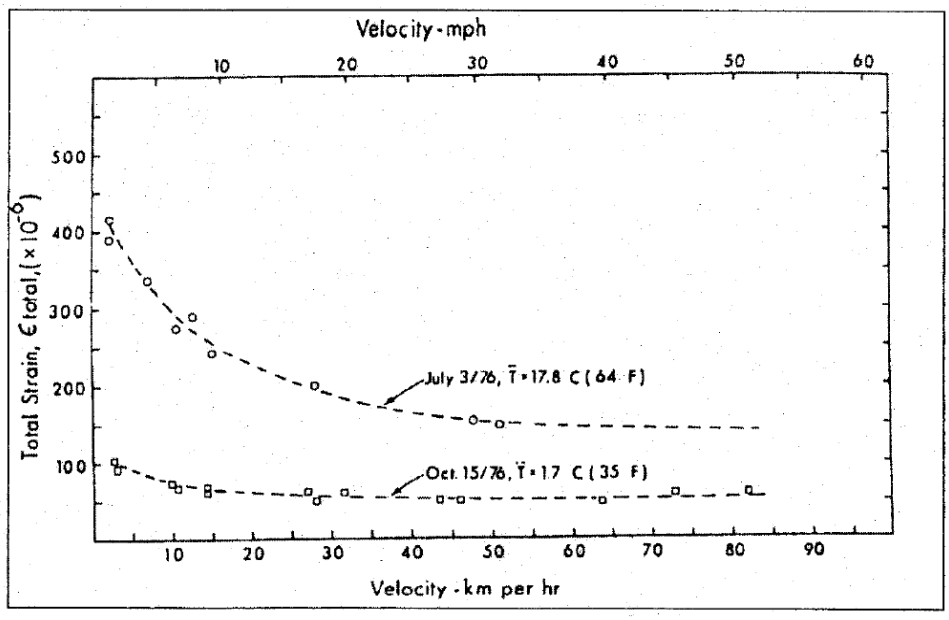

Figure 2-4: Asphalt Longitudinal Strain versus Vehicle Speed for July and October 1976 (Christison et al. 1978)

The average temperature was 17.8°C and 1.7°C during July and October, respectively. The measured strain was observed to be higher in July, and the difference was more pronounced at lower speed.

Doré and Duplain (2002) studied the effect of environmental parameters on measured asphalt longitudinal strain of the St-Célestin test road in Quebec. The test section, 150m long, consisted of 180mm of asphalt concrete, 300 mm of crushed-rock granular base, 450 mm granular subbase, and underlying 300 mm layer of silty sand over clay. The pavement sensors included strain gauges, multi-depth deflectometers, thermistors, moisture sensors, frost gages, piezometers, and heave gauges. A standard Benkelman beam truck, moving at 50 km/hr, was used to study pavement response during spring-thaw season, March and April, and recovery period, May. The authors reported that the strain at the bottom of the asphalt layer increased as the pavement temperature and the moisture content increased (Figure 2-5).

Solaimanian et al. (2006) measured the tensile strain in Penn State Test Track using various loading configurations and truck speeds in different seasons. The average tensile strain was 40μm/m in February, while 80μm/m was observed in September. The air temperature varied between 15 to 18°C in September and 4 to 5°C in February.

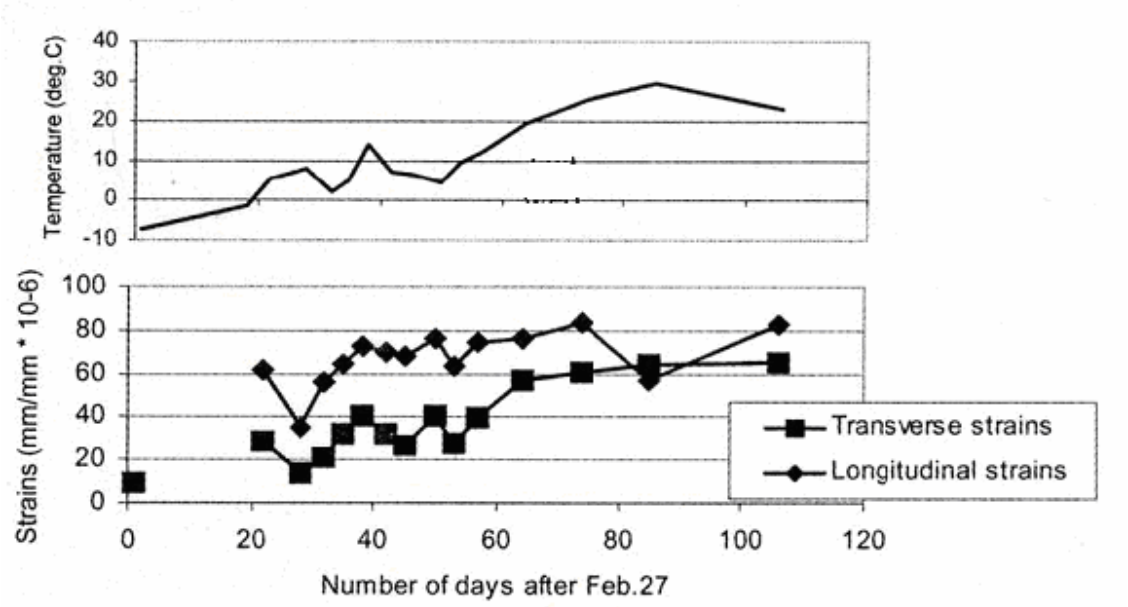

Figure 2-5: Asphalt Strain and Pavement Temperature during Spring Thaw (Doré and Duplain 2002).

Chapter 3: Flexible Pavement Response under Dynamic Wheel Loads-A CPATT Full-Scale Instrumented Test Road Study

3.1 Overview

In 2000, the Centre for Pavement and Transportation Technology (CPATT) commissioned a two lane test track in southern Ontario. In 2002, sensors were installed in the test track to monitor pavement environmental and load-associated responses. The unique CPATT test track facility is located in a climate with seasonal freeze/thaw events, and is equipped with a remote access data acquisition system with the capability to sample sensors using a high frequency sampling rate. In 2006, a series of controlled loading tests were performed to investigate pavement dynamic response due to various loading conditions. The paper describes the CPATT test site, the field instrumentation program, and the state-of-the-art remote access data acquisition systems. It describes the 2006 field test program and presents typical sensor data for asphalt strain gauges and total pressure cells. Field data is then used to determine wheel wander impacts on sensor readings and temperature effect on measured asphalt longitudinal strains. Testing found that 16 cm wheel wander can reduce asphalt longitudinal strain by 36 percent, and that daily temperature fluctuations can double the asphalt longitudinal strain.

3.2 Introduction

Over the past three decades, considerable advances have occurred in the design, construction, and monitoring of in situ pavement test sections - The Minnesota Road Research Project (Timm and Newcomb 2003; Tompkins et al. 2007; Worel et al. 2007), the Virginia Smart Road (Al-Qadi et al. 2004), the Ohio SHRP Test Pavement Sections (Sargand et al. 1997; Sargand et al. 2007), and the National Center for Asphalt Technology (NCAT) Test Track (Brown 2006; Priest et al. 2005; Timm et al. 2004). These studies are either in mild or cold climate with little seasonal variations. Currently, there is little published literature on flexible pavements subject to freeze/thaw environment typical of southern Ontario, Canada.

To address this issue, the Centre for Pavement and Transportation Technology (CPATT) commissioned, in 2000, a two- lane test track, 709m long and eight m wide, at the Regional Municipality of Waterloo Landfill located in Waterloo, Ontario, Canada. Weather data from the University of Waterloo weather station indicates that the site average monthly temperature typically varies from -10°C in January to 26°C in August and that frequent freeze/ thaw conditions are common during winter months. In the fall of 2002, pavement and environmental sensors were installed to measure pavement stresses, strains, temperature, and soil moisture content. In the summer of 2006, a field test program was completed to investigate pavement response due to tire type, tire pressure, truck speed, axle load, and sensor variation due to wheel wander.

This paper provides an overview of the CPATT field test facility, the field instrumentation program, and the state-of-the-art data acquisition system. Details of the 2006 field experimental program are presented along with typical sensor data.

3.3 CPATT Test Track

3.3.1 Site Information

The technological challenges regarding roads and pavements are substantial and include not only the need for asset preservation but also the provision of adequate levels of service and safety, as well as, the need for continuing innovation and advancement in all areas. These challenges formed the basis for a new research initiative in Canada – the University of Waterloo's Centre for Pavement and Transportation Technology (CPATT) integrated laboratory and field-tests facility. Support for the initiative came from a three-way partnership of the public sector (Federal, Provincial, Regional and Municipal), private sector (contractors, consultants, suppliers, and manufacturers), and academia.

In this study, environmental parameters and flexible pavement field response were measured at the CPATT test track (709m long and eight meters wide) located in Waterloo. The two-lane CPATT test track has asphalt overlay consisting of binder Hot Laid 3 (HL3) plus a surface mix consisting of HL3, Polymer-Modified Asphalt (PMA), and Stone Mastic Asphalt (SMA) or Superpave. The location and arrangement of each surface mix is shown in Figure 3-1.

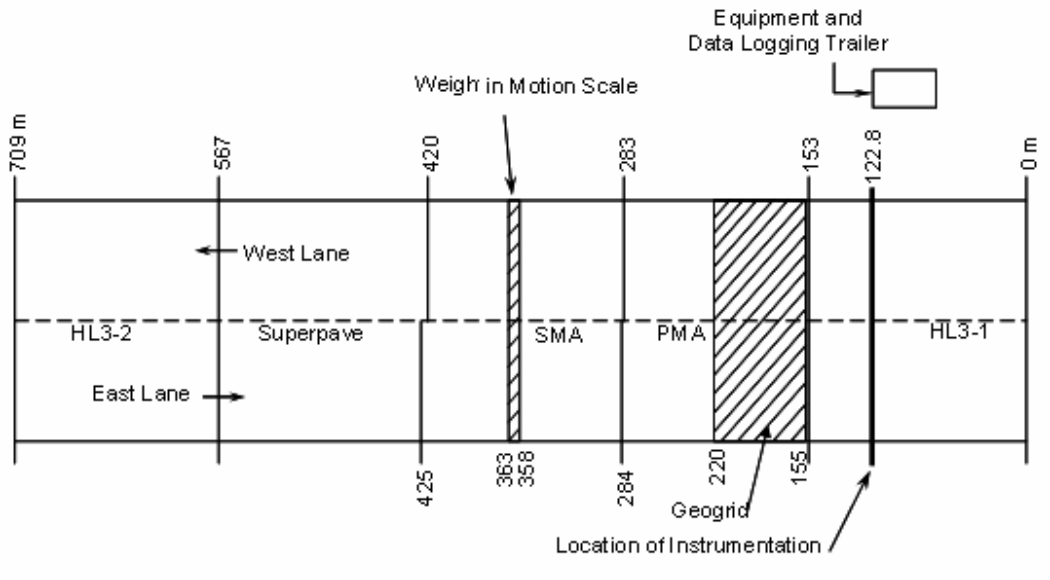

Figure 3-1: CPATT Test Track Facility Located at Waterloo Region

The instrumented test track section consists of 223 mm and 185 mm of HL3 on the west and east lane respectively. The HL3 mix consists of 40 percent crushed gravel, 45% asphalt sand, 15% screenings, and 5.3% PG 58-28 asphalt cement. Below the HL3 are 200mm of Granular A base aggregate and 300mm of Granular B subbase aggregate. Compacted Granular A, 900mm in depth, is located below the subbase aggregate. Below the compacted Granular A is site subgrade that consists of compacted fill and well compacted clayey silt with some gravel. Granular A, as defined in Ontario Provincial Standard Specification (OPSS) 1010, consists of crushed rock composed of hard, uncoated, fractured fragments reduced from rock formations or boulders of uniform quality while Granular B consists of clean, hard, durable uncoated particles from deposits of gravel or sand (MTO 2003). Further details on the test track facility including its construction and pavement performance can be found in Knight et al. (2004) and Tighe et al. (2003).

3.3.2 Field Monitoring Program

A state-of-the-art field instrumentation and data acquisition program was developed as part of the CPATT field monitoring program. Sensors were installed to measure asphalt and soil strain, vertical stress, soil moisture content, and ground temperature. Figure 3-2 shows sensor distribution (ASG is asphaltic strain gauge, TPC is total pressure cell, T is thermistors, and TDR is Time Domain Reflectometer). The following sections, adopted from Adedapo (2007), provide details on the pavement load and environmental sensors and the state-of-the-art data acquisition system.

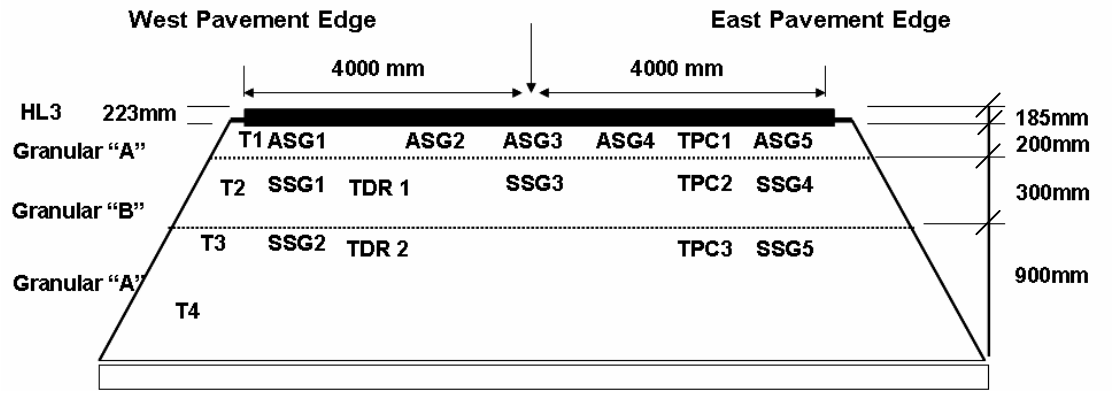

Figure 3-2: Instrumented Section Profile and Sensor Distribution Layout

3.3.2.1 Load Sensors

Asphalt Strain Gauges (ASG)

To measure asphalt longitudinal strains at the base of the asphalt layer, five ASG-152 H-type asphalt strain gauges, manufactured by Construction Technology Laboratories (CTL) Group Inc. were installed. These gauges were chosen due to their reliability, durability, low cost, short

delivery time, and excellent performance at other test sites. Prior to installation, calibration and functionality of each gauge was checked in the laboratory. Figure 3-2 shows the location of the five asphalt strain gauges (ASG1 to ASG5). ASG3 was placed at the road centerline, while ASG1 and ASG2 were placed 690mm and 2700 mm from the west pavement edge respectively. ASG5 and ASG4 were placed 1380mm and 3200mm from the east pavement edge respectively. To ensure that the asphalt strain gauges were bounded to the asphalt base course, all asphalt strain gauges were placed in a sand-asphalt binder mixture consisting of sand and PG 64-22 binder (Figure 3-3).

Figure 3-3: H-type Asphalt Strain Gauge Prior to Placement of HL3 Asphalt (Adedapo 2007)

Earth Pressure Cells (TPC)

To record changes in vertical stress during construction and vertical stress due to dynamic wheel loads, Campbell Scientific RST pressure cells were installed (RST TP -12-S, TP-9-S, and TP-6-S pressure cells with 172kPa, 345kPa and 690kPa stress capacity). Pressure cells were selected due

to their imprint size, sensitivity, availability, measurement range, capability to withstand HMA temperature, and previous successful use in other pavement research programs. TPC1, TPC2, and TPC3 were installed approximately 3200mm from the east edge of the pavement (Figure 3-2). TPC1, 150mm (6") in diameter, was placed at the base of the asphalt (top of the base course) while TPC2, 225mm (9") in diameter, was placed 592mm below the asphalt surface near the top of the Granular B subbase. TPC3, 300mm (12") in diameter, was placed 938mm below the asphalt surface near the top of the Granular A subgrade. Figure 3-4 shows the placement of TPC1 just below the base of the asphalt pavement.

Figure 3-4: Placement of Total Pressure Cell (Adedapo 2007)

Soil Strain Gauges (SSG)

To measure dynamic soil strains at the base-subbase and subbase-subgrade interfaces Geokon model 3900 embedment strain gauges were installed. The Geokon strain gauge has a length of 195mm, diameter of 26mm, and a flange diameter of 38mm. The flange diameter was larger than the maximum aggregate size used. Five soil strain gauges (SSG1 to SSG5) were installed as

shown in Figure 3-2. Soil strain gauges SSG1 and SSG2 were installed approximately 990mm from the west pavement edge and 601 and 969mm respectively below the asphalt surface. Soil strain gauges SSG4 and SSG5 were installed approximately 1350mm from the east pavement edge and 580 and 901mm below the base of the asphalt respectively. Gauge SSG3 was installed at the base of the asphalt (top of the base course) below the road centerline.

3.3.2.2 Environmental Sensors

Time-Domain Reflectometer Probes (TDR)

To measure base and subbase daily and seasonal water content changes, two Campbell Scientific CS616 TDR probes (TDR1 and TDR2) were installed 800 and 1150mm below the west lane asphalt surface respectively. The TDR probes were selected due to their performance, survivability, cost, and ability to integrate with available existing data acquisition loggers. The TDR probes consisted of two parallel conducting rods 300mm in length with a separation distance of 32mm. All sensors were calibrated prior to installation using site Granular A and B aggregates.

Thermistor Probes (T)

To measure daily and seasonal temperature changes in pavement structure, four Campbell Scientific T107B thermistors (T1 to T4) were installed 223, 530, 1134, and 1734mm below the west lane asphalt surface respectively. Campbell Scientific reports the thermistors precision to be ± 0.1 °C.

3.3.3 Data Acquisition

A Campbell Scientific CRX10 data logger was used to monitor the thermistors and the TDR probes using a sampling rate of 0.0033Hz (1 reading every 5 minutes). This sampling rate was deemed sufficient to record daily sensor changes. All other sensor data was collected using Somat eDAQ-plus®, a data logger with the sampling rate set at 0.01Hz (1 reading every 1.67 minutes) in idle mode and 1500Hz when triggered by a traffic load. The high sampling rate was used to capture the millisecond truck load moving over the sensors while the low sampling rate was used to record sensor changes due to environmental factors. The CPATT test track is one of the few instrumented test tracks that has the ability to collect sensor data at a high sampling rate. The Somat eDAQ system is a compact, rugged, and modular data acquisition system capable of collecting a wide range of signal types directly from sensors - strain, analog to ±80V, digital, frequency, and temperature. The eDAQ unit used for this research has the following modules: processor, high-level simultaneous sampling board, and high level board. The processor speed is 266MHz with integrated floating point and 256MB on board DRAM is available for the operating system. The speed of the master sample clock is 100kHz and it has a 2GB memory capacity for onboard data storage. The PC-to-eDAQ communication is via Ethernet 100BaseT and RS232 serial communication. Test Control software (TCE), a Windows ™ based software application, was used to set up and define test requirements in the eDAQ. TCE software was used to: create the test setup files that define and calibrate transducer channels; define data modes and computed channels for online data calculations and analyses; specify triggering conditions for collection of sensor data; monitor sensors using run-time displays; and initialize, start, stop, and upload sensor stored data.

3.3.4 Power Supply and Management

For long-term field monitoring in remote locations, power supply and management plays a critical role for the operation and collection of sensor data. For this project, power was supplied using two 12V deep cycle batteries that were recharged using a solar panel (Figure 3-5).

To conserve battery power during the winter - when the duration of solar recharge was limited - a programmable timer was used to automatically turn the system off and on at predefined times. This power system was found to work well, to be robust, and a cost- effective method to power the sensors and the eDAQ data acquisition system.

Figure 3-5: Solar Panel for Recharging Batteries at Test Site (Adedapo 2007)

3.3.5 Remote Monitoring System

A unique remote monitoring system was developed so that the eDAQ field computer could be monitored and the sensor data could be downloaded using a secure internet connection. Figure 3-6 shows the secure remote monitoring system. The remote monitoring system allowed for daily data upload and the ability to check sensor functionality without the need for site visit. During one data check, several asphalt strain gauges were found not to be working. A site visit revealed that sensor wires had been accidentally cut during grass mowing. All wires were promptly fixed resulting in only a short period with limited data collection.

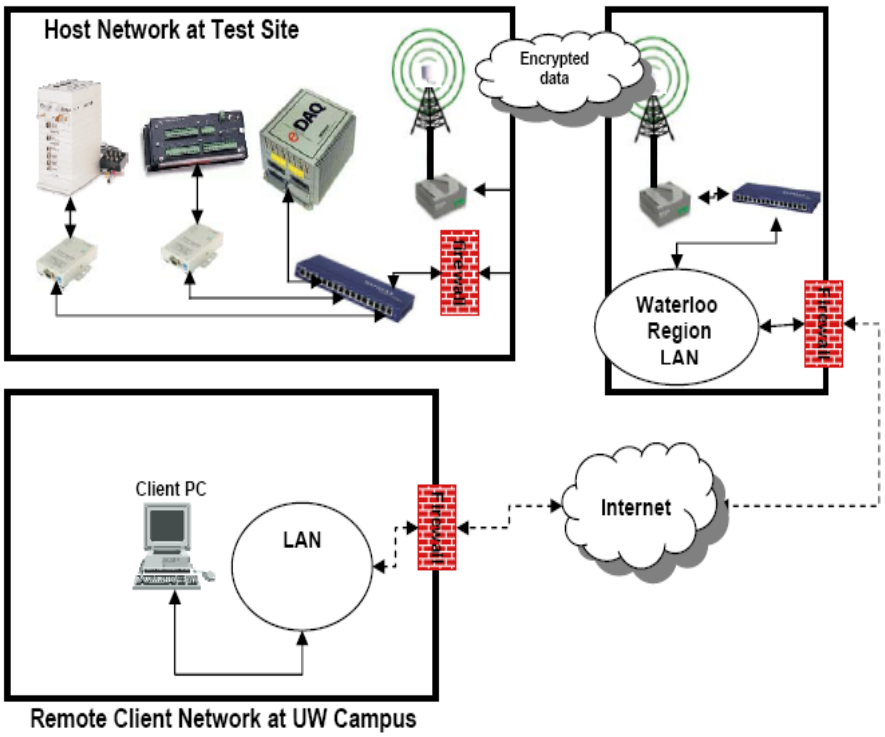

Figure 3-6: Schematic of Developed Secured Remote Monitoring System (Adedapo 2007)

3.3.6 Instrumentation Survivability

To date, all sensors, except for ASG4, have remained operational. Thus daily sensor data were continuously collected over a six year period. ASG4 stopped working shortly after installation.

3.4 2006 Field Testing Program

From June 11 to 16, 2006, controlled wheel loading tests were performed to investigate the effects of various axle and tire configurations on pavement response. A trailer with two axles and a movable load passed over ASG1 and ASG5 at a speed of 5, 25 and 40 km/hr. A Challenger Motor Freight Inc. 2712 truck (Figure 3-7), with single steering axle and tandem driving axle, hauled the trailer. All tests were completed using the trailer in a single axle configuration as shown in Figure 3-7.

Figure 3-7: Challenger 2712 Truck Used in CPATT Test Track

The trailer was configured so that a single axle load could be quickly changed to prescribed values between 7,000 to 15,000kg. All axle loads were set using a mobile scale placed under each axle tire as shown in Figure 3-8. Tests were completed using six tire types: 11R22.5, 275/80R22.5, 295/75R22.5, and 285/70R22.5 dual tires, and 455/55R22.5 and 445/50R22.5 wide-base tires. Tire inflation pressures ranged from 482 to 827kPa.

Figure 3-8: Mobile Scale Used to Verify Single Axle Loads

Multiple passes of the trailer were conducted for each load configuration to ensure that at least three wheel loads passed over the sensors within a prescribed offset limit (50 mm). Video cameras along with pavement markings (Figure 3-9) were used to verify when a wheel passed within the prescribed limit.

For each axle load and tire configuration the tire contact area was measured by obtaining a static tire imprint. Pressure-sensing pads were also used to determine the tire static contact pressure (Figure 3-10).

Figure 3-9: Camera and Pavement Markings Used to Verify Wheel Load Location over ASG1 and ASG5

Figure 3-10: Pressure Sensor Pad used to Measure Tire Contact Pressure

3.5 Data Collection and Analysis

Pavement sensor data was collected at a rate of 1500Hz for each wheel pass. Test Control software (TCE) was used to set up test requirements in eDAQ data acquisition system and to specify triggering conditions for collection of test data. The recorded high speed signals were processed using Infield Somat field analysis software program that is optimized for use with Somat hardware. This software allowed for quick analysis of the large data files. Typical asphalt longitudinal strain gauge and total pressure cell data are shown in Figure 3-11 and Figure 3-12 respectively.

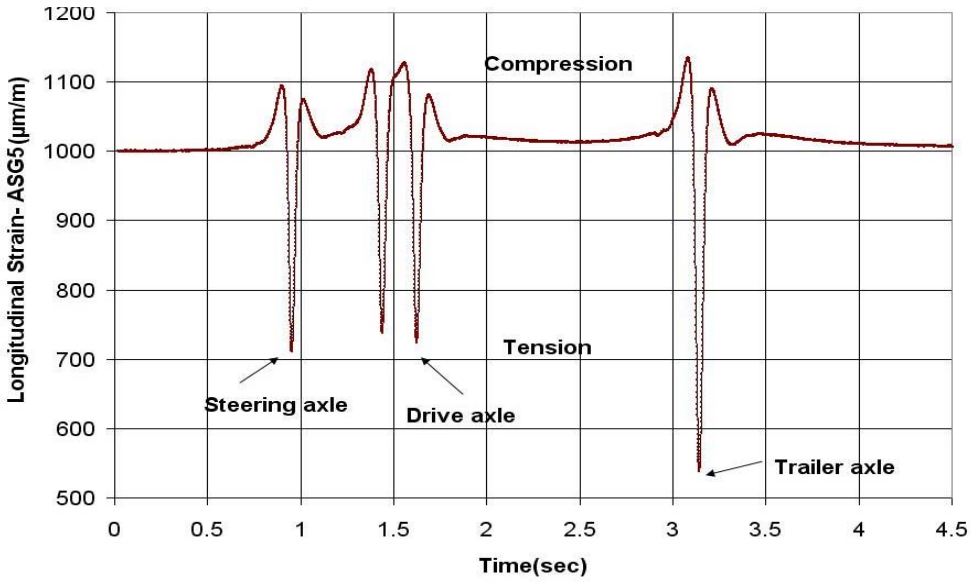

Figure 3-11: Asphalt Strain Gauge (ASG5) Response during the Passing of the Truck and Trailer Wheel Loads

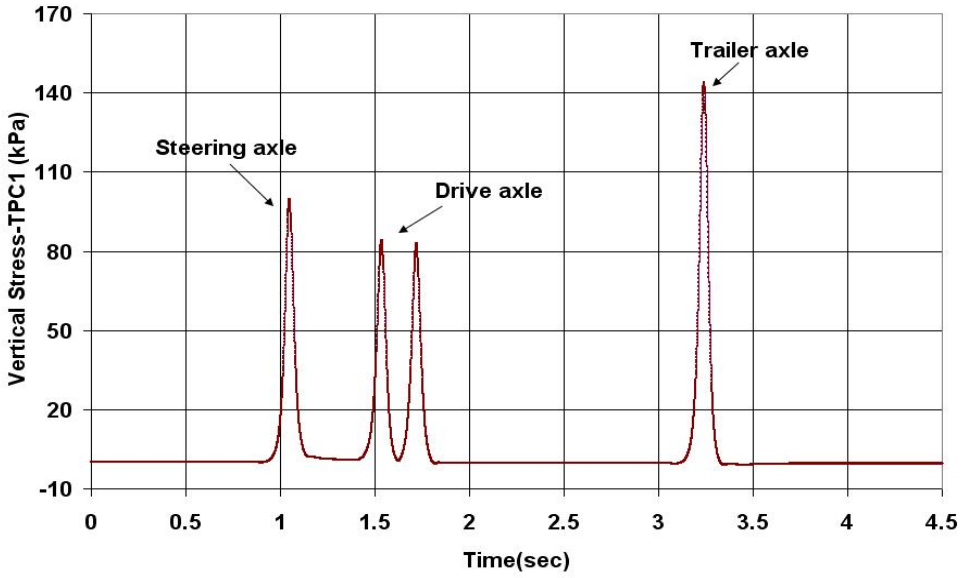

Figure 3-12: Total Pressure Cell (TPC1) Response during the Passing of the Truck and Trailer Wheel Loads

Figure 3-11 shows ASG5 asphalt longitudinal strain measured at the bottom of asphalt pavement layer under a wheel load of 49kN moving at a speed of 25km/hr. The first pulse, at 1 second, represents the passing of the truck steering axle over the strain gauge. The following two pulses, at approximately 1.4 and 1.6 seconds, are the truck's dual tandem drive wheels passing over the strain gauge. The third pulse, at approximately 3.2 seconds, represents the passing of the prescribed trailer wheel load. All wheel passes show the following characteristic behavior – asphalt compression followed by asphalt tension then a second compression wave. Following each truck and trailer pass, the strain gauge was observed to quickly return to its preloading strain values (approx. 1000 μm/m). Sebaaly and Mamlook (1987), Al-Qadi et al. (2004), Immanuel and Timm (2006), and Stoffels et al. (2006) reported similar asphalt longitudinal

strain gauge responses. Figure 3-12 shows TPC1 vertical stress when the truck and trailer with a 49kN wheel load passed over ASG5 at a speed of 25km/hr. The first peak pressure response, at approximately 1 second, represents the passing of the steering axle while the two following pressure peaks represent the passing of the truck dual tandem drive wheels. The third pressure peak, at approximately 3.3 seconds, represents the passing of the prescribed trailer wheel load. Sebaaly and Mamlook (1987), Al-Qadi et al. (2004), Immanuel and Timm (2006), Loulizi et al. (2001), and Priest et al. (2005) reported similar total pressure cell responses.

Temperature and soil moisture content data were recorded at five minute intervals throughout the week of testing. Figure 3-13 shows changes in thermistor probes T-1, T-2, T-3, and T-4 during the week. Temperature data from all probes show a sinusoidal distribution with decreasing magnitude as the probe depth below the asphalt surface increases. It also shows that T-1 minimum and maximum daily temperature increased each day and that the daily temperature variation ranged from 5 to 7.8ºC. Daily air temperatures were found to range from a low of 15ºC to a high of 35ºC with the nightly low and afternoon high increasing throughout the week. Asphalt surface temperatures were also recorded for every run using a heat sensor gun. Soil moisture content was recorded to be 13 and 21 percent at TDR1 and TDR2 respectively during the week of testing.

The following section presents a partial analysis of the field data collected to determine the impact of wheel wander and daily temperature changes on asphalt strain gauge readings during the passing of a constant wheel load.

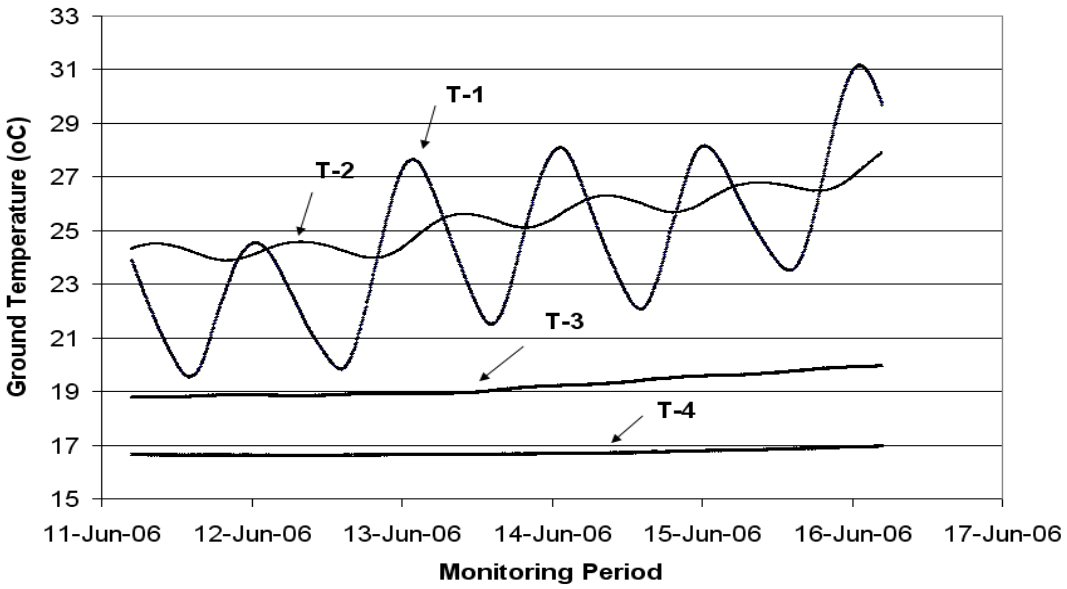

Figure 3-13: Temperature Variation at T-1, T-2, T-3, and T-4 during the Tests

3.5.1 Impact of Wheel Wander on Asphalt Strain Gauge Response

The impact of wheel wander on asphalt strain gauge response was investigated using ASG5 test data from a 44.4kN wheel load moving at a speed of 25km/hr directly over the strain gauge, with 8 and 16cm of offset. Pavement markings were used to guide the driver directly over the strain gauges placed in the east and west lanes, and to determine the exact position of the wheel load with respect to sensor locations. Figure 3-14 shows ASG5 asphalt longitudinal strain response with and without wheel wander.

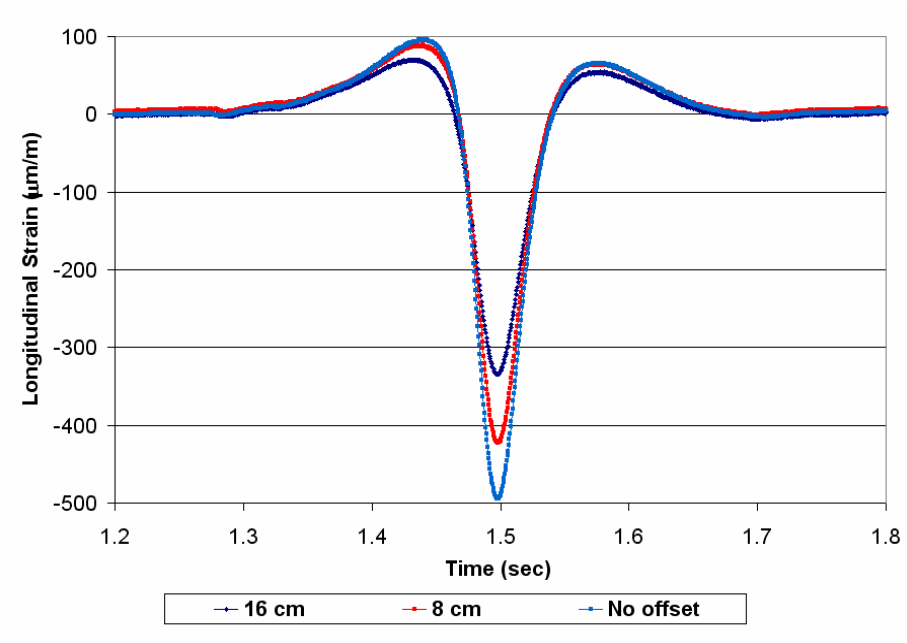

Figure 3-14: ASG5 Strain Response under Different Wheel Lateral Offset

Figure 3-14 shows that when the wheel load passes directly over the strain gauge it results in 500µm/m of asphalt longitudinal strain, while 8 and 16cm of wheel wander results in 420 and 330µm/m respectively. Thus, 16cm of wheel wander reduces the measured asphalt longitudinal strain by 36 percent. Figure 3-14 also shows that the compression part of the wave is not very sensitive to wheel wander.

Figure 3-15 and Figure 3-16 show west and east lanes wheel wander distributions for 270 wheel passes. In these figures, positive offset means that the wheel passed towards the edge of the pavement, and negative offset means that the wheel passed towards the road centerline. The distributions show that -25 to 20cm of wheel wander occurred in the west lane while -20 to 30cm occurred in the east lane. The asymmetrical shape of distributions indicates that the driver had a bias towards the road centerline when travelling in the west lane and towards the road shoulder when travelling in the east lane.

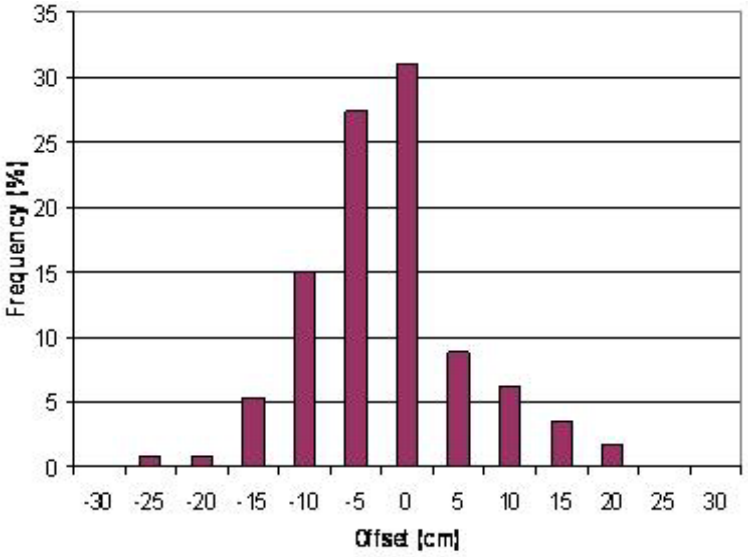

Figure 3-15: Lateral Offset Distribution of the Runs - West Lane

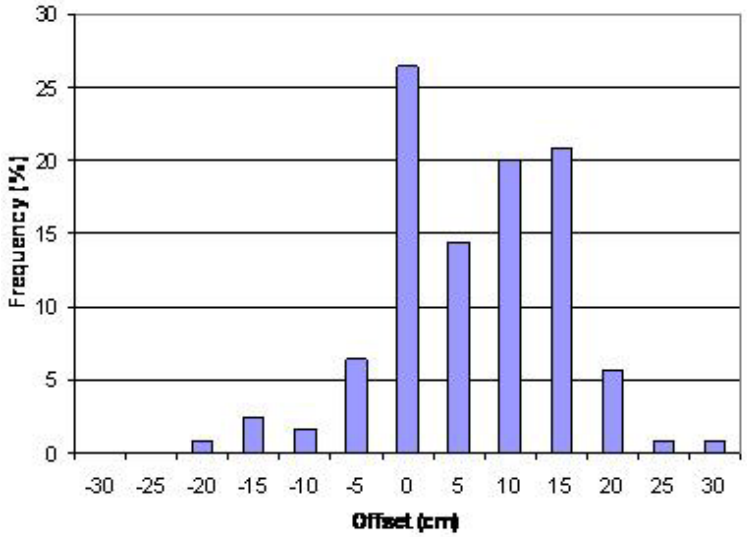

Figure 3-16: Lateral Offset Distribution of the Runs - East Lane

3.5.2 Effect of Temperature on Measured Longitudinal Strains

To determine the impact of temperature changes on the measured asphalt longitudinal strain with a constant wheel load, test data from the following test configuration was used - dual tires

(11R22.5D) with a tire inflation pressure of 689kPa, an axle load of 49kN moving directly over (no wheel wander) the sensors at a speed of 25km/hr. Figure 3-17 shows ASG5 and ASG1 asphalt longitudinal strain variation with asphalt mid-depth temperature. The asphalt mid-depth temperature was determined by averaging the heat gun measured asphalt surface temperature and the temperature measured at base of the asphalt layer (T-1). Figure 3-17 shows that ASG5 asphalt longitudinal strain doubled from 250μm/m at 20.5ºC to 500μm/m at 34ºC while ASG1 almost doubled from 185μm/m at 20.5ºC to 390μm/m at 34ºC. Both strain gauges indicate that asphalt longitudinal strain is sensitive to small changes in asphalt mid-depth temperature. It should be noted that ASG1 consistently had lower strain than ASG5. This lower measured strain is inferred to be the result of the thickness of the west lane asphalt being 38mm more than the east lane. Analysis of the field data showed that exponential relationships, with R^2 of greater than 0.9, exist between asphalt longitudinal strain and mid-depth temperature. Al-Qadi et al. (2002), Loulizi et al. (2002), Priest et al. (2005), and Stoffels et al. (2006) also reported exponential relationships between measured asphalt longitudinal strain and asphalt temperature.

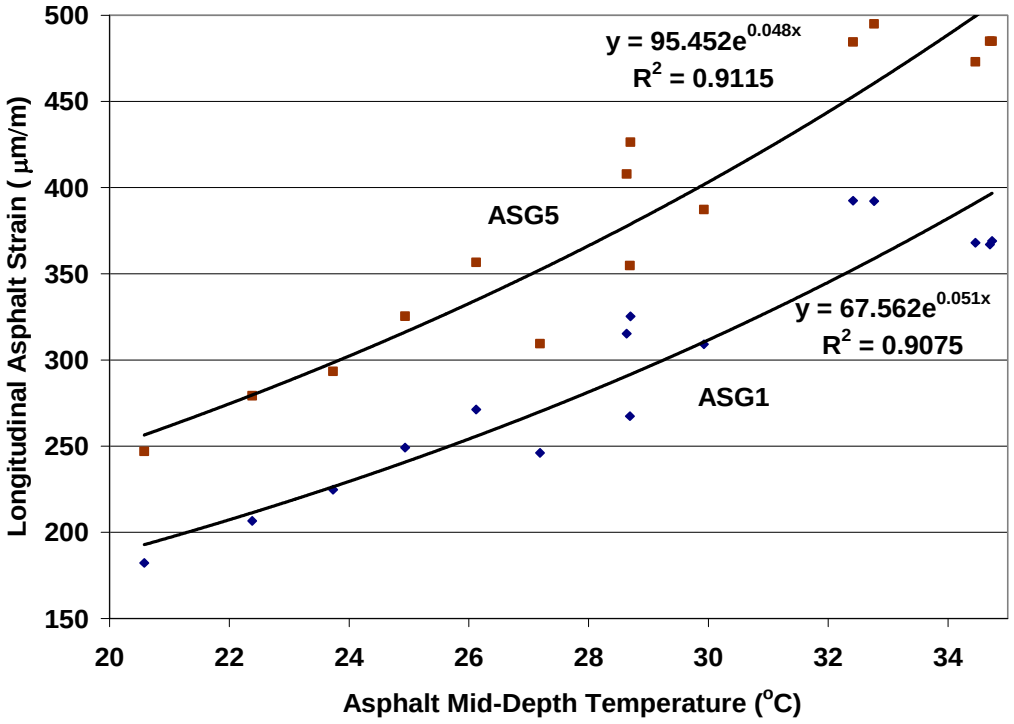

Figure 3-17: Asphalt Longitudinal Strain Variation with Asphalt Mid-Depth Temperature

3.6 Summary and Conclusions

An overview of the CPATT test track, field instrumentation, and the state-of-the-art data acquisition system is presented. This unique facility, located in a climate with seasonal freeze/thaw events, is equipped with an internet accessible data acquisition system capable of reading and recording sensors using a high sampling rate (1500 Hz). Field data was analyzed to determine the effects of wheel wander and changes in asphalt temperature on sensor readings.

Main conclusions drawn from this study are:

- The CPATT instrumentation system has worked exceptionally well for over six years with a survivability rate of approximately 95%.

- Two data acquisition systems were implemented – low frequency to record daily temperature and soil moisture content changes and high frequency to record pavement stresses and strains due to passing wheel loads.

- The remote monitoring system considerably reduced the required site visits and resulted in ensuring that continuous data collection occurred with limited site visits.

- Longitudinal strain response shows that the pavement fully recovers after each truck and trailer wheel pass.

- 16 cm of wheel wander reduced measured pavement strains by 36 percent.

- An exponential relationship was found between asphalt longitudinal strains and asphalt mid-depth temperature.

3.7 Acknowledgment

The authors would like to thank the Natural Science and Engineering Research Council of Canada (NSERC) and CPATT for providing research funding. We would also like to acknowledge the Ministry of Transportation Ontario (MTO), Challenger Motor Freight Inc., and Michelin Canada for their help in organizing and developing the 2006 field test program.

Chapter 4: Validation of Hot-Mix Asphalt Dynamic Modulus using Field Measured Pavement Response

4.1 Overview

The current Mechanistic–Empirical Pavement Design Guide (MEPDG) proposes using the laboratory dynamic modulus test to determine the time-temperature dependent properties of Hot Mix Asphalt (HMA) materials. To date, limited measurements have been performed to compare the HMA behavior of laboratory dynamic modulus test with the field measured pavement response. The objective of this study was to compare and validate laboratory determined HMA dynamic modulus with the results of field measured asphalt longitudinal strains. Under constant loading frequency, the laboratory determined dynamic modulus for Hot Laid 3 (HL3) was found to decrease exponentially when the temperature of the asphalt mix increased. Controlled wheel load experiments, performed using a constant truck speed, found that HL3 asphalt longitudinal strain increased exponentially with an increase in asphalt mid-depth temperature. The comparison of both exponential relationships showed that the laboratory determined dynamic modulus was inversely proportional to the field measured asphalt longitudinal strain.

4.2 Introduction

The current Mechanistic–Empirical Pavement Design Guide (MEPDG), introduced by the recently completed NCHRP Project 1-37A and currently under evaluation by transportation agencies, proposes the use of the time-temperature dependant complex modulus (E^*) of HMA (NCHRP 2004). Dynamic modulus test is also being used as a Simple Performance Test to predict rutting and fatigue cracking in HMA (NCHRP 2004).

The use of complex modulus (E^*) in the design guide has several advantages over stiffness parameters such as resilient modulus (M_R). Loulizi et al. (2006) compared laboratory dynamic modulus and resilient modulus test data for HMA. In this study, resilient and dynamic modulus tests were performed at five temperatures on two typical mixes used in the Commonwealth of Virginia and the test results compared. The dynamic modulus was determined using six frequencies and the resilient modulus test was determined at one loading frequency. The authors found a strong relationship between the dynamic modulus test performed at 5Hz and the resilient modulus. The authors concluded that the dynamic modulus test provides a better characterization of HMA than the resilient modulus test due to its full characterization of the mix over a range of temperatures and loading frequencies.

To date, limited measurements have been performed to compare the HMA behavior of laboratory dynamic modulus test with the field measured pavement response. This paper describes a series of laboratory dynamic modulus test performed on Hot Laid 3 (HL3) asphalt mix used at the Centre for Pavement and Transportation Technology (CPATT) test track. It also discusses field controlled wheel load experiments performed at the CPATT test track facility, and presents typical HL3 pavement response. An analytical approach is then proposed to validate laboratory

measured dynamic modulus with the result of field wheel load experiments. Conclusions and recommendations are then presented.

4.3 Dynamic Modulus Test

Uzarowsky (2006) presents the results of dynamic modulus tests performed on several mixes including HL3 - the mix used in the instrumented section of CPATT test track. The HL3 mix was designed using the Marshall methodology to meet requirements of Ontario Provincial Standard Specification (OPSS) 1150 (MTO 2003). The HL3 mix consisted of 40 percent crushed gravel, 45% asphalt sand, 15% screenings, and 5.3% PG 58-28 asphalt cement. HL3 specimens, 150mm in diameter, were prepared in accordance with AASHTO TP62-03 standard (AASHTO 2003) using a Superpave Gyratory Compactor. Dynamic modulus test specimens, 100 mm in diameter, were then cored from the 150mm specimens and the average air void was determined to be 6.2 percent. An Interlaken UniTest Control System with pre-programmed software was then used to determine the dynamic modulus of HL3 at five testing temperatures (-10, 4.4, 21.1, 37.8, and 54.4 ^{o}C) and at six loading frequencies (0.1, 0.5, 1.0, 5.0, 10.0, and 25.0 Hz). AASHTO (2003) procedures were used to determine the dynamic modulus ($\left|E^*\right|$) over the last five loading cycles using Equation 4-1:

$$\left|E^*\right| = \frac{\sigma_o}{\varepsilon_o} \qquad (4\text{-}1)$$

where:

σ_o =Average peak stress

ε_o = Average peak strain

HL3 dynamic modulus test results, reported by Uzarowsky (2006), are summarized in Table 4-1.

Table 4-1: HL3 Dynamic Modulus

Loading Frequency (Hz)	**Dynamic Modulus (MPa)**				
	-10°C	**4.4 °C**	**21.1 °C**	**37.8 °C**	**54.4 °C**
25	29035.6	18234.1	8517.0	3677.7	1771.9
10	26140.9	15782.4	6724.6	2531.6	1241.3
5	23758.5	14155.5	5632.2	2001.5	1062.6
1	19463.9	8970.2	3567.4	1324.5	789.3
0.5	17024.6	8410.7	2903.3	1139.1	723.1
0.1	12462.5	5904.9	1923.6	876.3	543.0

4.3.1 Changes in Dynamic Modulus with Temperature

Figure 4-1 shows the dynamic modulus with respect to temperature for each loading frequency. This figure shows that for each loading frequency, the dynamic modulus decreases exponentially with increasing temperature. Using the least squared regression method, Equation 4-2, an exponential relationship, was found to fit the test data with a R^2 of 0.99:

$$\left|E^*\right|(T) = a \cdot e^{b \cdot T} \qquad for \qquad f = f_o \tag{4-2}$$

where:

$\left|E^*\right|(T)$ = Dynamic modulus as a function of temperature (MPa)

f = Test loading frequency (Hz)

f_o = Constant loading frequency (Hz)

T = Test temperature (^{o}C)

a, b = Regression coefficients

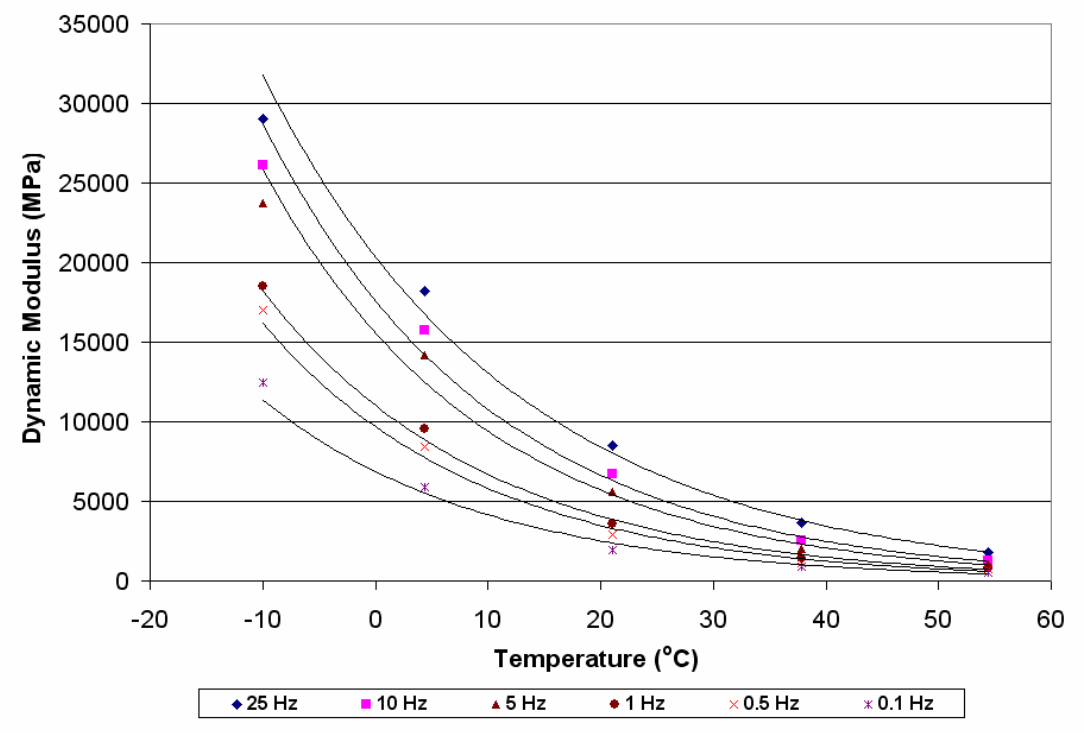

Figure 4-1: Dynamic Modulus versus Temperature for Each Loading Frequency.

Table 4-2 presents regression constants a, b and R^2 values for each loading frequency. The table illustrates that the regression constant b does not vary significantly for various loading frequencies and is relatively constant over the frequency range of 0.1 to 25Hz.

Table 4-2: a, b and R^2 Values for Each Loading Frequency

Loading Frequency	***a***	***b***	R^2
25	20,381	-0.045	0.99
10	17,615	-0.049	0.99
5	15,594	-0.050	0.99
1	11,028	-0.050	0.99
0.5	9,688	-0.051	0.99
0.1	6,862	-0.050	0.98

4.3.2 Changes in Dynamic Modulus with Frequency

Dynamic modulus versus frequency for each testing temperature is shown in Figure 4-2. This figure shows that for each testing temperature the dynamic modulus increases non-linearly when the frequency increases. Using the least squared regression method, Equation 4-3, a non-linear relationship, was found to fit the test data with a R^2 of 0.97 to 0.99:

$$\left|E^*\right|(f) = c.f^{d} \qquad for \quad T = T_o \qquad (4\text{-}3)$$

where:

$\left|E^*\right|(f)$ = Dynamic modulus as a function of frequency (MPa)

T = Test temperature (^{o}C)

T_o = Constant test temperature (^{o}C)

f = Test loading frequency (Hz)

c, d = Regression coefficients

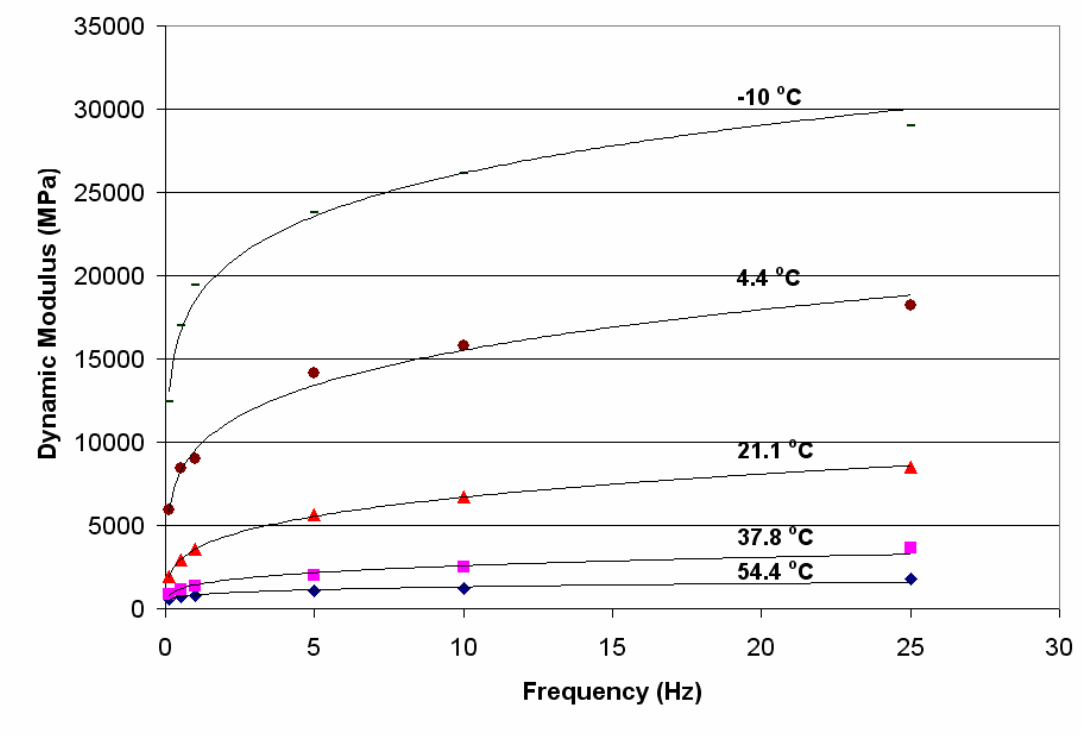

Figure 4-2: Dynamic Modulus versus Frequency for Each Testing Temperature

Table 4-3 presents regression coefficients c, d and R^2 values for each testing temperature. This table shows that the d value for all testing temperatures varied from 0.151 to 0.273 over the temperature range of -10 to 54.4 °C, while the d value is relatively constant over the same range.

Table 4-3: c, d and R^2 Values for Each Testing Temperature

Test Temperature(^{o}C)	c	d	R^2
-10	18,490	0.151	0.99
4.4	9,550	0.211	0.99
21.1	3,573	0.273	0.99
37.8	1,428	0.257	0.97
54.4	824	0.203	0.97

4.4 CPATT Field Test Facility

In this study, flexible pavement field response was measured at the CPATT test track (709m long and eight meters wide) located in Waterloo, Ontario, Canada. The instrumented test track section consists of 223mm and 185mm of HL3 on the west and east lane respectively. The HL3 mix is the same as that tested by Uzarowsky (2006). Below the HL3 are 200mm of Granular A base aggregate and 300mm of Granular B subbase aggregate. Compacted Granular A, 900mm in depth, is located below the subbase aggregate. Below the compacted Granular A is site subgrade that consists of compacted fill and well compacted clayey silt with some gravel. Granular A, defined in OPSS 1010, consists of crushed rock composed of hard, uncoated, fractured fragments, produced from rock formations or boulders of uniform quality. Granular B, defined in OPSS 1010, consists of clean, hard, durable uncoated particles from deposits of gravel or sand (MTO 2003).

A state-of-the-art field instrumentation and data acquisition program was developed as part of the CPATT field monitoring program. The field instrumentation consisted of sensors installed to measure asphalt and soil strain, vertical stress, soil volumetric water content, and ground

temperature. Figure 4-3 shows the instrumented section profile and sensor distribution layout (ASG is asphaltic strain gauge, TPC is total pressure cell, T is thermistors, and TDR is Time Domain Reflectometer).

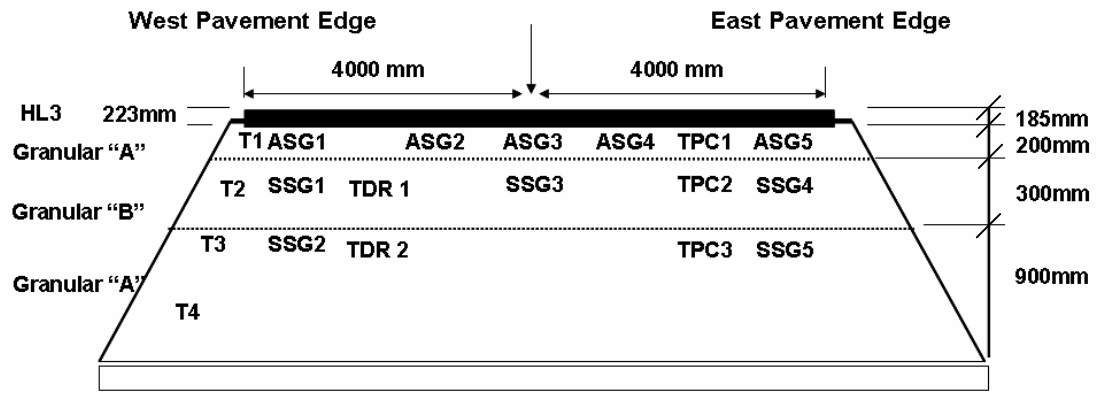

Figure 4-3 : Instrumented Section Profile and Sensor Distribution Layout

All load sensor data was collected using a Somat eDAQ-plus®, data logger with the sampling rate set at 0.01 Hz (1 reading every 1.67 minutes) in idle mode and 1500 Hz when triggered by a traffic load. The high sampling rate was used to capture the millisecond truck load moving over the sensors while the low sampling rate was used to record sensor changes due to environmental changes. The CPATT test track is one of the few instrumented test tracks that has the ability to collect sensor data at a high sampling rate. Tighe et al. (2003) report details on the CPATT test track facility construction and pavement performance.

4.5 Field Testing Program

A series of controlled wheel loading tests was carried out on the instrumented CPATT test track section with the objective of quantifying the pavement response to truck loading under different

wheel load configurations and varying daily temperature. A Challenger Motor Freight Inc. 2712 truck, with a single steering axle and a tandem driving axle was used to haul a trailer in a single axle configuration so that the outer trailer tire passed over ASG1 and ASG5 at a speed of 5, 25 and 40km/hr. Multiple passes of the truck were conducted for each load configuration to ensure that at least three wheel loads passed directly over the sensors. Video cameras along with pavement markings were used to verify when a wheel passed directly over each strain gauge. The vertical stress and asphalt longitudinal strains were measured and recorded at a frequency of 1500Hz. Figure 4-4 shows measured ASG5 longitudinal strain at the bottom of asphalt layer under a wheel load of 49kN moving at a speed of 25km/hr. The first strain pulse, at 1 second, represents the passing of the truck steering axle over the strain gauge. The following two strain pulses, at approximately 1.4 and 1.6 seconds, are the truck's dual tandem drive wheels passing over the strain gauge. The third pulse, at approximately 3.2 seconds, represents the passing of the prescribed trailer wheel load. Figure 4-5 shows TPC1 vertical stress when the truck and trailer with a 49kN wheel load passed directly over ASG5 at a speed of 25km/hr. The first peak pressure response, at approximately 1 second, represents the passing of the steering axle while the two following pressure peaks represent the passing of the truck dual tandem drive wheels. The third pressure peak, at approximately 3.3 seconds, represents the passing of the prescribed trailer wheel load.

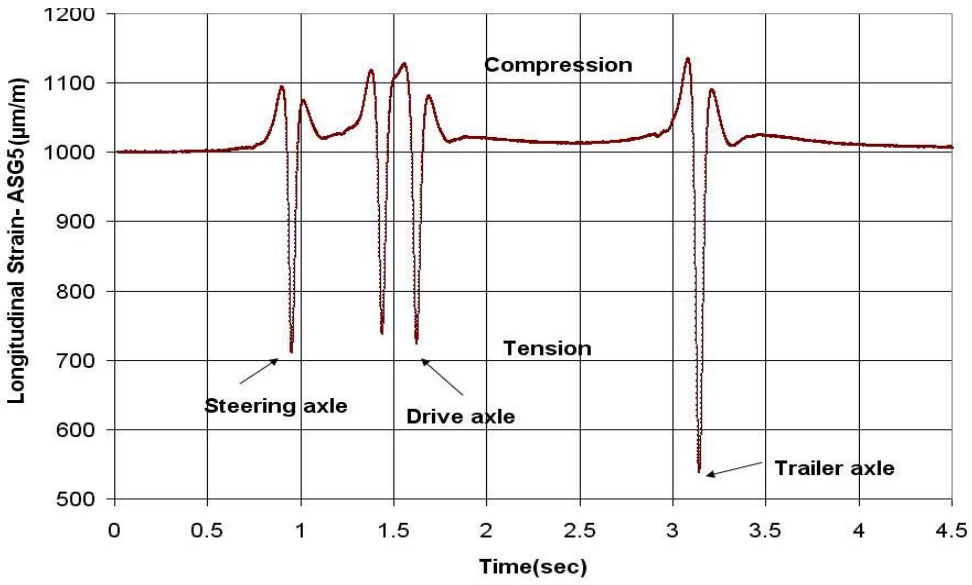

Figure 4-4: Asphalt Strain Gauge (ASG5) Response during the Passing of the Truck and Trailer Wheel Loads

4.5.1 Effect of Temperature on Measured Asphalt Longitudinal Strains

To determine the impact of temperature changes on the measured asphalt longitudinal strain, test data from the following test configuration were used - dual tires (11R22.5D) with a tire inflation pressure of 689kPa and a wheel load of 49kN moving directly over the sensors at a speed of 25km/hr. Figure 4-6 shows ASG1 and ASG5 asphalt longitudinal strain variation with asphalt mid-depth temperature. The asphalt mid-depth temperature was determined by averaging the measured asphalt surface temperature and the temperature measured at the base of the asphalt layer (T1).

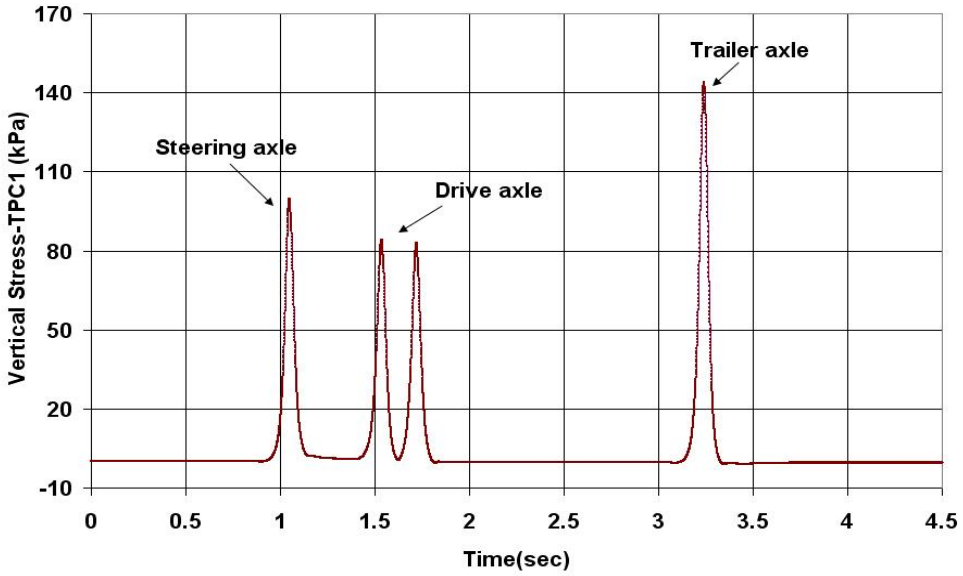

Figure 4-5: Total Pressure Cell (TPC1) Response during the Passing of the truck and Trailer Wheel Loads

Figure 4-6 shows that under a constant truck speed that ASG1 and ASG5 asphalt longitudinal strain increases with increasing asphalt temperature. Similar findings are reported by Loulizi et al. (2002). It should be noted that ASG1 consistently had lower strain than ASG5. This lower measured strain is inferred to be the result of the west lane asphalt thickness being 38mm more than that of the east lane. Using the least squared regression method (Equation 4-4), an exponential relationship was found to fit the test data with a R^2 of 0.91.

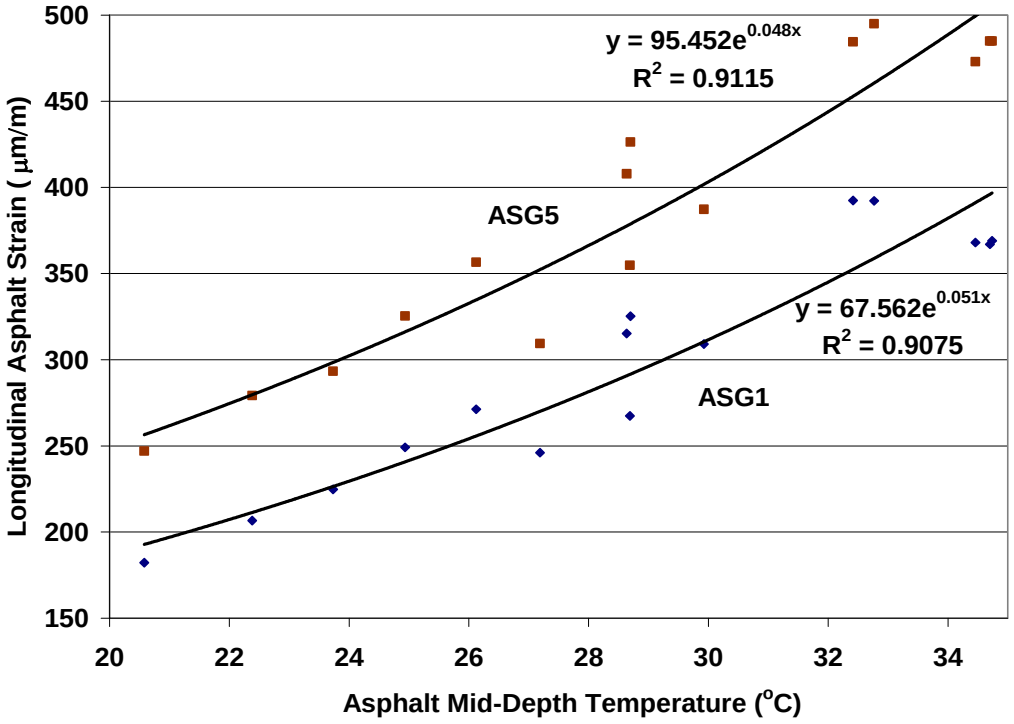

Figure 4-6: Asphalt Longitudinal Strain Variation with Asphalt Mid-Depth Temperature

$$\varepsilon_x(T) = a_1 \cdot e^{b_1 \cdot T} \qquad for \quad S = S_o \qquad (4\text{-}4)$$

where:

$\varepsilon_x(T)$ = Asphalt longitudinal strain as a function of temperature (μm/m)

T = Asphalt mid-depth temperature (°C)

S = Truck speed (km/hr)

S_o = Constant truck speed (km/hr)

a_1, b_1 = Regression coefficients

For a truck speed of 25km/hr and wheel load of 49kN, a_1 values were found to be 67.6 and 95.5 for ASG1 and ASG5 respectively, and b_1 constants were found to be 0.051 and 0.048. It should be noted that ASG1 and ASG5 have approximately the same b_1 constants.

4.5.2 Effect of Truck Speed on Measured Asphalt Longitudinal Strains

To determine the impact of truck speed changes on the measured asphalt longitudinal strain with a constant wheel load, test data from the following test configuration were used - dual tires (11R22.5D) with a tire inflation pressure of 689kPa and a wheel load of 49kN moving directly over the sensors at a speed of 5, 25 and 40 km/hr and 32^{o}C asphalt temperature. Figure 4-7 shows maximum ASG1 and ASG5 asphalt longitudinal strain gauge readings under the three truck speeds. This figure shows that under a constant temperature of 32^{o}C, the asphalt longitudinal strains decrease with increasing truck speed.

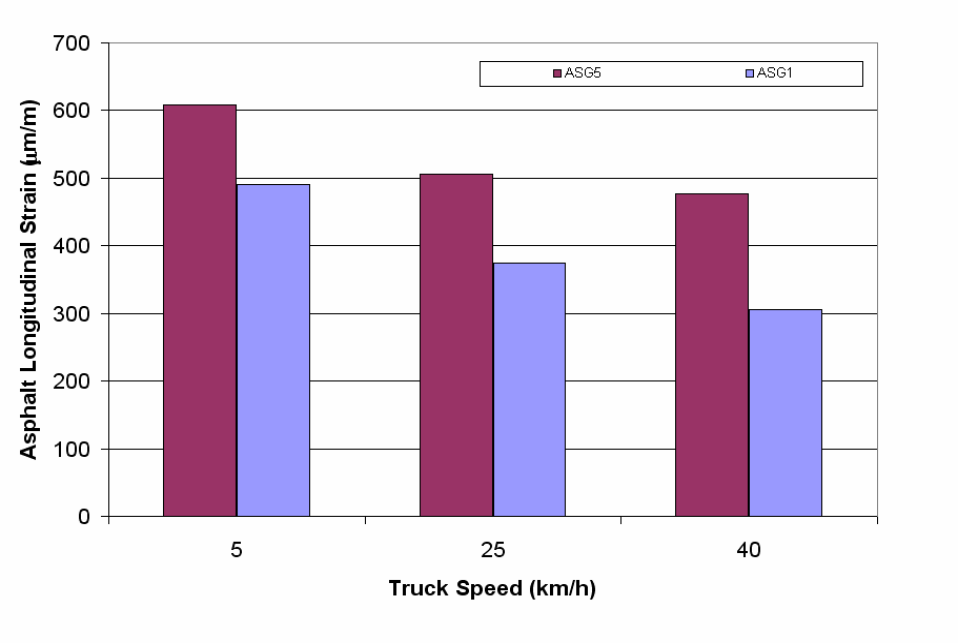

Figure 4-7: Maximum ASG1 and ASG5 Asphalt Longitudinal Strain under Various Truck Speeds

4.5.3 Truck Speed and Loading Frequency

To compare dynamic modulus test data with pavement field response, the loading frequency for each truck speed was determined. Huang (1993) and Loulizi et al. (2002) reported that the loading time (duration) of the applied pulse is dependent on the truck speed and the depth beneath the pavement surface. Figure 4-8 shows the measured vertical stress pulse when the dual tires (11R22.5D) with a tire inflation pressure of 689kPa and a wheel load of 49kN at a speed of 25km/hr passed over ASG5. TPC1, TPC2, and TPC3 are located 225, 592, and 938mm below the pavement surface respectively.

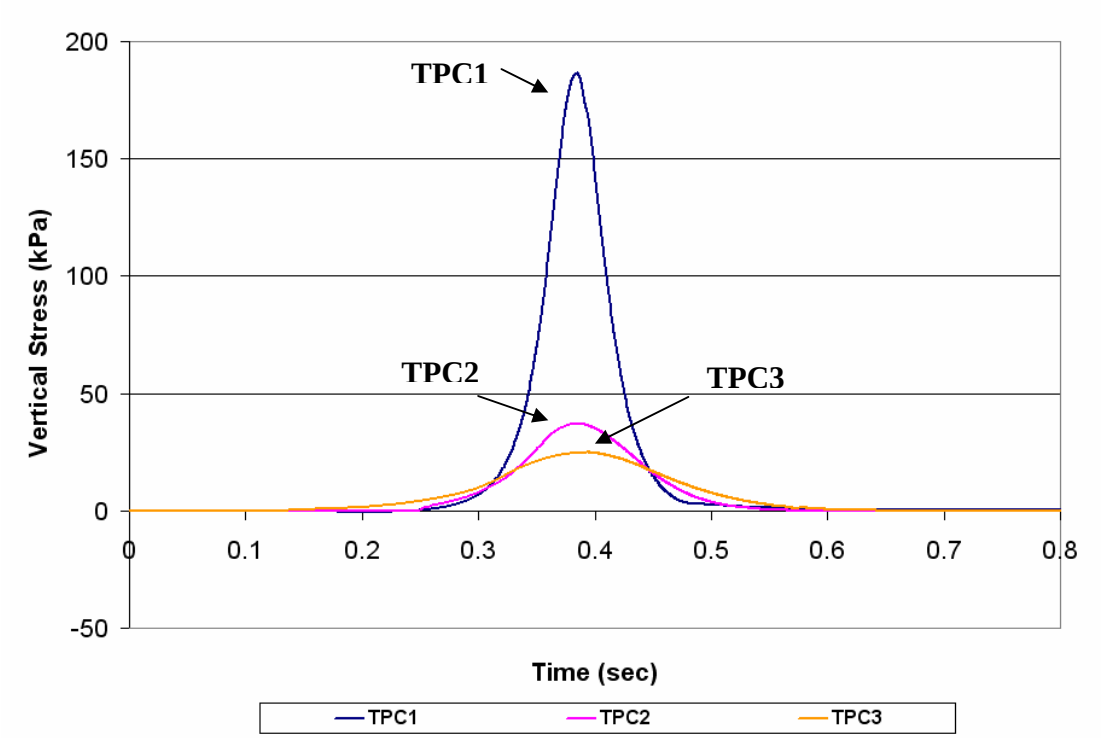

Figure 4-8: Measured Vertical Stress at TPC1, TPC2, and TPC3

Figure 4-8 confirms that loading time is a function of depth below the asphalt surface as TPC1 has a shorter loading time than TPC3. Since TPC1 is approximately at the same elevation of ASG1 and ASG5, TPC1 loading time can be used to determine the loading frequency.

Figure 4-9 shows TPC1 vertical stress pulse with a truck speed of 5, 25, and 40 km/hr. This figure shows that the loading time decreases when the truck speed increases. The shape of the measured vertical stress pulse was also found to be slightly asymmetrical as the stress pulse tail was found to be slightly more elongated when the truck moves onto the sensor. Loulizi et al. (2002) also showed that the stress pulse was slightly asymmetrical. To determine the loading frequency, the inverse of the loading time, the first half of the stress pulse was used. For truck

speeds of 5, 25, and 40km/hr, the loading frequency was determined to be 0.7, 3.5, and 5.5Hz respectively.

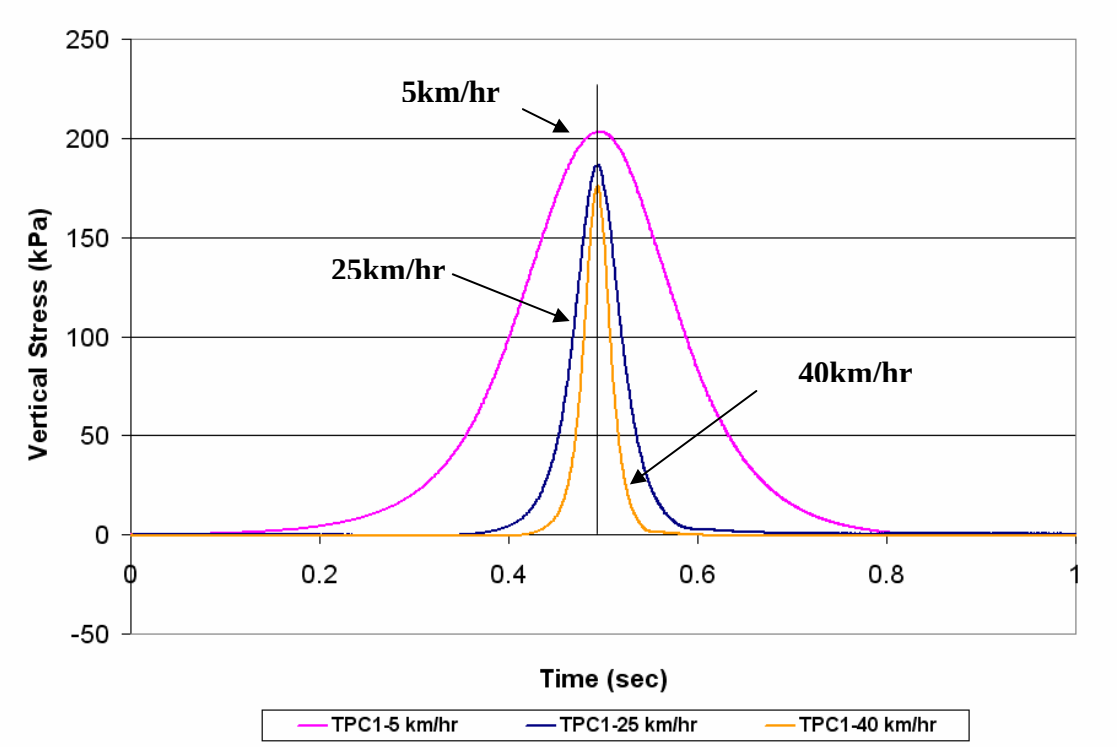

Figure 4-9: TPC1 Vertical Stress under Truck Speed of 5, 25, and 40 km/hr

4.6 Comparison of Dynamic Modulus Test to Pavement Field Response

Equation 4-2, developed using the laboratory dynamic modulus test data, shows that the dynamic modulus can be represented by an exponential function of temperature when the loading frequency is constant. Equation 4-4, developed from the controlled wheel load test, also shows that the asphalt longitudinal strain can be represented by an exponential function of temperature when the truck speed is constant. It should be noted that Equations 4-2 and 4-4 have the same form, and Table 4-2 shows that the b values are approximately -0.050 when the frequency is 10 Hz or less. Figure 4-6, developed for a constant speed of 25 km/hr (3.5 Hz), also indicates ASG1

and ASG5 to have b_1 constants of 0.051 and 0.048 respectively. Thus, b constants for the dynamic modulus test and b_1 constant for the wheel load test are similar in magnitude but opposite in sign. This indicates that the laboratory measured dynamic modulus is inversely proportional to the field measured longitudinal strain. This is in agreement with Equation 4-1 that shows that the dynamic modulus is inversely proportional to the measured strain.

4.7 Summary and Conclusions

The paper presents the results of laboratory measured dynamic modulus tests performed on HL3 asphalt mix and the results of a field controlled wheel load experiments. Using this data the following conclusions are drawn.

- Laboratory dynamic modulus tests show that the dynamic modulus is an exponential function of the test temperature when loading frequency is constant, and that the dynamic modulus is a non-linear function of the loading frequency when the test temperature is constant.

- Field controlled wheel load tests found that HL3 asphalt longitudinal strain is an exponential function of pavement mid-depth temperature when the truck speed and wheel loading is constant, and that the loading time is a function of depth below the pavement surface and truck speed.

- Using the stress pulse of the pressure cell at the elevation of the asphalt strain gauges the frequency of loading was found for three truck speeds and that the laboratory dynamic modulus is inversely proportional to the field measured asphalt longitudinal strain. This indicates that the dynamic modulus can simulate the pavement behavior under wheel load.

4.8 Acknowledgment

The authors would like to thank the Natural Science and Engineering Research Council of Canada (NSERC) and CPATT for providing research funding. We would also like to acknowledge the Ministry of Transportation Ontario (MTO), Challenger Motor Freight Inc., and Michelin Canada for their help in organizing and developing the 2006 field test program.

Chapter 5: Investigation of Flexible Pavement Structural Response for the Centre for Pavement and Transportation Technology (CPATT) Test Road

5.1 Overview

This study was conducted to investigate structural responses of flexible pavements at the Center for Pavement and Transportation Technology (CPATT) test track located at Waterloo, Ontario, Canada. A comprehensive field testing program was carried out to examine flexible pavement responses to a variety of loading conditions. Tests were completed using six tire types: 11R22.5, 275/80R22.5, 295/75R22.5, and 285/70R22.5 dual tires, and 455/55R22.5 and 445/50R22.5 wide-base tires, and tire inflation pressures ranged from 482 to 827kPa. A two dimensional finite element model was developed using MichPave to predict pavement responses. A simplified method was proposed to characterize HMA properties using the laboratory dynamic modulus test. The developed model simulations approximated the field measured responses to all loading configurations.

5.2 Introduction

Mechanistic-Empirical (M-E) methods for the design of flexible pavements have gained significant interest and continue to advance toward full implementation by transportation agencies (Selvaraj 2007). The response models that predict pavement response (i.e., stress, strain, and deflection) under traffic loads and/or environmental conditions are the core component of the M-E design procedure (NCHRP 2004). Therefore, the validity of response models is an important prerequisite for reliable design and performance prediction of the flexible pavement.

Traditionally, the common practice is to use multi-layered elastic theory to predict pavement responses under wheel load. Concerns regarding accuracy of this type of model arise when considering Hot Mix Asphalt (HMA) materials which exhibit viscoelastic behavior and dynamic loads which are applied by moving traffic (Liao 2007). Over the years, numerous finite element (FE) models, capable of modeling viscoelastic HMA behavior and performing dynamic analysis, have been developed (Loulizi et al. 2006) . However, the application of these programs requires considerable expertise from the user and demands a large amount of computation time. Therefore, the layered elastic models continue to be the state-of-the practice for most pavement design and analysis applications (Selvaraj 2007).

In 2006, a series of controlled loading tests were performed at the Center for Pavement and Transportation Technologies (CPATT) test track to investigate pavement dynamic response due to various loading conditions. This paper discusses field controlled wheel load experiments performed at the CPATT test track facility and presents the asphalt longitudinal strain responses. It also explains a three step procedure implemented to simplify incorporating laboratory determined viscoelastic properties of HMA into a finite element (FE) model to accurately

simulate the behavior of HMA. The developed model is validated using results of field experiments.

5.3 CPATT Field Test Facility

In this study, flexible pavement field response was measured at the CPATT test track (709m long and eight meters wide) located in Waterloo, Ontario, Canada. The instrumented test track section consists of 223 and 185mm of Hot Laid 3 (HL3) on west and east lane respectively. The HL3 mix consists of 40 percent crushed gravel, 45% asphalt sand, 15% screenings, and 5.3% PG 58-28 asphalt cement. Below the HL3 are 200mm of Granular A base aggregate and 300mm of Granular B subbase aggregate. Compacted Granular A, 900mm in depth, is located below the subbase aggregate. Below the compacted Granular A is site subgrade that consists of compacted fill and well compacted clayey silt with some gravel. Granular A, as defined in Ontario Provincial Standard Specification (OPSS) 1010, consists of crushed rock composed of hard, uncoated, fractured fragments, reduced from rock formations or boulders of uniform quality while Granular B consists of clean, hard, durable uncoated particles from deposits of gravel or sand (MTO 2003). Further details about the test track facility including its construction and pavement performance can be found in Knight et al. (2004) and Tighe et al. (2003).

A state-of-the-art field instrumentation and data acquisition program was developed as part of the CPATT field monitoring program. The field instrumentation consisted of sensors installed to measure asphalt and soil strain, vertical stress, soil moisture content, and pavement temperature. Figure 5-1 shows instrumented section profile and sensor distribution layout (ASG is asphaltic strain gauge, TPC is total pressure cell, T is thermistors, and TDR is Time Domain Reflectometer). A Campbell Scientific CRX10 data logger was used to monitor the thermistors

and TDR probes using a sampling rate of 0.0033Hz (1 reading every 5 minutes). All other sensor data was collected using a Somat eDAQ-plus®, data logger with the sampling rate set at 0.01 Hz (1 reading every 1.67 minutes) in idle mode and 1500Hz when triggered by a traffic load. The high sampling rate was used to capture the millisecond truck load moving over the sensors while the low sampling rate was used to record sensor changes due to environmental changes. The CPATT test track is one of the few instrumented test track that has the ability to collect sensor data at a high sampling rate.

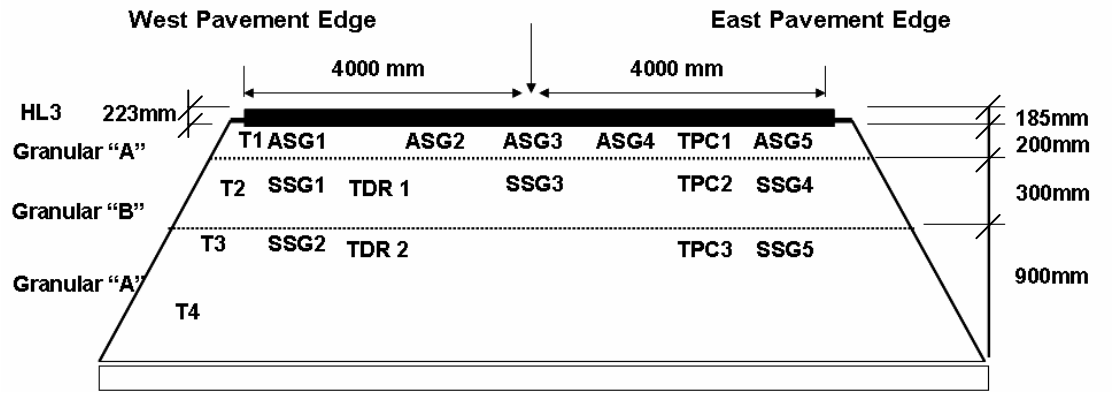

Figure 5-1: Instrumented Section Profile and Sensor Distribution Layout

5.4 Field Testing Program

A series of controlled wheel loading tests was carried out on CPATT test track with the objective of quantifying the pavement response to truck loading under different wheel load configurations and varying daily temperature. A Challenger Motor Freight Inc. 2712 truck (Figure 5-2), with a single steering axle and a tandem driving axle was used to haul a trailer in a single axle

configuration so that the outer trailer tire passed over ASG1 and ASG5 at a targeted speed of 5, 25 and 40km/hr.

Figure 5-2: Challenger Motor Freight Inc. 2712 Truck Used for Field Test

The trailer was configured so that a single axle load could be quickly adjusted to prescribed values between 7,000 to 15,000kg. All axle loads were set using a mobile scale placed under each axle tire. Multiple passes of the truck were collected for each load configuration to ensure at least three wheel loads passed over the sensors. Video cameras along with pavement markings were used to verify when a wheel passed directly over each strain gauge. For each axle load and tire configuration the tire contact area was measured by obtaining a static tire imprint. Pressure-sensing pads were also used to determine the tire static contact pressure.

The vertical stress and asphalt longitudinal strains were measured and recorded at a frequency of 1500Hz for each wheel pass. Test Control software (TCE) was used to set up test requirements in eDAQ data acquisition system and to specify triggering conditions for collection of test data. The recorded high speed signals were processed using Infield Somat field analysis software program that is optimized for use with Somat hardware. This software allowed for quick analysis of the large data files. Typical asphalt longitudinal strain gauge and total pressure cell data are shown in Figure 5-3 and Figure 5-4 respectively.

Figure 5-3 shows ASG5 longitudinal strain measured at the bottom of asphalt layer under a wheel load of 49kN moving at a speed of 25km/hr. The first pulse, at 1 second, represents the passing of the truck steering axle over the strain gauge. The following two pulses, at approximately 1.4 and 1.6 seconds, are the truck's dual tandem drive wheels passing over the strain gauge. The third pulse, at approximately 3.2 seconds, represents the passing of the prescribed trailer wheel load.

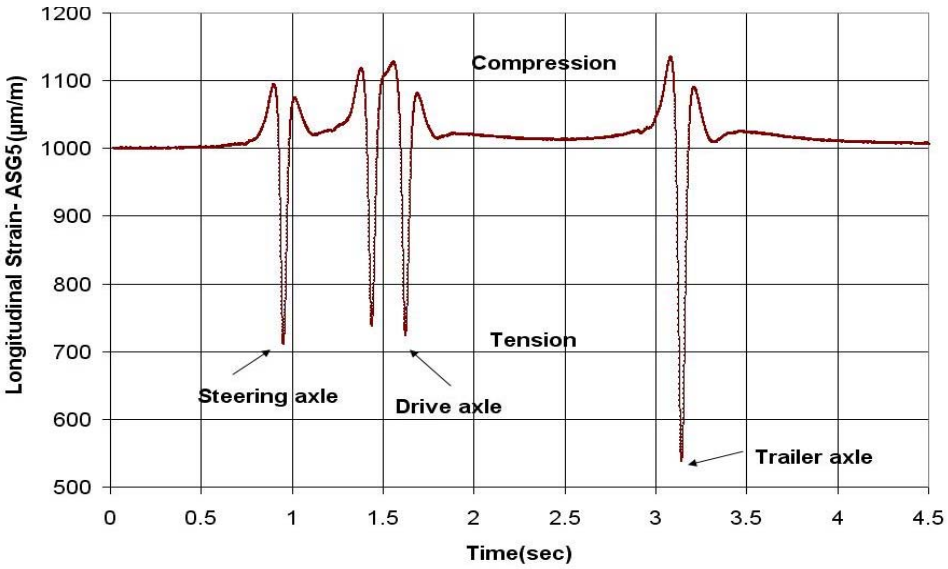

Figure 5-3: Asphalt Strain Gauge (ASG5) Response during the Passing of the Truck and Trailer Wheel Loads

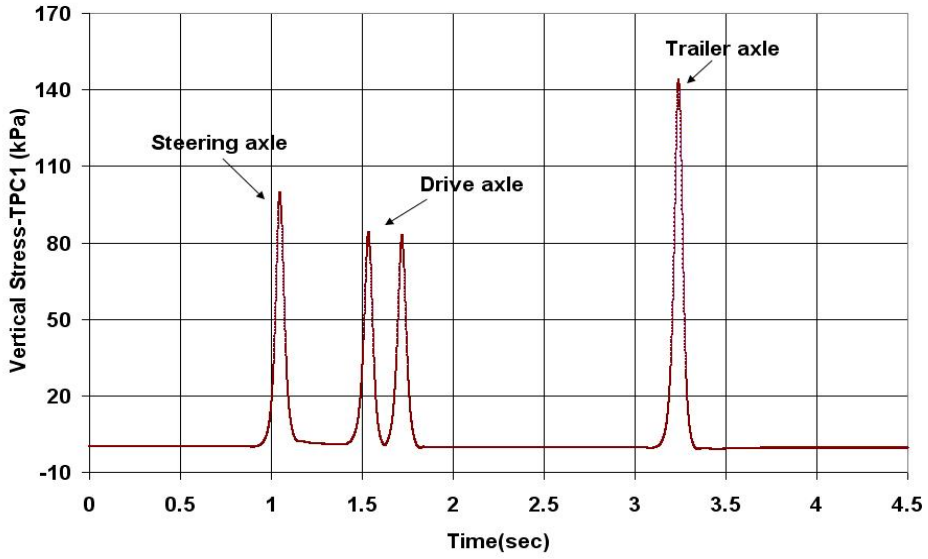

Figure 5-4 Total Pressure Cell (TPC1) Response during the Passing of the truck and Trailer Wheel Loads

Figure 5-4 shows TPC1 vertical stress when the truck and trailer with a 49kN wheel load passed over ASG5 at a speed of 25km/hr. The first peak pressure response, at approximately 1 second, represents the passing of the steering axle while the two following pressure peaks represent the passing of the truck dual tandem drive wheels. The third pressure peak, at approximately 3.3 seconds, represents the passing of the prescribed trailer wheel load.

Tests were completed using six tire types: 11R22.5, 275/80R22.5, 295/75R22.5, and 285/70R22.5 dual tires, and 455/55R22.5 and 445/50R22.5 wide-base tires. Tire inflation pressures ranged from 482 to 827kPa. Table 5-1 to Table 5-4 summarize the test configuration and ASG1 and ASG5 maximum asphalt longitudinal strain for each loading configuration.

ASG1 has consistently lower strain than ASG5. This lower measured strain is inferred to be the result of the west lane asphalt being 38mm thicker than the east lane. The asphalt mid-depth temperature was determined by averaging the measured asphalt surface temperature and the temperature measured at the base of the asphalt layer (T-1).

Table 5-1: Test Configuration and Asphalt Strain Gauge Response- 455/55R22.5 Wide Base Tire

Run ID	Wheel Load (kg)	Tire Pressure		Truck Speed (km/hr)	Mid-Depth Temp. (^{o}C)	Maximum Asphalt Longitudinal Strain (μm/m)	
		psi	*kPa*			ASG1	ASG5
1	4525	110	758.4	25.5	23.2	240.7	339.9
11	5025	125	861.8	24.7	22.3	243.8	351.1
12	4500	110	758.4	25.5	24.6	237.4	351.0
13	4085	95	655.0	25.3	26.4	241.1	350.0
14	3500	80	551.6	24.3	28.9	238.5	347.2
25-6	4450	110	758.4	26.0	29.3	293.0	441.0
35	4450	110	758.4	5.0	30.1	398.0	623.0
37	4450	110	758.4	35.7	29.9	310.0	443.0

Table 5-2: Test Configuration and Asphalt Strain Gauge Response- 445/50R22.5 Wide Base Tire

Run ID	**Wheel Load (kg)**	**Tire Pressure**		**Truck Speed (km/hr)**	**Asphalt Mid-Depth Temp. (^{o}C)**	**Maximum Asphalt Longitudinal Strain (μm/m)**	
		psi	***kPa***			**ASG1**	**ASG5**
16	4540	115	792.9	25.0	33.6	390.8	542.0
17	4100	100	689.5	25.3	31.9	338.5	482.4
18	3500	85	586.1	25.7	31.3	285.8	412.1
27-8	4450	110	758.4	27.1	26.9	249.0	409.0

Table 5-3: Test Configuration and Asphalt Strain Gauge Response- 11R22.5 Dual Tire

Run ID	Wheel Load (kg)	Tire Pressure		Truck Speed (km/hr)	Asphalt Mid-Depth Temp. (°C)	Maximum Asphalt Longitudinal Strain (μm/m)	
		psi	*kPa*			ASG1	ASG5
2	4000	70	482.6	25.3	26.0	204.3	267.1
3	4550	85	586.1	24.5	28.0	288.6	379.0
4	5025	100	689.5	23.6	28.0	316.8	410.0
5	5500	115	792.9	24.2	29.5	346.8	437.5
6	6100	120	827.4	25.1	28.4	336.1	448.4
7	6560	120	827.4	25.4	27.0	332.3	422.3
10	5025	100	689.5	23.3	19.7	183.2	248.2
15	5000	100	689.5	25.1	34.2	368.0	473.0
23	4960	100	689.5	25.3	22.1	205.0	277.0
41	4900	100	689.5	5.0	31.9	481.0	597.0
50	4925	100	689.5	39.6	30.1	325.0	430.0

Table 5-4: Test Configuration and Asphalt Strain Gauge Response- 275/80R22.5, 295/75R22.5, and 285/70R22.5

Run ID	Tire Type	Wheel Load (kg)	Tire Pressure		Truck Speed (km/hr)	Asphalt Mid-Depth Temp. (^{o}C)	Maximum Asphalt Longitudinal Strain (μm/m)	
			psi	*kPa*			ASG1	ASG5
45	275\80	4950	107	737.7	21.0	32.2	393.0	487.0
46	295\75	4960	100	689.5	26.0	32.6	389.0	491.0
47	285\70	4810	110	758.4	26.0	24.2	243.0	317.0

5.5 Finite Element (FE) Modeling

MichPave software, developed for pavement applications, was used to model pavement responses. MichPave is a nonlinear FE program developed by Michigan State University, and is part of the Michigan Flexible Pavement Design System (MFPDS) for integrated and comprehensive analysis and design of flexible pavements (Harichandran et al. 1990).

5.5.1 Model Formulation and Assumptions

The software uses an isotropic axisymmetric formulation, which reduces the 3D pavement structure mathematically to 2D by assuming constant properties in all horizontal planes. The program computes displacements, stresses, and strains within the pavement due to a single circular wheel load, and is able to account for the stress-dependent behavior of granular and cohesive soil layers in the pavement cross section. Each layer in a pavement cross section is assumed to extend infinitely in the horizontal direction, and the bottom layer is assumed to be

infinitely deep. All the pavement layers are assumed to be fully bonded so that no interlayer slip occurs due to applied load (Harichandran et al. 1990).

MichPave uses rectangular four-nodded elements with linear interpolation functions (Harichandran et al. 1990). A lateral boundary is placed at a radial distance of 15a to 40a from the center of the wheel contact area, where *a* is the radius of the wheel contact area. A default mesh generation is used for the analysis, but it can be modified when necessary. Figure 5-5 shows the developed FE mesh in MichPave.

The default mesh has the following characteristics:

- In the radial direction, the total width is divided into four regions: 0 to a, a to 3a, 3a to 6a, and 6a to the lateral boundary. All elements within a region have the same horizontal dimension. The default location of the lateral boundary varies from 15a to 40a depending on the thickness of the asphalt concrete layer.

- Within any layer, all elements have the same vertical dimension.

- The aspect ratio of all elements is less than 1:4.

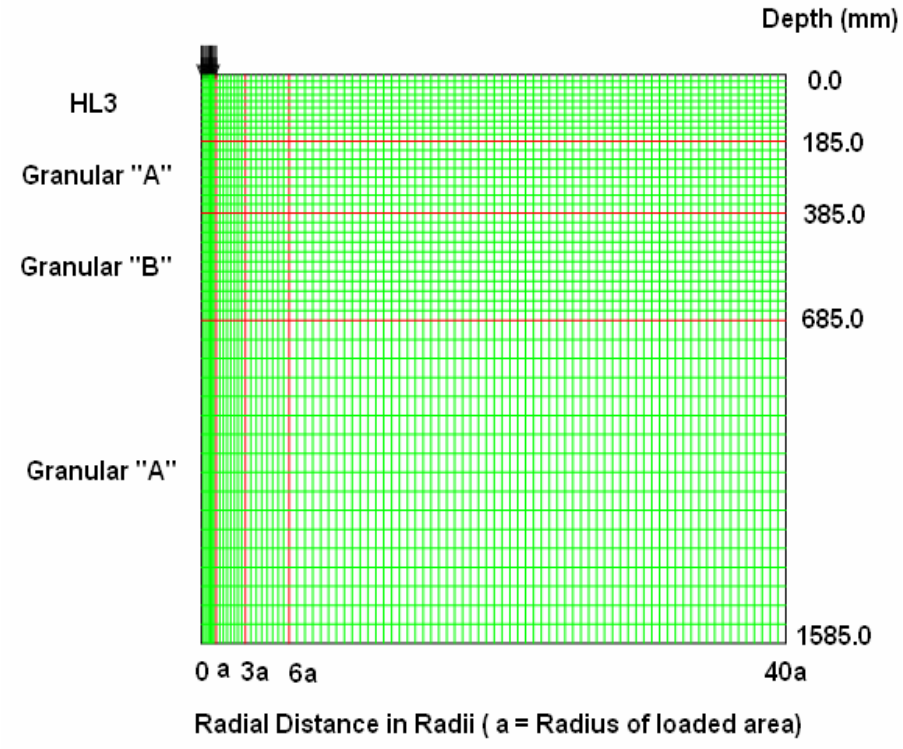

Figure 5-5: MichPave Finite Element Mesh- East Lane

5.5.2 HMA Modulus Characterization

MichPave treats HMA as an elastic material and uses resilient modulus for HMA characterization. However, unlike elastic solids, the HMA materials are viscoelastic and their behavior depends strongly on temperature and loading frequency. In this study, the dynamic modulus test was chosen to determine viscoelastic properties of HMA material. A three step procedure was proposed and used to incorporate laboratory determined viscoelastic properties of HMA into the MichPave FE Model. The implemented procedure is as follows:

5.5.2.1 Step 1: Laboratory HL3 Dynamic Modulus under Various Temperature and Loading Frequencies

The laboratory dynamic modulus test data was used to determine the HL3 dynamic modulus under different temperature and loading frequencies. Uzarowsky (2006) presents the results of dynamic modulus tests performed on several mixes including HL3 - the mix used in the instrumented section of CPATT test track. The HL3 mix was designed using the Marshall methodology to meet requirements of OPSS 1150 (MTO 2003). HL3 specimens, 150mm in diameter, were constructed in accordance with AASHTO TP62-03 standard (AASHTO 2003) using a Superpave Gyratory Compactor. Dynamic modulus test specimens, 100 mm in diameter, were cored from the 150mm specimens. The measured average air void was determined to be 6.2 percent. An Interlaken UniTest Control System with pre-programmed software was used to determine the dynamic modulus of HL3 at five testing temperatures (-10, 4.4, 21.1, 37.8, and 54.4^{o}C) and six loading frequencies (0.1, 0.5, 1.0, 5.0, 10.0, and 25.0Hz). HL3 dynamic modulus ($\left|E^{*}\right|$) test results reported by Uzarowsky (2006) are summarized in Table 5-5.

Table 5-5: HL3 Dynamic Modulus (Uzarowsky (2006))

Loading Frequency (Hz)	**Dynamic Modulus (MPa)**				
	-10^{o}C	**4.4 ^{o}C**	**21.1 ^{o}C**	**37.8 ^{o}C**	**54.4 ^{o}C**
25	29035.6	18234.1	8517.0	3677.7	1771.9
10	26140.9	15782.4	6724.6	2531.6	1241.3
5	23758.5	14155.5	5632.2	2001.5	1062.6
1	19463.9	8970.2	3567.4	1324.5	789.3
0.5	17024.6	8410.7	2903.3	1139.1	723.1
0.1	12462.5	5904.9	1923.6	876.3	543.0

Figure 5-6 shows changes in dynamic modulus with temperature for each loading frequency.

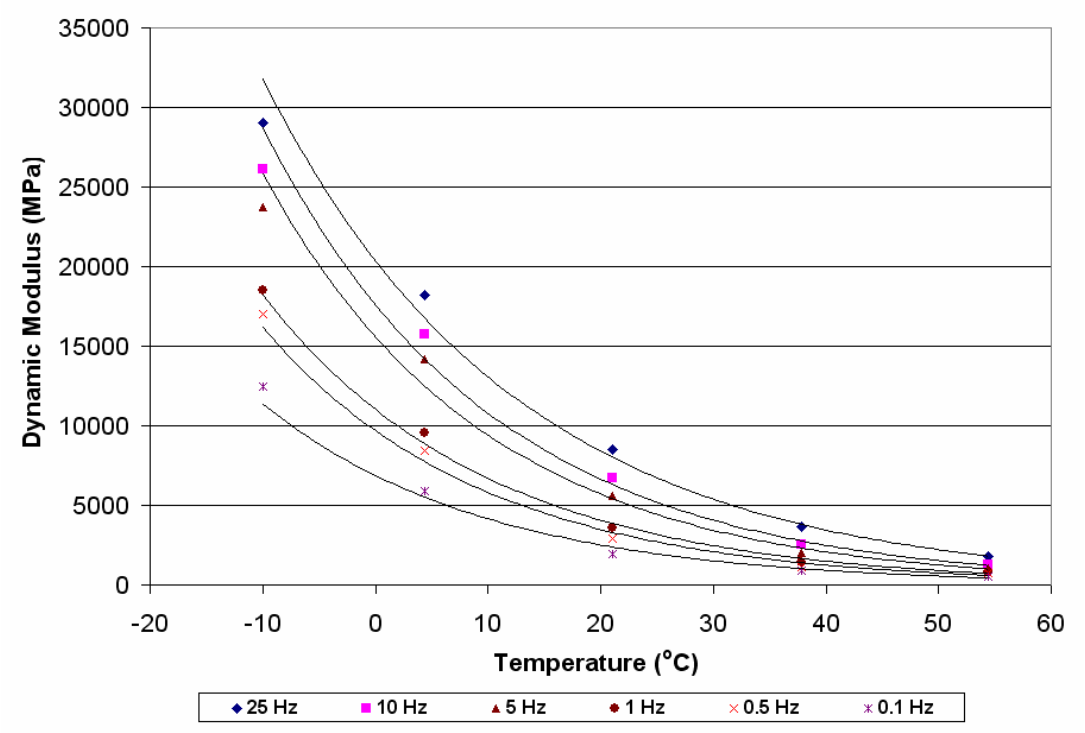

Figure 5-6: Dynamic Modulus versus Temperature for Each Loading Frequency.

5.5.2.2 Step 2: Wheel Load Frequency for Each Truck Speed

For each truck speed, loading frequency was determined using the TPC1 pressure wave. Huang (1993) and Loulizi et al. (2002) report that the loading time (duration) of the applied pulse is dependent on the truck speed and the depth beneath the pavement surface. Since TPC1 is at the same elevation as ASG1 and ASG5, TPC1 loading time can be used to determine the frequency of loading. Figure 5-7 shows TPC1 vertical stress pulse with a truck speed of 5, 25, and 40 km/hr when the dual tires (11R22.5D) with a tire inflation pressure of 689kPa and a wheel load of 49kN passed over ASG5. This figure shows that the loading time decreases with an increase in truck speed.

The shape of the measured vertical stress pulse was found to be slightly asymmetrical. When the truck moves away from the sensor the stress pulse tail was found to be slightly more elongated than when the truck moves onto the sensor. Loulizi et al. (2006) also showed that the stress pulse was slightly asymmetrical. To determine the loading frequency, the inverse of the loading time, the first half of the stress pulse was used. For truck speeds of 5, 25, and 40km/hr, the loading frequency was determined to be 0.7, 3.5, and 5.5Hz respectively.

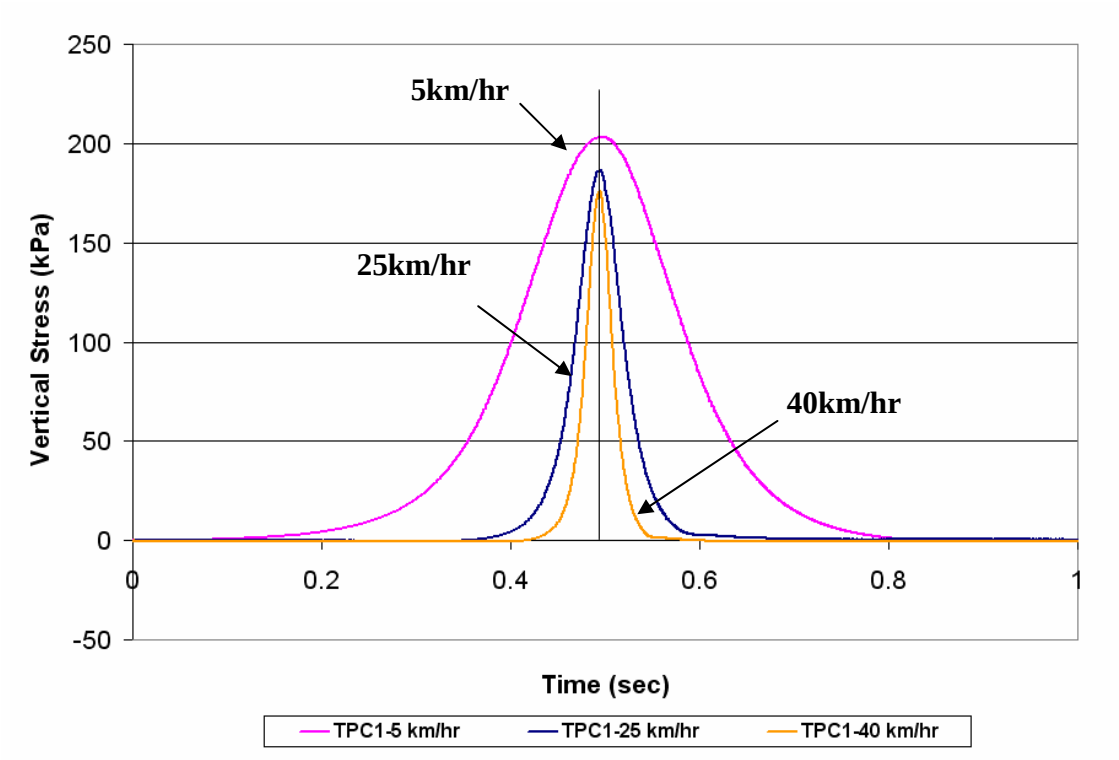

Figure 5-7: TPC1 Vertical Stress under Truck Speed of 5, 25, and 40 km/hr

5.5.2.3 Field Represented Dynamic Modulus

Changes in dynamic modulus with temperature for loading frequency of 0.7, 3.5, and 5Hz were interpolated using the data shown in Table 5-5 (Figure 5-6).

Asphalt mid-depth temperature was determined by averaging the measured asphalt surface temperature and the temperature measured at the base of the asphalt layer (T-1). Table 5-1 to Table 5-4 present the asphalt mid-depth temperature for each loading configuration.

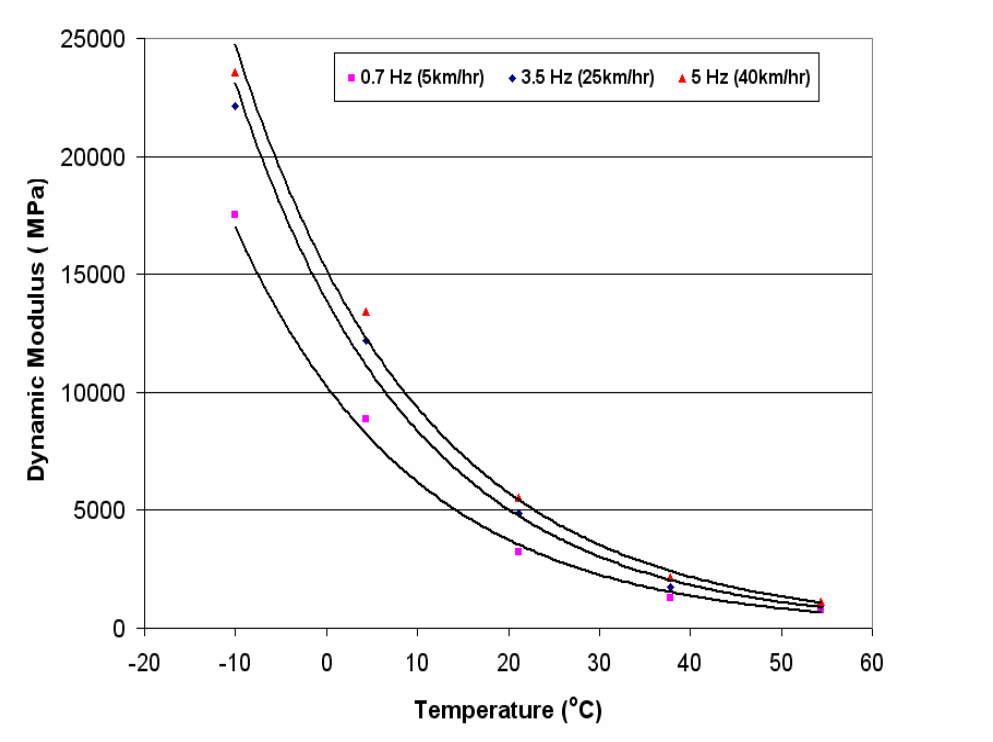

Figure 5-8: HL3 Dynamic Modulus under Loading Frequency of 0.7, 3.5, and 5 Hz (Corresponding to Truck Speed of 5, 25, and 40 km/hr)

Figure 5-8 was used to calculate the field represented dynamic modulus using asphalt mid-depth temperature and loading frequency (truck speed). The field represented dynamic modulus was then used as an elastic modulus of HMA in FE analysis.

5.5.3 Granular Material Characterization

The so-called K-σ_3 model was used to characterize the resilient modulus of granular materials. This model is of the form:

$$M_R = K_1 \cdot \sigma_3^{K_2} \quad (5\text{-}1)$$

where:

M_R = Resilient Modulus (MPa)

σ_3 = Confining pressure (MPa)

K_1, K_2 = Constant values

The average in-situ density of the soil immediately below the subbase and on top of the subbase was determined to be 20.5 and 21.75 kN/m^3 respectively. The material properties assigned to the Granular A and Granular B, shown in Table 5-6, were obtained from the results of extensive laboratory tests on compacted soils published by Selig (1988).

Table 5-6: Summary of Granular Material Properties Used for Simulation

Soil	**Type**	
Properties	**Granular A**	**Granular B**
K_1	5994	8834
K_2	0.6	0.43
Friction Angle (degree)	48	42
Density (kg/m^3)	2200	1800

5.6 Validation of the FE model

Calculated asphalt longitudinal strains from FE model were compared to field measurements, and the results are shown in Figure 5-9 to Figure 5-12.

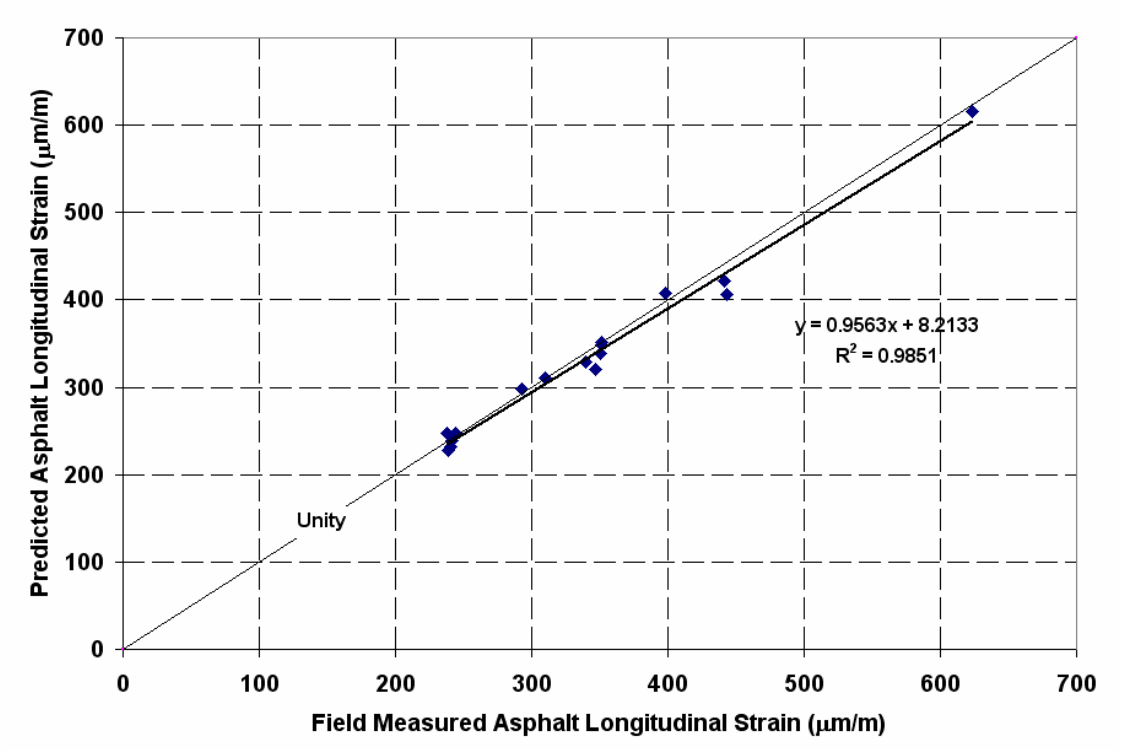

Figure 5-9: Comparison of Field Measured and Calculated Asphalt Longitudinal Strain - 455/55R22.5 Wide Base Tire

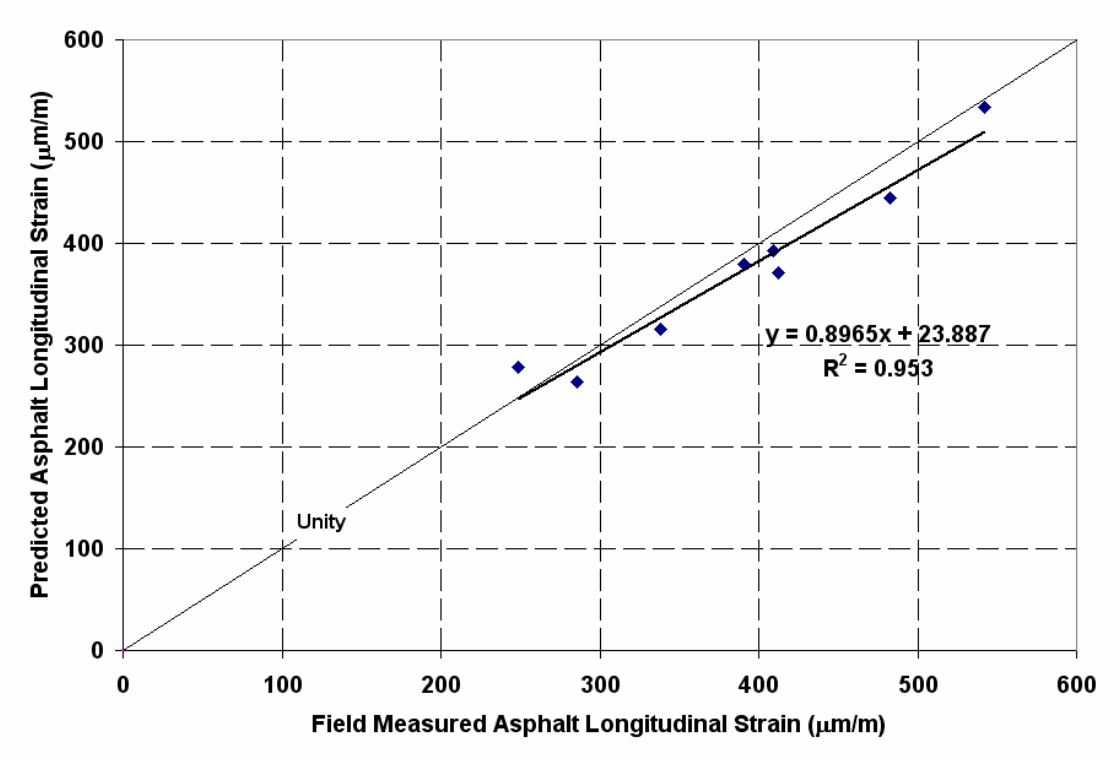

Figure 5-10: Comparison of Field Measured and Calculated Asphalt Longitudinal Strain - 445/55R22.5 Wide Base Tire

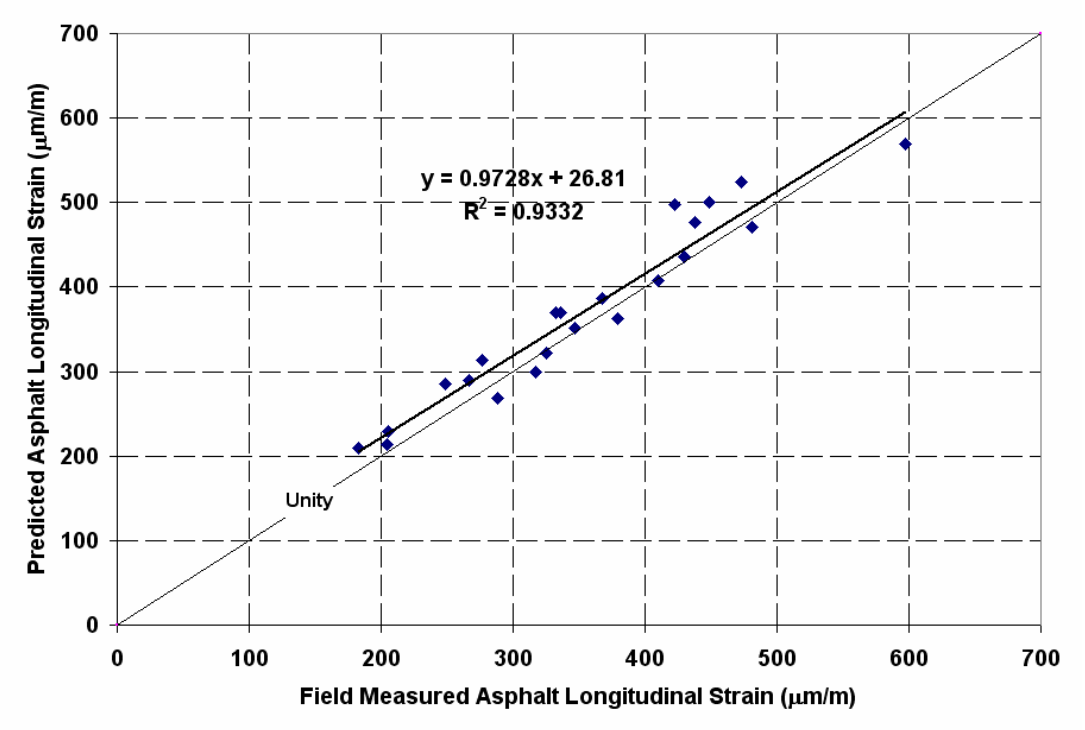

Figure 5-11: Comparison of Field Measured and Calculated Asphalt Longitudinal Strain - 11R22.5 Dual Tire

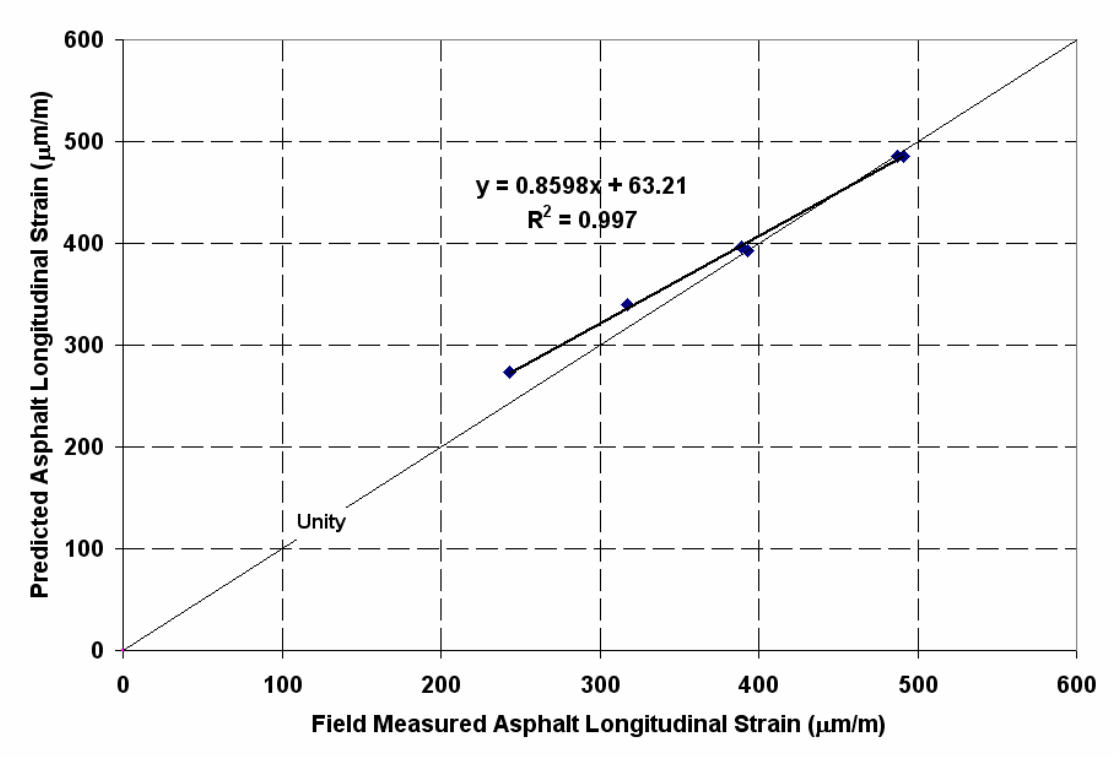

Figure 5-12: Comparison of Field Measured and Calculated Asphalt Longitudinal Strain - 275/80R22.5, 295/75R22.5, and 285/70R22.5

It can be seen that overall the FE model yielded reasonably close predictions compared with field measured values.

5.7 Summary and Conclusions

The paper presents the results of field controlled wheel load experiments performed at CPATT test track. The following conclusions are drawn. Tests were completed using six tire types: 11R22.5, 275/80R22.5, 295/75R22.5, and 285/70R22.5 dual tires, and 455/55R22.5 and 445/50R22.5 wide-base tires, and tire inflation pressures ranged from 482 to 827kPa. A two dimensional FE model was developed using MichPave to predict pavement responses. A three

step procedure was implemented to incorporate laboratory determined viscoelastic properties of HMA into the model. The developed model was validated using the result of field experiments. The results demonstrated that the developed simplified method for incorporating laboratory determined viscoelastic properties of HMA into FE model can predict pavement responses accurately.

5.8 Acknowledgements

The authors acknowledge the Natural Sciences and Engineering Research Council of Canada (NSERC), Canada Foundation for Innovation (CFI), Ontario Innovation Trust (OIT), Ontario Research and Development Challenge Fund (ORDCF), along with the Center for Pavement and Transportation Technologies (CPATT) private and public sector partners for providing research funding. The authors also acknowledge the University of Waterloo technical staff, Ken Bowman, Terry Ridgway, and Doug Hirst, for their guidance, help, and assistance with the field instrumentation.

Chapter 6: Long-Term Monitoring of Environmental Parameters to Investigate Flexible Pavement Response

6.1 Overview

A research program is developed and implemented in a climate subjected to freeze-thaw cycles to investigate the impact of environmental parameters on flexible pavement response. Details of the field data collection system implemented at the Centre for Pavement and Transportation Technologies (CPATT) field test facility located in Waterloo, Ontario, Canada are presented. Data processing and data analysis are also discussed. Temperature, soil moisture content, asphalt longitudinal strain, Falling Weight Deflectometer (FWD), and resilient modulus readings recorded over a two year period are presented and discussed. Field results presented in this study show that: 1) the pavement is subjected to several freeze-thaw cycles during the winter months; 2) rapid fluctuations occur in the soil moisture probe readings when the ground is subjected to freeze-thaw cycles; 3) FWD and soil resilient modulus are highly correlated to soil moisture content; 4) asphalt longitudinal strain fluctuated between 600 and 650μm/m during spring and summer months.

6.2 Introduction

Pavement response has been shown to be correlated to environmental conditions, such as moisture content and temperature (Salem 2004; Zuo 2003). Akhter and Witczak (1985), Drumm et al. (1997), Li and Selig (1994), and Park et al. (2001) report that moisture content influences unbound material modulus and temperature influences asphalt stiffness and pavement response. Al-Qadi et al. (2005), Monismith et al. (1966), and Haas (1968) also report that temperature changes induce asphalt strains. Field monitoring programs have been used to understand pavement response due to environmental conditions (Salem 2004; Zuo 2003). To date most published field studies have been completed in relatively mild climatic conditions (Watson and Rajapakse 2000). Limited published environmental data exist for pavements subjected to climates with freeze-thaw cycles (such as southern Canada).

A field investigation program was developed at the University of Waterloo to investigate in-situ flexible pavement response due to environmental conditions in a climate subjected to freeze-thaw cycles. Figure 6-1 shows the overall field program implemented at the test track facility located in Waterloo, Ontario, Canada. The primary objectives of the investigation program were: (i) monitor and measure daily and seasonal changes in moisture and temperature of the pavement structure and (ii) evaluate pavement response (i.e. deflections and strains) due to changes in soil moisture and air temperature. To ensure a successful data collection system, the following components were considered: 1) sensors must be compatible with the research objectives; 2) sensors need to be calibrated prior to installation; 3) the data acquisition system (DAS) must be compatible with sensors; and 4) DAS must have the ability to monitor and record sensors readings at the required frequency.

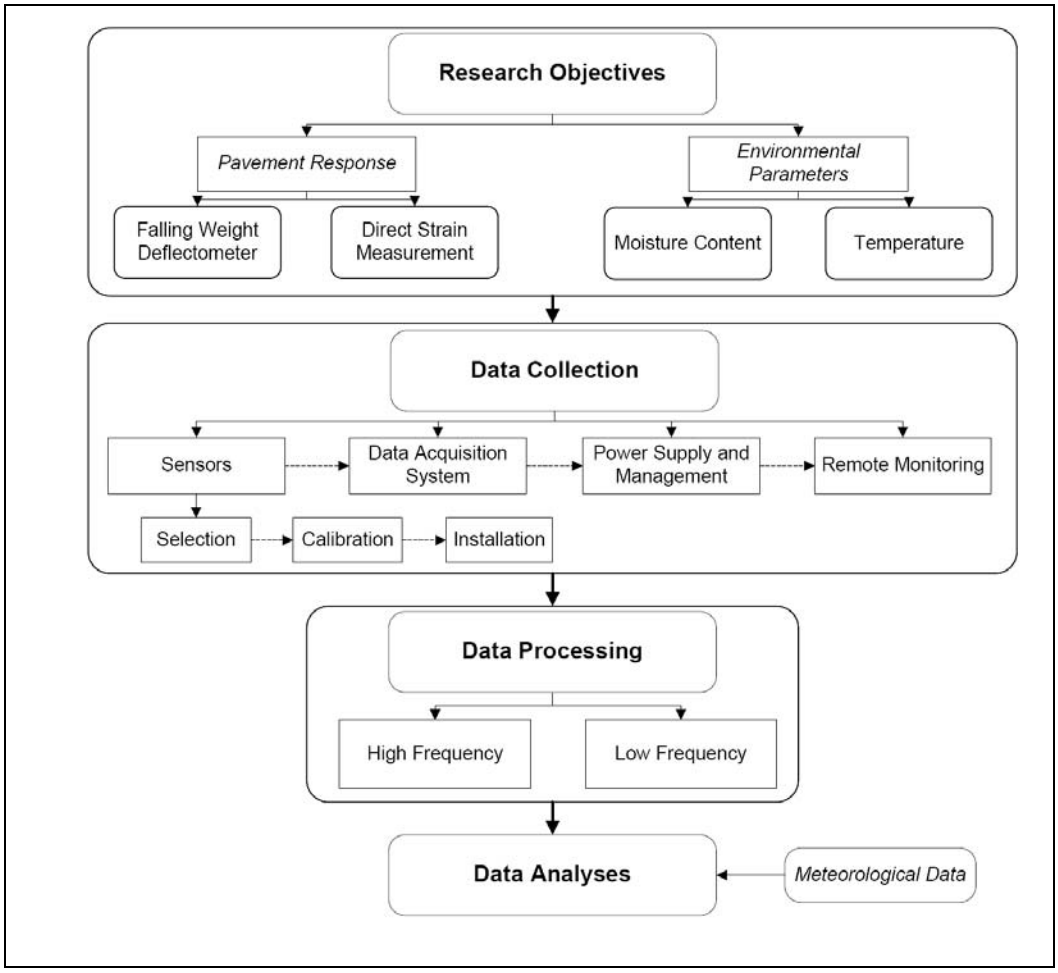

Figure 6-1: Research Process

For this study, the DAS had the ability to collect load sensor data at a high frequency and environmental sensor data at low frequency. For long-term field monitoring in remote locations, power supply and management play a critical role in the successful operation and collection of sensor data. To effectively and efficiently analyze large data sets, careful consideration must be given to data formats and to the selection of specialized software tools.

This paper provides an overview of the field test facility, and the data collection, processing, and analysis. Two years of environmental data that has freeze-thaw cycles is also presented and discussed.

6.3 Site Information

In this study, environmental parameters and flexible pavement field response was measured at the CPATT test track (709m long and eight meters wide) located in Waterloo, Ontario, Canada. The two lane CPATT test track has asphalt overlay consisting of binder Hot Laid 3 (HL3) plus a surface mix consisting of HL3, Polymer-Modified Asphalt (PMA), and Stone Mastic Asphalt (SMA) or Superpave. Figure 6-1 shows the location and arrangement of each surface mix.

The instrumented test track section consists of 223 mm and 185 mm of HL3 on the west and east lane respectively. The HL3 mix consists of 40 percent crushed gravel, 45% asphalt sand, 15% screenings, and 5.3% PG 58-28 asphalt cement. Below the HL3 are 200mm of Granular A base aggregate and 300mm of Granular B subbase aggregate. Compacted Granular A, 900mm in depth, is located below the subbase aggregate. Below the compacted Granular A is site subgrade that consists of compacted fill and well compacted clayey silt with some gravel. Granular A, as defined in the Ontario Provincial Standard Specification (OPSS) 1010, consists of crushed rock composed of hard, uncoated, fractured fragments, reduced from rock formations or boulders of uniform quality while Granular B consists of clean, hard, durable uncoated particles from deposits of gravel or sand (MTO 2003). Further details about the test track facility including its construction and pavement performance can be found in Tighe et al. (2003).

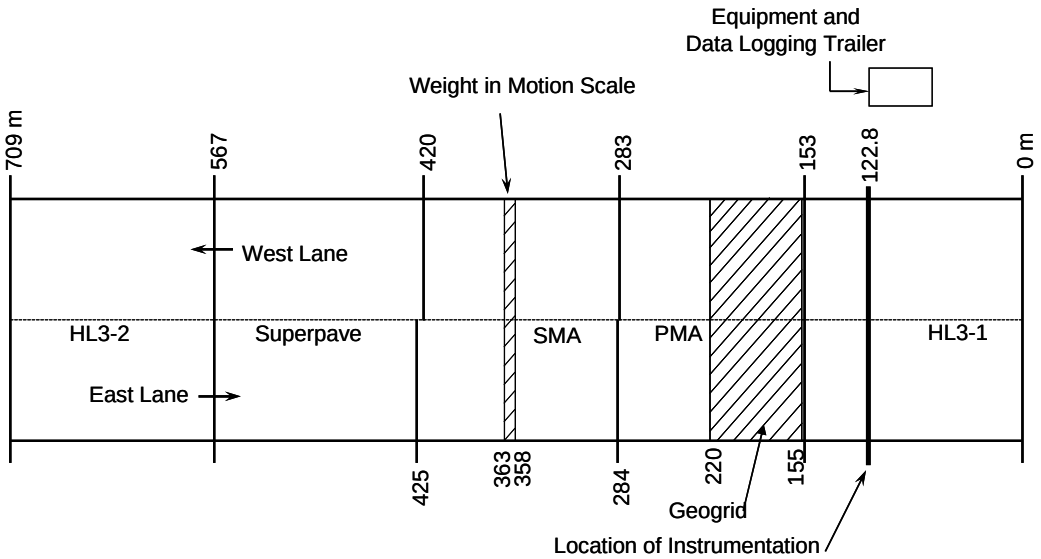

Figure 6-2: CPATT Test Track Facility Located at Waterloo Region

6.4 Data collection

6.4.1 Sensors

A state-of-the-art field instrumentation system was developed and installed to measure environmental conditions and pavement structural responses. Environmental measurements pertinent to this work included temperature of the asphalt, base, and subgrade materials, and moisture content of the base and subgrade layers. Time Domain Reflectometr (TDR 1 and TDR 2) probes and thermistors (T-1 to T-4) were installed, as shown in Figure 6-3, to measure moisture and ground temperatures, respectively.

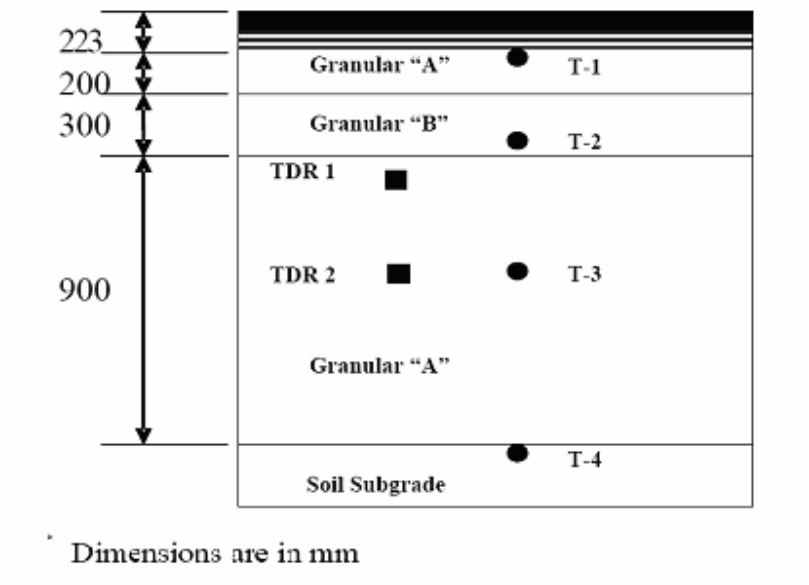

Figure 6-3: Pavement Profile and Environmental Sensor Distribution

Instrumentation also included asphalt strain gauges (ASG1 to ASG5), as shown in Figure 6-4, to measure asphalt longitudinal strain. The following sections, adopted from Adedapo (2007), provide details of the environmental and load sensors.

6.4.1.1 Time-Domain Reflectometry Probes (TDR)

To measure base and subbase daily and seasonal moisture content changes, two Campbell Scientific CS616 TDR probes (TDR1 and TDR2) were installed respectively 800 and 1150mm below the west lane asphalt surface. The TDR probes were selected due to their performance, survivability, cost, and ability to integrate with available existing data acquisition loggers. The TDR probes consisted of two parallel conducting rods, 300mm in length, with a separation distance of 32mm. All sensors were calibrated prior to installation using site Granular A and B aggregates.

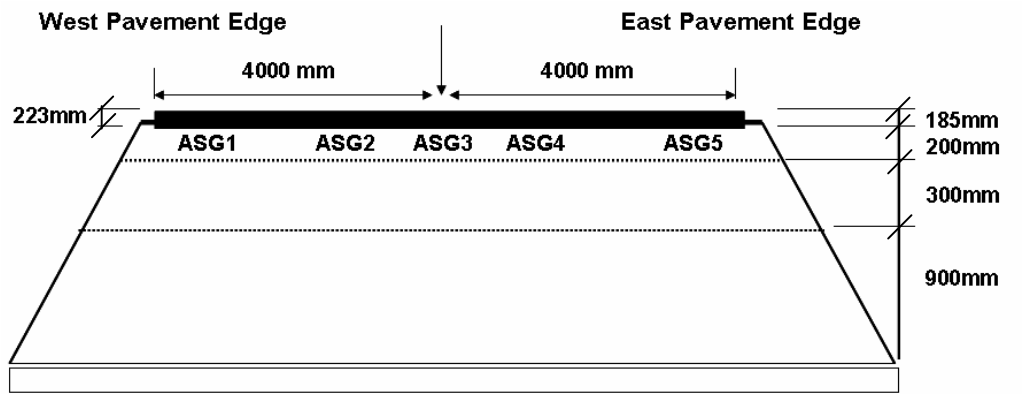

Figure 6-4: Asphalt Strain Gauge Distribution

6.4.1.2 Temperature Probes

Four Campbell Scientific T107B thermistors (T-1 to T-4) were installed 223, 530, 1134, and 1734mm below the west lane asphalt surface. Campbell Scientific reports the thermistors precision to be ± 0.1 °C between -35° to 50°C.

6.4.1.3 Asphalt Strain Gauges (ASG)

To measure asphalt longitudinal strains at the base of the asphalt layer, five ASG-152 H-type asphalt strain gauges, manufactured by Construction Technology Laboratories (CTL) Group Inc., were installed. These gauges were chosen due to their reliability, durability, low cost, short delivery time, and excellent performance at other test sites. Prior to installation, each gauge's calibration and functionality was checked in the laboratory. As shown in Figure 6-4, ASG3 was placed on the road centerline, while ASG1 and ASG2 were placed 690 and 2700mm from the west pavement edge respectively. ASG5 and ASG 4 were placed 1380 and 3200mm from the east pavement edge respectively. To ensure that the asphalt strain gauges were bound to the

asphalt base course, all asphalt strain gauges were placed in a sand-asphalt binder mixture consisting of sand and PG 64-22 binder.

6.4.2 Data Acquisition Systems (DAS)

A Campbell Scientific CRX10 data logger was used to monitor the thermistors and TDR probes using a sampling rate of 0.0033Hz (1 reading every 5 minutes). This sampling rate was deemed sufficient to record daily sensor changes.

Asphalt strain gauge data was collected using a Somat eDAQ-plus® data logger with the sampling rate set at 0.01 Hz (1 reading every 1.67 minutes) in idle mode and 1500 Hz when triggered by a traffic load. The high sampling rate was used to capture the millisecond traffic load moving over the sensors. The low sampling rate was used to record sensor readings due to environmental changes. The CPATT test track is unique due to its ability to record sensor data at low and high frequency. The compact, rugged, and modular Somat eDAQ system has the capability to collect a wide range of signal types directly from sensors (i.e., strain, analog to ±80V, digital, frequency, and temperature). The eDAQ system used in this study had the following layers: Base Processor, High Level, and Simultaneous High Level. The Base Processor has a 266 MHz processor with integrated floating point, master sample clock speed of 100 kHz, 256MB of on board DRAM, and 2GB memory for onboard data storage. The High Level Layer consists of 16 multiplexed singled-ended channels with a 16 bit A/D converter with a channel-to channel skew of approximately 25μsec with a maximum sampling rate of 2500Hz. An onboard excitation source provides ±10V with 30mA output for sensor conditioning. The Simultaneous High Level layer has 16 general-purpose analog inputs channels. Each input was independently set to measure down to 3.8μV resolution or have a full-scale input range of ±80 volts. Each

channel has its own 16-bit analog-to-digital converter (ADC) running at a frame check sequence (FCS) master sample clock rate of 100 kHz. The ADCs output was down-sampled to the user-selected rate between 0.1 to 100,000 samples per second. The settings for full-scale range, sample rate, digital filtering, and transducer power voltage level was fully independent for each channel. Each of the 16 channels collected data using different sample rates, digital filters, and transducer power levels. Transducer power was set from +3V to +28V in one volt increments with an accuracy of ±50mV. Each channel was power-limited to 400mW. Multiple transducer power outputs were combined to drive a transducer. Each channel has an input impedance of 10MΩ for ranges up to ±10V and 100kΩ for ranges greater then ±10V. Common mode input voltages of up to ±80V were provided with 100kΩ input impedance. Small conditioning modulus, called Smart Modulus, was used to condition strain gauge and thermocouple inputs. Ethernet 100BaseT and RS232 serial communication provides the PC-to-eDAQ communication. Test Control software (TCE), a Windows ^{TM} based software application, was used to set up and define test requirements in the eDAQ. This included: creation of the test setup files that define and calibrate transducer channels; creation of data modes and computed channels for online data calculations and analyses; specification of triggering conditions for collection of sensor data; sensor monitoring via run-time displays; and initialization, starting, stopping, and uploading of sensor stored data.

6.4.3 Power Supply and Management

For long-term field monitoring in remote locations, power supply and management play a crucial role for the operation and collection of sensor data. For this project, power was supplied using two 12V deep cycle batteries that were recharged using a solar panel (Figure 6-5).

Figure 6-5: Solar Panel for Recharging Batteries at Test Site (Adedapo 2007)

To conserve battery power during the winter time - when the duration of solar recharge was limited - a programmable timer was used to automatically turn the system off and on at predefined times. A power regulator was also used to prevent batteries from overcharging and discharging, and to prevent power flow from the batteries to the solar panel. Safety disconnect switches were installed so that the system power could be turned off without the need to disconnect wires. This power system was found to work well, be robust, and a cost effective method to power the sensors, Somat eDAQ-plus®, and Campbell Scientific CRX10.

6.4.4 Remote Monitoring System

A unique remote monitoring system was developed to allow the monitoring of the eDAQ field computer and the downloading of the sensor data over a secure internet connection. Figure 6-6 shows the secure remote monitoring system used at the site.

This remote monitoring system allowed for daily data upload and the ability to check sensor functionality without the need to travel to the site. During one data check, several asphalt strain gauges were found not to be functioning. After a site visit it was found that sensors wires had been accidentally cut during grass mowing. All wires were promptly fixed resulting in only a short period of limited data collection. The Campbell Scientific CRX10 data was downloaded manually on a weekly basis.

6.4.5 Pavement Response Surveys

Falling Weight Deflectometer (FWD) pavement surveys were performed by Applied Research Associates Inc. along the test track at 20m intervals Details on the pavement condition and performance were reported by Popik and Tighe (2006). FWD test results for each survey station include back calculated subgrade resilient modulus.

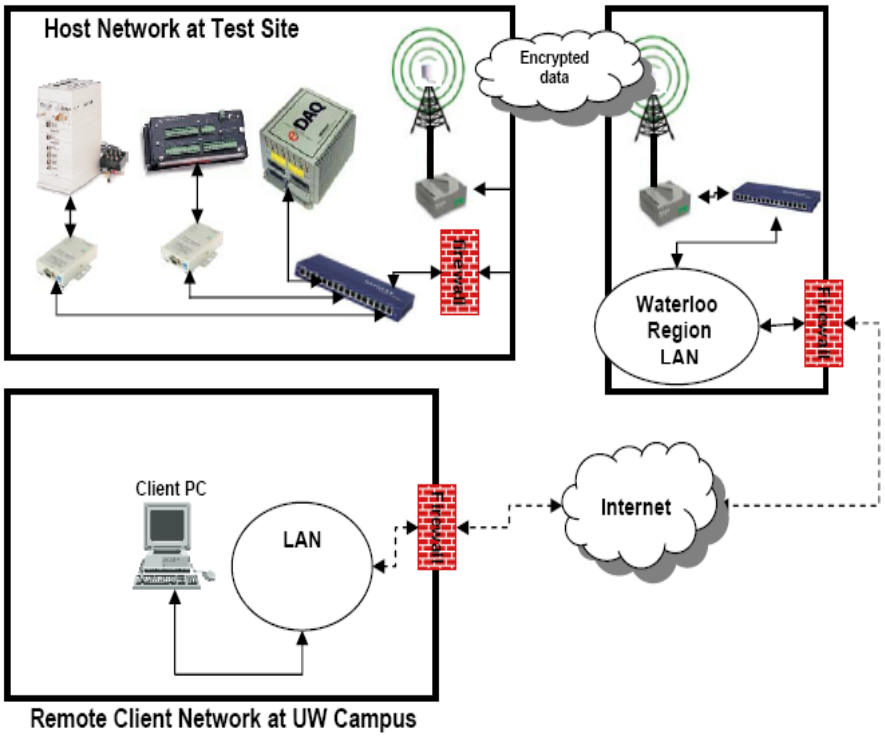

Figure 6-6: Schematic of Developed Secured Remote Monitoring System (Adedapo 2007)

6.5 Data Processing

Field monitoring programs require the ability to store and to efficiently process large volumes of data. For this study, approximately 5 gigabytes/year of field data was collected. Somat InField and MS Excel programs were used to process and display the results of the load and environmental sensors.

Asphalt strain gauge data were processed with SoMat InField, a versatile, powerful software application optimized for use with the eDAQ data acquisition system. Infield allows sensor data to be read from the eDAQ file (.SIF) and displayed graphically. It also contains different data processing functions that allow for easy data combining and exporting of approximately 87,500

data files that represent 8 million data points to MS Excel. MS Excel macros were used to extract and process sensor data.

Campbell Scientific CRX10, TDR, and thermistors data files (.DAT) were imported into MS Excel for data processing. A database that has 210,240 data points was constructed, and MS Excel macros were developed to extract and process the data.

6.6 Data Analysis

6.6.1 Ground and Ambient Air Temperature Variation

Figure 6-7 to Figure 6-10 show ground and ambient air temperature variation for the period from April 2004 to May 2005. Ambient air temperature data was obtained from the University of Waterloo weather station, located approximately five kilometers north east of the CPATT test site. The March 2005 data gap, shown in Figure 6-7 to Figure 6-10, corresponds to a period of 13 days when the Campbell Scientific CRX10 data logger was removed from the site.

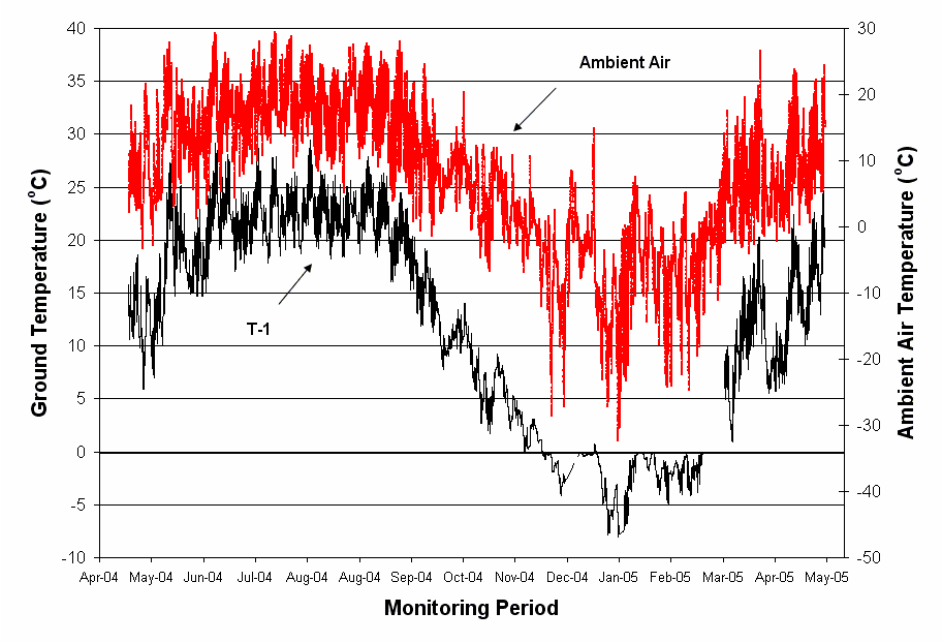

Figure 6-7: 2004-2005 T-1 Temperature Readings

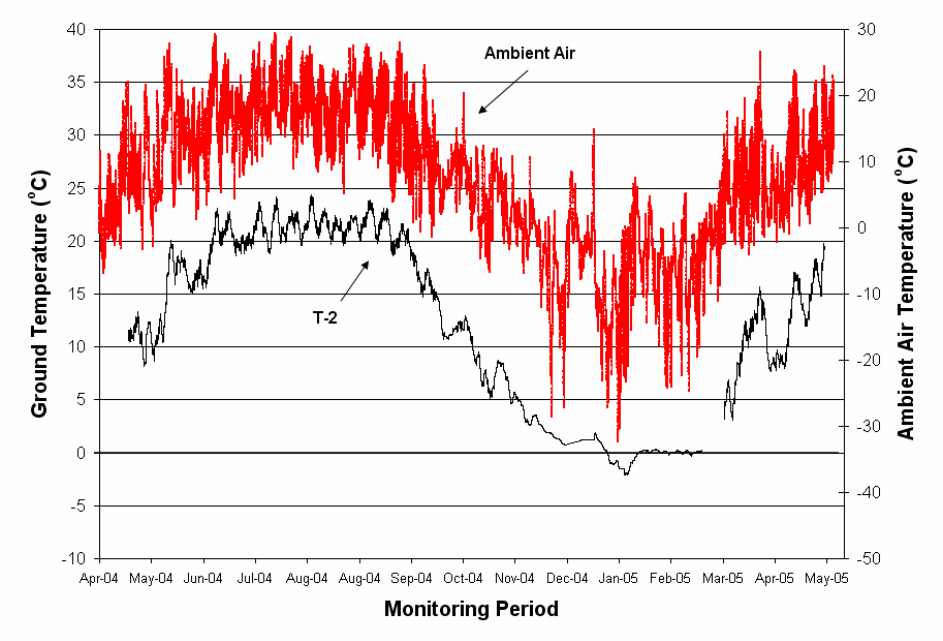

Figure 6-8: 2004-2005 T-2 Temperature Readings

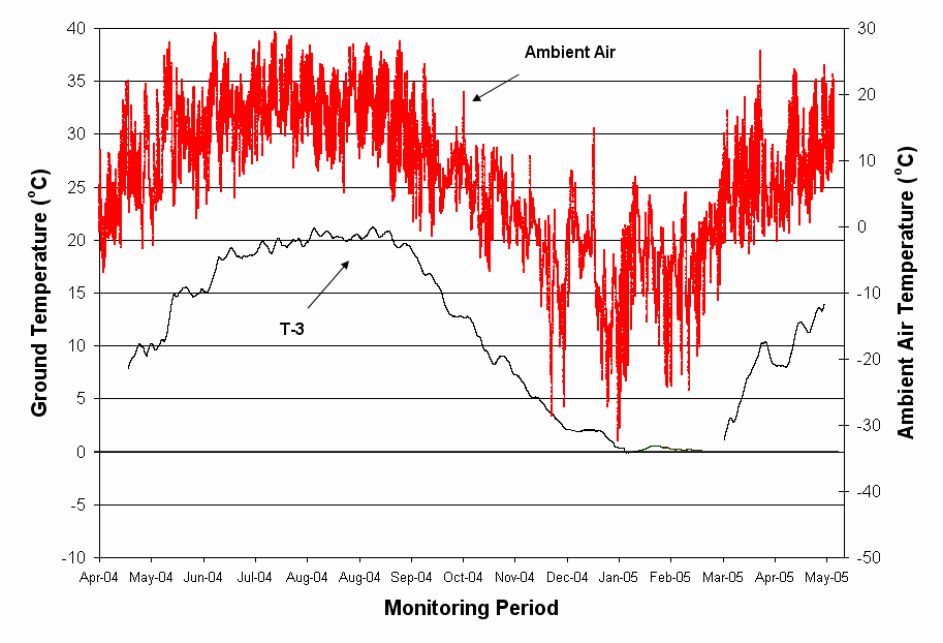

Figure 6-9: 2004-2005 T-3 Temperature Readings

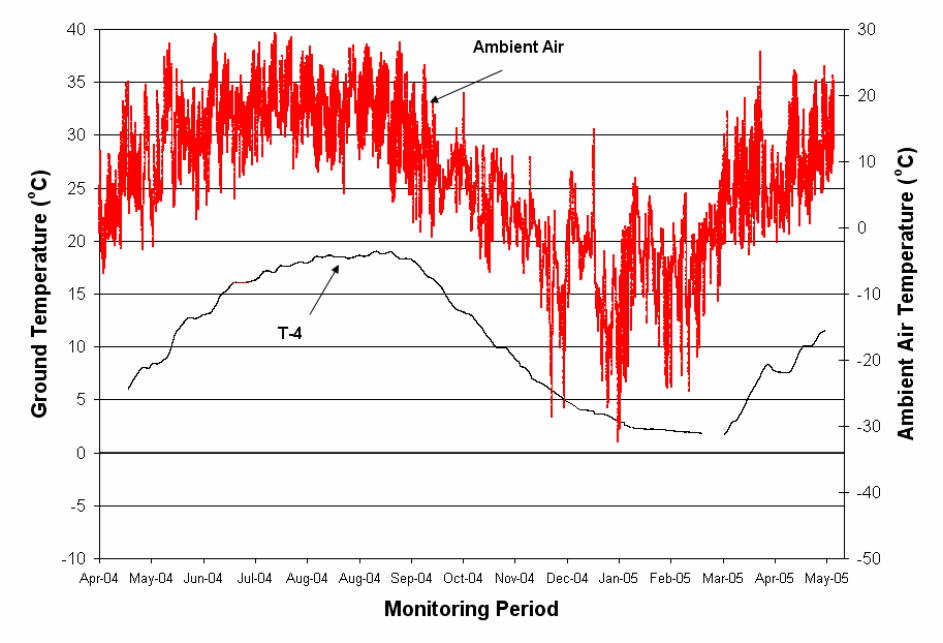

Figure 6-10: 2004-2005 T-4 Temperature Readings

All temperature probes show a sinusoidal response with decreasing temperature variation and sensitivity with depth. For example, temperature probe T-1, located 223mm below the asphalt layer, has a temperature variation of 38°C with daily temperature fluctuations of 10 to 20°C while T-4 shows a temperature variation of 17 °C with daily temperature fluctuations of 1°C. Figure 6-7 shows that T-1 recorded freezing ground conditions from November to the end of March while Figure 6-8 and Figure 6-9 indicate freezing or near freezing ground conditions starting in late December to early January respectively. Figure 6-10 indicates no ground freezing occurred at 1734mm. Thus, the frost depth was between 1134 and 1734mm below the asphalt surface.

6.6.2 Average Daily Temperature

Figure 6-11 shows the average daily temperature with depth below the asphalt surface and the average ambient air temperature from April 2004 to March 2005. This figure shows that all average daily temperatures have a response similar to the average ambient air temperature, and that the average ambient air temperature was always lower than the average ground temperature for T-1, T-2, and T-3. It also shows that during the warming period from April 2004 until September 2004 the average daily temperature decreases with depth. Therefore, the ground has a temperature gradient. In September 2004, the average daily temperature was constant resulting in a negligible temperature gradient (all temperature probes had average value of 17.5 ^{o}C). After September 2004, the average ground temperature was found to increase with depth. Thus, the ground has a reversed temperature gradient compared to the period prior to September 2004. This reversed temperature gradient continues until March 2005, when the average daily temperature becomes constant (all temperature probes had average value of 4 ^{o}C).

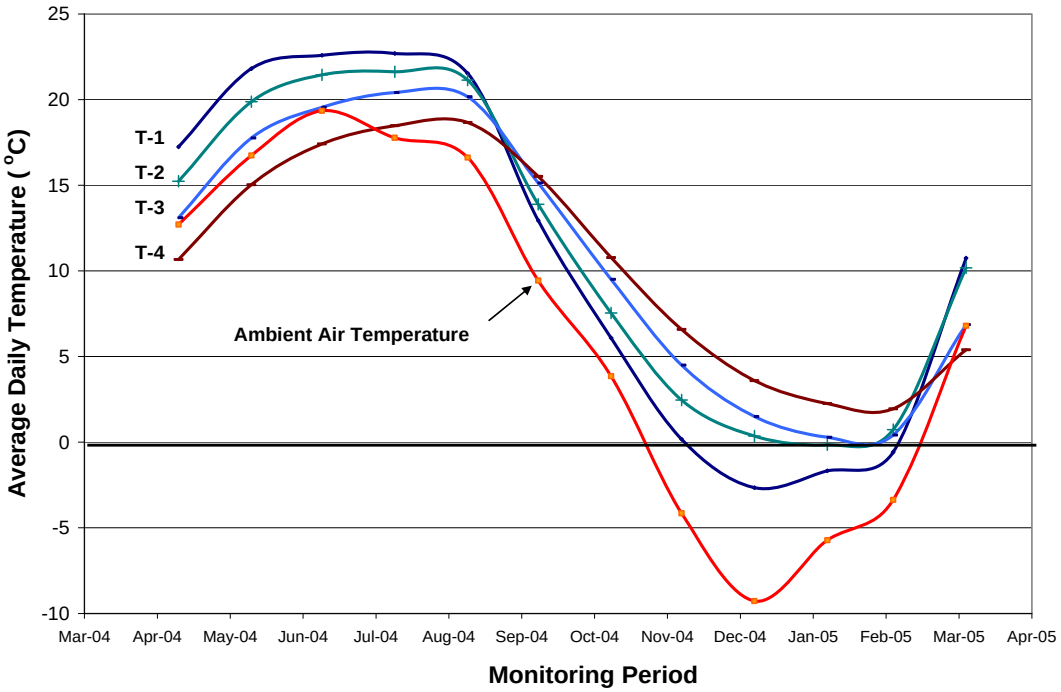

Figure 6-11: 2004-2005 Average Daily Ambient Air Temperature and Average Daily Ground Temperature below the Asphalt

6.6.3 Moisture Content Variation over Monitoring Period

Figure 6-12 shows TDR1 (upper) and TDR2 (lower) seasonal moisture content changes from March 2004 to February 2006. The small data gap, in March 2005, corresponds to a period of 13 days when the Campbell Scientific CRX10 data logger was removed from the site.

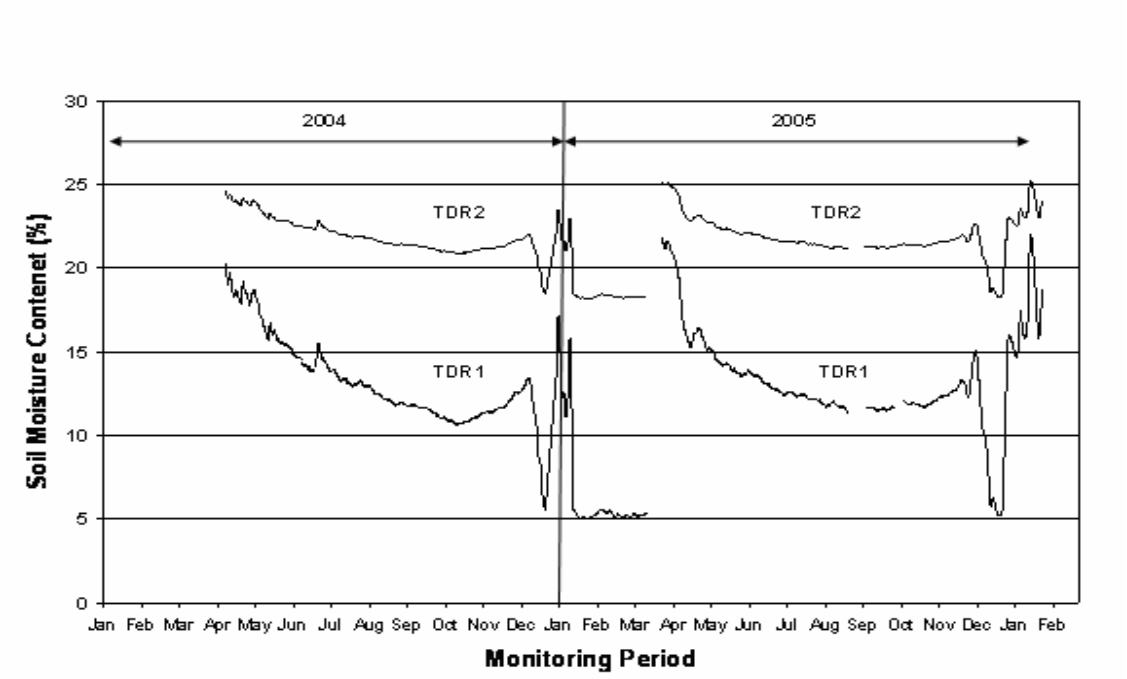

Figure 6-12: 2004-2005 TDR1 and TDR2 Soil Moisture Content Readings

Both TDR probes showed the following response:

- Maximum soil moisture occurred during March to April.
- Soil moisture decreased from April to October.
- Soil moisture increased from October to November/December.
- Soil moisture showed a period of high and low moisture content when the ground freezes and thaws during the winter months (November to February).

During the monitoring period, TDR1 indicated soil moisture content between 5 to 22 percent while TDR2 had soil moisture content between 17 to 25 percent.

6.6.4 Moisture and Pavement Performance Variation with Time

Figure 6-13 shows soil moisture content and FWD peak deflections from April 2004 to February 2005.

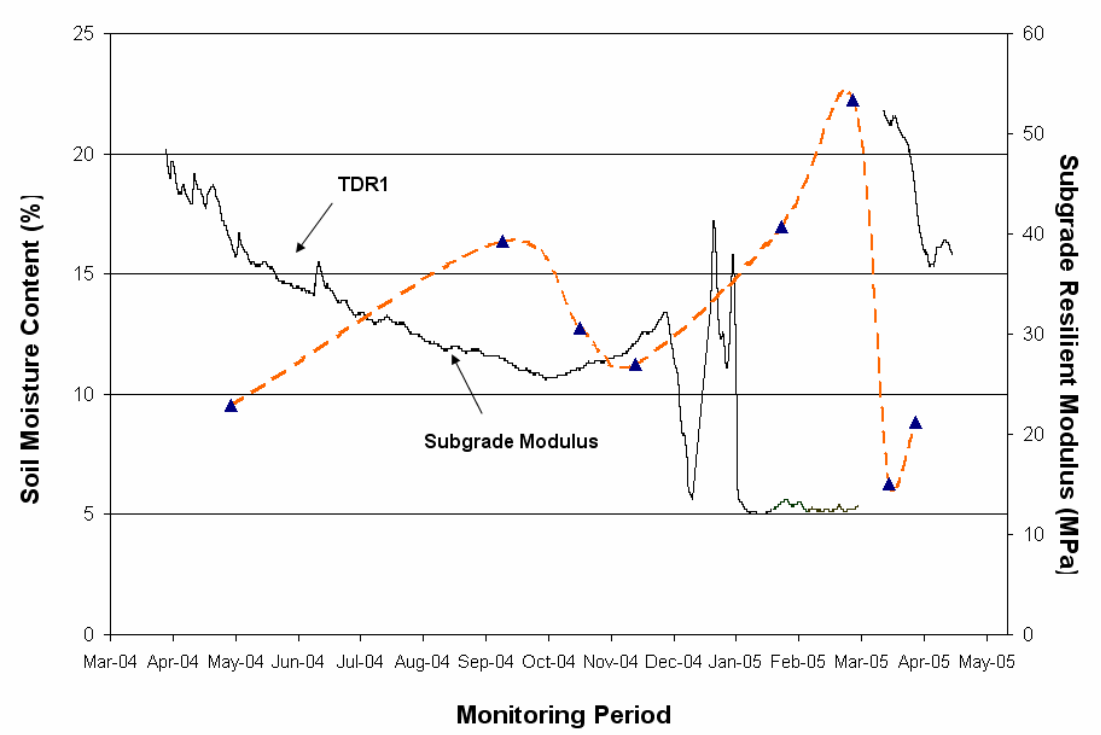

Figure 6-13: Subgrade Resilient Modulus and Soil Moisture Content Readings

The above figure shows an inverse correlation between resilient modulus and moisture content (i.e., the highest modulus occurs during winter months when the ground is frozen and lowest occurring during the spring ground thaw). Salem (2004) also reported an inverse correlation between resilient modulus and soil moisture content. Using a nonlinear regression analysis, Equation 6-1, with an R^2 of 0.91, was found to fit the data.

$$M_R = 211.17e^{-0.0694 \cdot \omega} \qquad (6\text{-}1)$$

where M_R is the subgrade resilient modulus (MPa), *e* is natural logarithm, and ω is soil moisture content in percentage.

6.6.5 Thermal Induced Strain

Figure 6-14 shows the measured asphalt longitudinal strain and ambient air temperature for ASG5 from August 21 to October 10, 2004.

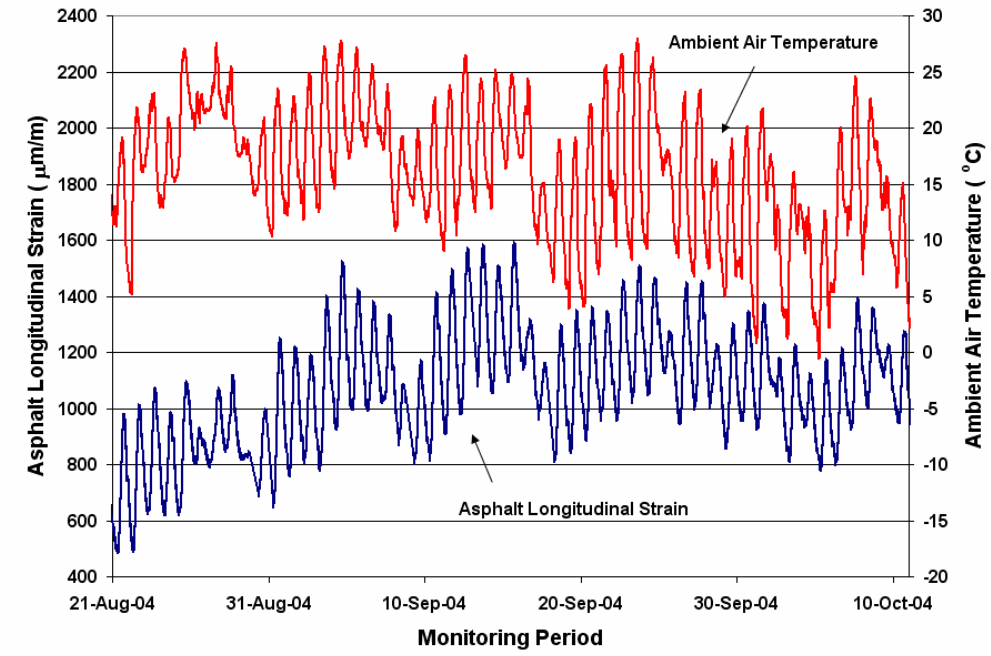

Figure 6-14: August 21 to October 10, 2004 Ambient Air Temperature and ASG5 Asphalt Longitudinal Strain Readings

This figure shows that the asphalt longitudinal strain varied with daily temperature changes to a maximum magnitude of approximately 500μm/m. Al-Qadi (2005) also reported similar asphalt longitudinal strain observation with a maximum magnitude of 350 μm/m. Figure 6-15 shows asphalt longitudinal strain daily fluctuation from January 2004 to January 2005.

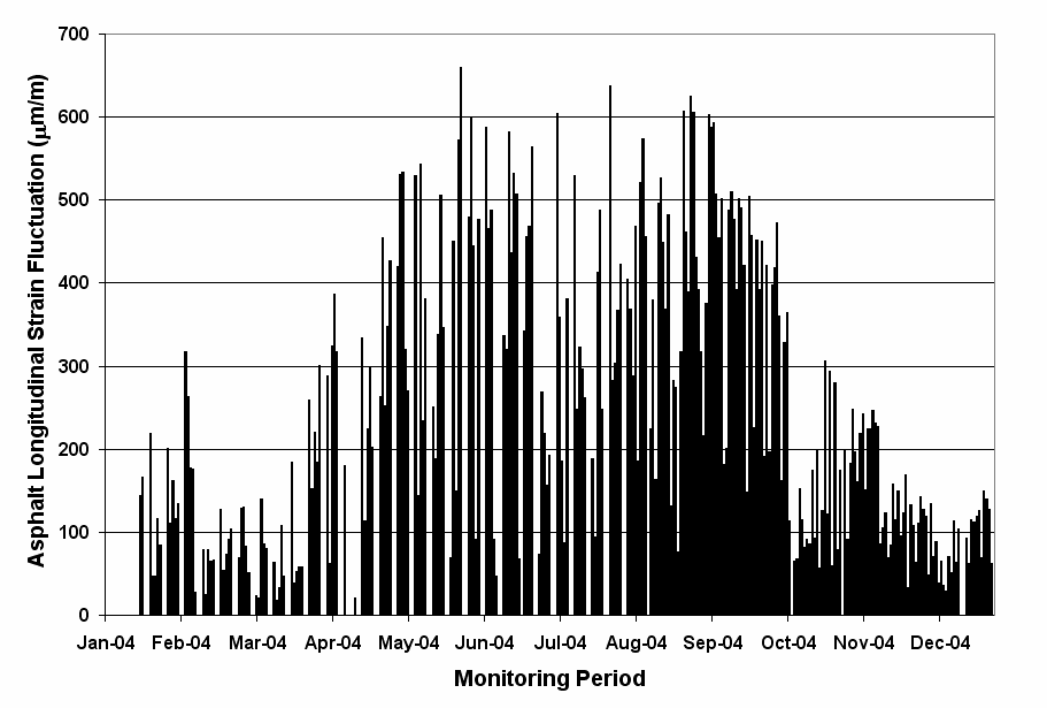

Figure 6-15: 2004 Thermal Induced ASG5 Asphalt Longitudinal Strain Fluctuations

This figure shows that daily strain fluctuations between 600 and 650μm/m can occur due to daily temperature changes. All strain gauges showed a similar trend. Largest daily strain fluctuations were observed from April to October 2004 which is the spring and summer seasons. Al-Qadi (2005) reported that the largest strain fluctuation occurred during the spring season.

6.7 Conclusions

This paper provides an overview of the CPATT test facility, the environmental sensor instrumentation program, and the data acquisition system. The CPATT facility is unique as it is located in a climate that is subject to seasonal freeze-thaw cycles. The data acquisition system is similarly unique as it allows remote monitoring and collecting of environmental and pavement

response data at a low and high frequency. Details of the data collection, data processing, and data analysis are also presented.

Based on two years of environmental and pavement response data obtained from the site the following conclusions are drawn.

- For long-term field studies, careful consideration must be given to the development of efficient and effective data collection, data processing, and data analysis so that the research objectives are achieved. This is especially important when large volumes of data are collected daily.
- Somat eDAQ-plus® data logger and TCE software are ideal for programming sensors and long-term sensor data monitoring and collection at high and low frequencies. Somat Infield software also allowed for rapid and easy processing and exporting of the large data files. This saved numerous hours and days of data processing and analysis.
- Temperature data showed that the pavement structure is frozen to a depth between 1134 and 1734mm below the asphalt surface. It also showed that the pavement went through several freeze-thaw cycles during the winter months.
- TDR probes showed a period of low and high moisture contents when the ground freezes and thaws during the winter months.
- Subgrade resilient modulus and soil moisture content have a strong correlation with an R^2 of 0.91.
- Daily asphalt longitudinal strain fluctuations are found to be correlated with daily temperature changes and asphalt longitudinal strain fluctuations as high as 650μm/m were recorded. The maximum daily strain fluctuations in this study were significantly higher than the 350 μm/m reported in Al-Qadi (2005).

6.8 Acknowledgement

The authors acknowledge the Natural Sciences and Engineering Research Council of Canada (NSERC), Canada Foundation for Innovation (CFI), Ontario Innovation Trust (OIT), Ontario Research and Development Challenge Fund (ORDCF), along with the Center for Pavement and Transportation Technologies (CPATT) private and public sector partners for providing research funding. The authors also acknowledge the University of Waterloo technical staff, Ken Bowman, Terry Ridgway, and Doug Hirst, for their guidance, help, and assistance with the field instrumentation.

Chapter 7: Observed Seasonal Variation of Environmental Factors and Their Impact on Flexible Pavement Performance Subject to Annual Freeze/ Thaw

7.1 Overview

This paper presents the results obtained over two years of field monitoring of environmental parameters and pavement performance using a state-of-the-art field monitoring system installed in the Center for Pavement and Transportation Technology (CPATT) test track located in Waterloo, Ontario, Canada. The objective of the study was to quantify the seasonal variation of environmental factors and pavement performance in a climate subject to freeze/thaw events. Site data collected included soil moisture content, pavement temperature, Falling Weight Deflectometer (FWD) subgrade resilient modulus, and meteorological data (rainfall and air temperature). Soil moisture content and subgrade resilient modulus changes in the pavement structure can be divided into three distinct Seasonal Zones. Seasonal Zone I consists of a decreasing soil moisture content trend, Seasonal Zone II consists of an increasing soil moisture trend, and Seasonal Zone III consists of frozen ground conditions.

7.2 Introduction

Transportation agencies are currently considering the implementation of Mechanistic-Empirical (M-E) method for pavement design. This methodology requires input of traffic and environmental data to predict the pavement response and performance (NCHRP 2004) .

The M-E Design Guide uses an Enhanced Integrated Climatic Model (EICM) to estimate unbound material resilient modulus. The EICM model records user-supplied resilient modulus for all unbound layer materials at an initial or reference condition. Using climatic data, the EICM evaluates changes in moisture content from an initial or a reference condition. Changes in soil moisture content are then used to modify the initial user-supplied resilient modulus. It also considers the effects of freezing, thawing and recovery on the reference resilient modulus. The M-E design method uses changes in subgrade resilient modulus over time to predict pavement response parameters and damage at various points within the pavement system.

Long-term field monitoring programs have been used to investigate seasonal variations of environmental parameters and their effects on pavement response and performance (Salem 2004; Zuo 2003). To date field studies have been completed in relatively mild climatic conditions (Watson and Rajapakse 2000). Limited published environmental data exists for pavements subject to seasonal freeze-thaw events, typical of the southern Canadian climatic conditions, to validate or calibrate the M-E design method.

In this study, environmental factors and pavement performance were monitored over a two- year period using a state-of-the-art field monitoring system installed at the Centre for Pavement and Transportation Technology (CPATT) test track located in Waterloo, Ontario, Canada. Site data collected included soil moisture content, pavement temperature, Falling Weight Deflectometer

(FWD) subgrade resilient modulus, and meteorological data (rainfall and air temperature). The goal of this study was to quantify the seasonal variation of environmental factors and pavement performance in a climate subject to freeze/ thaw events. This will be accomplished by (1) investigating seasonal changes in soil moisture content and pavement temperature; (2) determining correlations between meteorological data and measured changes in environmental factors; and (3) evaluating pavement performance due to changes in environmental factors. The use of the presented data for evaluation of M-E design approach will also be discussed.

7.3 CPATT Test Track

In this study, environmental parameters and flexible pavement field response was measured at the CPATT test track (709m long and eight meters wide) located in Waterloo, Ontario, Canada. The instrumented test track section consists of 223 mm of Hot-Laid 3 (HL3) mix, consisting of 40 percent crushed gravel, 45% asphalt sand, 15% screenings, and 5.3% PG 58-28 asphalt cement. Below the HL3 are 200mm of Granular A base aggregate and 300mm of Granular B subbase aggregate. Compacted Granular A, 900mm in depth, is located below the subbase aggregate. Below the compacted Granular A is site subgrade that consists of compacted fill and well compacted clayey silt with some gravel. Granular A, as defined in the Ontario Provincial Standard Specification (OPSS) 1010, consists of crushed rock composed of hard, uncoated, fractured fragments, reduced from rock formations or boulders of uniform quality while Granular B consists of clean, hard, durable uncoated particles from deposits of gravel or sand (MTO 2003).

Based on historical weather data from the University of Waterloo weather station, the average monthly temperature at the site typically varies from -10°C during the winter months to 26 °C during the summer months.

7.4 Data Collection System

This section provides details on the state-of-the-art field instrumentation system implemented at CPATT test track, meteorological data collected from the University of Waterloo weather station, and FWD pavement surveys performed at the instrumented section.

7.4.1 Pavement Instrumentation

A state-of-the-art field instrumentation system was developed and installed to measure temperature of the asphalt, base, and subgrade materials, and soil moisture content in the granular base and subgrade materials. Pavement temperatures were measured and recorded using a Campbell CRX10 data logger with four Campbell Scientific T107B thermistors (T-1 to T-4) installed 223, 530, 1134, and 1734mm below the asphalt surface respectively. Soil moisture was measured and recorded using two Campbell Scientific CS616 Time Domain Reflectometer probes (TDR 1 and TDR 2) installed 800 and 1150mm below the asphalt surface respectively connected to Campbell CRX10 data logger. Figure 7-1 shows the distribution of the thermistors and the TDR probes in the instrumented section. Probe data was collected at a rate of 1 reading every 5 minutes (0.0033Hz). This sampling rate was deemed sufficient to record daily changes in probe readings.

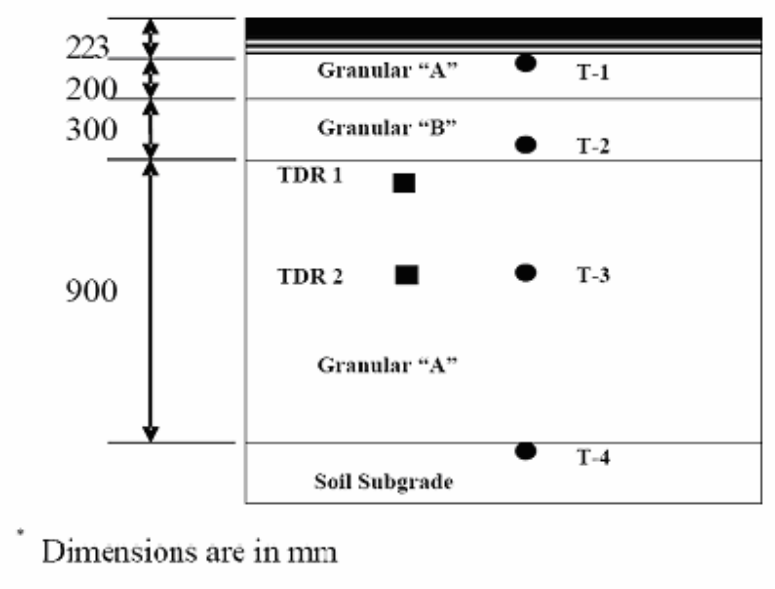

Figure 7-1: Pavement Profile and Sensors Location

Power was supplied to the data logger and probes using two 12V deep cycle batteries that were recharged using a solar panel. To conserve battery power during the winter time - when the duration of solar recharge was limited - a programmable timer was used to automatically turn the system off and on at predefined intervals. A power regulator was also used to prevent batteries from overcharging and discharging, and to prevent power flow from the batteries to the solar panel.

Campbell Scientific CRX10, TDR, and thermistors data files (.DAT) were imported into a data base consisting of 210,240 data points.

Further details about the field monitoring program can be found in Adedapo (2007).

7.4.2 Meteorological Data

For this study precipitation and air temperature data were obtained from the University of Waterloo weather station, located approximately five kilometers North East of the instrumented test site. Data obtained from this weather station was deemed to be representative of the conditions at the instrumented test site.

7.4.3 Pavement Performance Surveys

FWD pavement surveys were performed on the instrumented test section by Applied Research Associate Inc. to record changes in pavement performance during the two year monitoring period. Test results provided by Applied Research Associate Inc. include pavement deflection and the back-calculated subgrade resilient modulus.

7.5 Moisture Content Variation during Monitoring Period

Figure 7-2 shows TDR1 (upper) and TDR2 (lower) moisture content changes from March 2004 to February 2006. The data gap in March 2005 corresponds to a period of 13 days when the data logger was removed from the site. Figure 7-2 illustrates that the two TDR probes showed similar response during the 2004-2005 and 2005-2006 monitoring period. The trends observed during the monitoring period are noted below:

- The March to April period has the highest recorded soil moisture content.
- The April to October period has a decreasing trend in soil moisture content
- The October to November/December period has an increasing trend in soil moisture content.

- The November to February period (winter months) has rapid and sudden fluctuations in soil moisture content

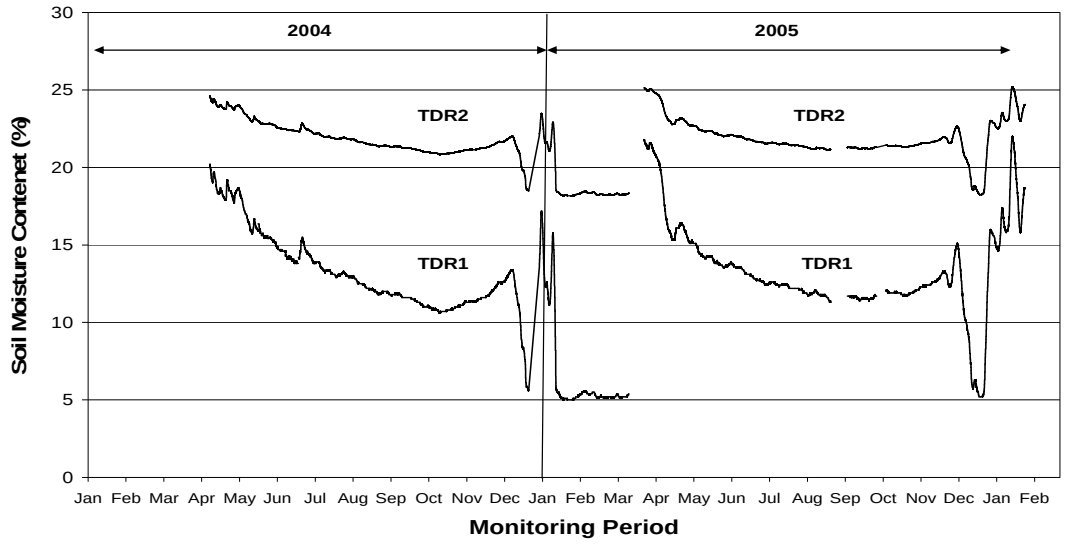

Figure 7-2 : 2004-2005 TDR1 Moisture Content

7.6 Pavement Temperature Variation over Monitoring Period

Figure 7-3 shows pavement temperatures probes T-1, T-2, T-3 and T-4 variation from April 2004 to May 2005. This figure shows that all the temperature probes have a sinusoidal response. It also shows that the daily and seasonal pavement temperature fluctuation decreases with depth below the asphalt surface. For example, temperature probe T-1, located 22.3cm below the asphalt layer, recorded a seasonal temperature variation of 38°C with daily temperature fluctuations in the order of 10 to 20°C, while T-4 showed a seasonal temperature variation of 17 °C with daily temperature fluctuations in the order of 1°C.

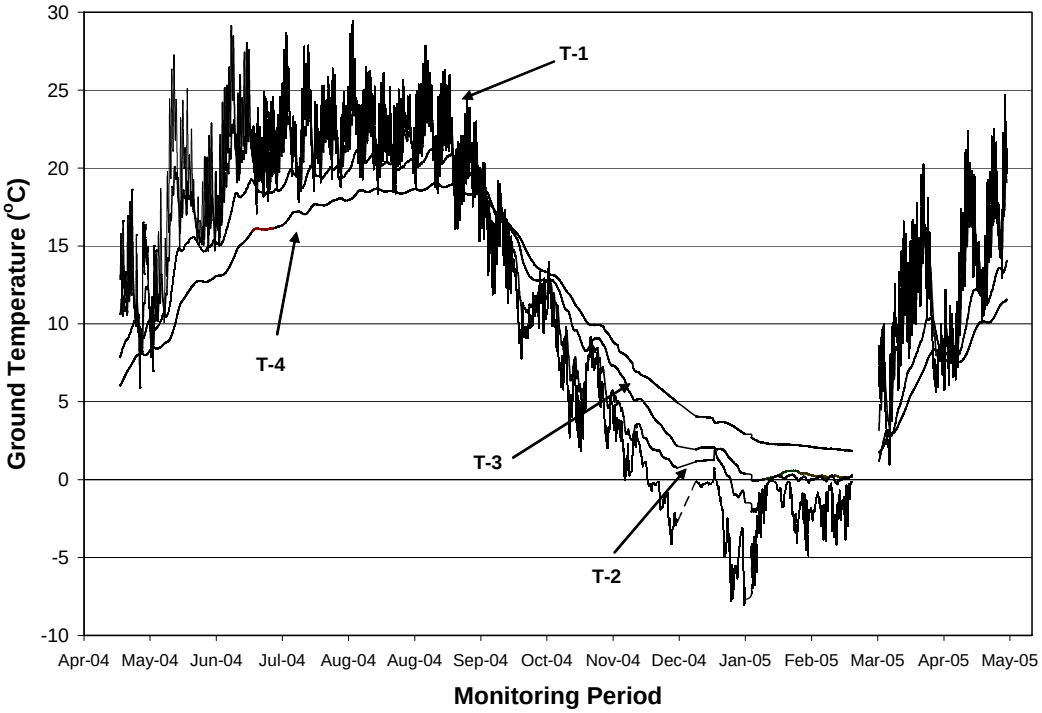

Figure 7-3: Temperature Variation at T-1, T-2, T-3, and T-4

Thermistor T-1, located 223 mm below the asphalt surface, indicates that freezing ground conditions (temperature below 0^{o}C) occur from November 2004 to the end of March 2005. Thermistors T-2 and T-3, located 530 and 1134mm below the asphalt surface, indicate that freezing ground conditions occur from December 2004/January 2005 to the end of March 2005. Thermistor T-4, located 1734mm below the asphalt surface, indicates that no freezing ground conditions occur over the monitoring period. For the site, the freezing depth is between 1134 and 1734mm below the asphalt surface. This correlates with the findings of the Ontario Ministry of Transportation and Communications (now Ontario Ministry of Transportation) which initiated a five year program aimed at measuring frost penetration in different subgrade soils throughout

Ontario. The depth of frost measured on Highway 7 in Guelph, Ontario, Canada between 1970 and 1975 ranged between 1.22m and 1.57m (Chisholm and Phang 1983).

The Guelph site is the closest instrumented site to the CPATT test facility. The CPATT measured frost penetration depth is in agreement with the frost depth reported in the Ontario Ministry of Transportation and Communications study.

7.6.1 Average Monthly Temperature Distribution

Average monthly changes in pavement temperature from April 2004 to March 2005 are plotted in Figure 7-4 and Figure 7-5. The temperature at depth zero is the average monthly air temperature while the thermistor temperatures (T-1 to T-4) are from below the asphalt surface. Figure 7-4 and Figure 7-5 show that the average monthly temperature at the base of the asphalt (T-1) is always greater than the average monthly air temperature. From April to September 2004 (Figure 7-4), the base and subbase temperature generally decreases linearly with depth at approximately 0.037°C/cm. From October 2004 to March 2005 (Figure 7-5), the base and subbase temperature generally increases linearly with depth at approximately 0.035°C/cm. Figure 7-5 shows that the pavement temperature, up to a depth of 120 cm, was at or below zero degree Celsius from December 2004 to March 2005.

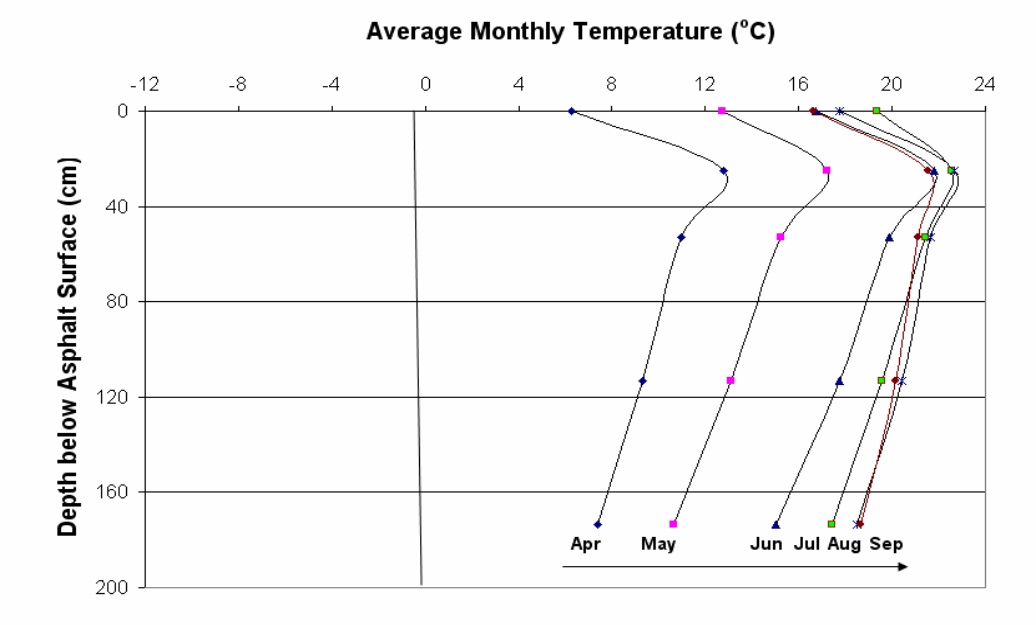

Figure 7-4: Monthly Temperature Distributions at Different Depth below Asphalt Surface – April to September

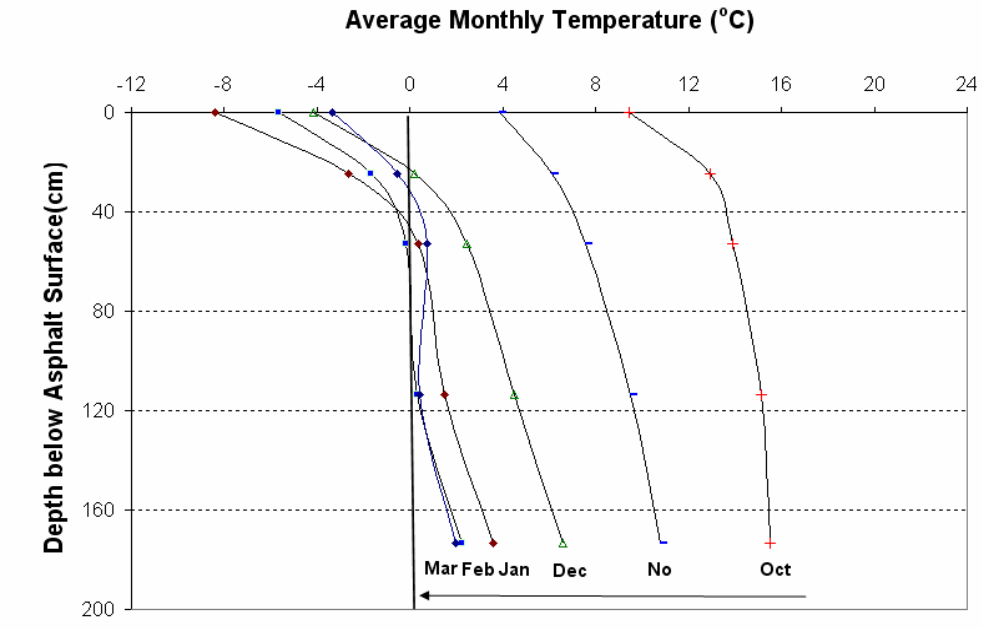

Figure 7-5: Monthly Temperature Distributions at Different Depth below Asphalt – October to March

7.7 Seasonal Zones

Soil moisture changes were subdivided into three Seasonal Zones shown in Figure 7-6.

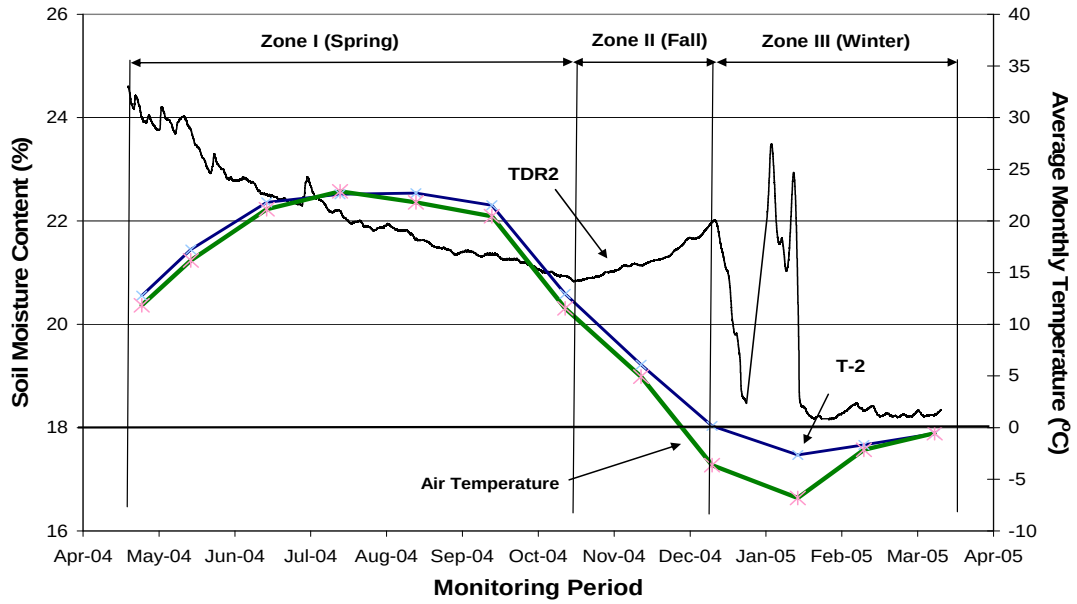

Figure 7-6: Moisture Content Zones for TDR2

Seasonal Zone I occurs during the spring and summer seasons when the soil moisture content shows a decreasing trend. In Figure 7-6 Seasonal Zone I occurs from April to October 2004 when the soil moisture content decreases from approximately 25 to 21 percent. The decreasing moisture content trend is inferred to be due to evaporation. Soil moisture content along with rainfall precipitation from April 18 to May 28, 2004 is shown in Figure 7-7. This figure indicates that temporary increases in soil moisture content occur with each significant precipitation event.

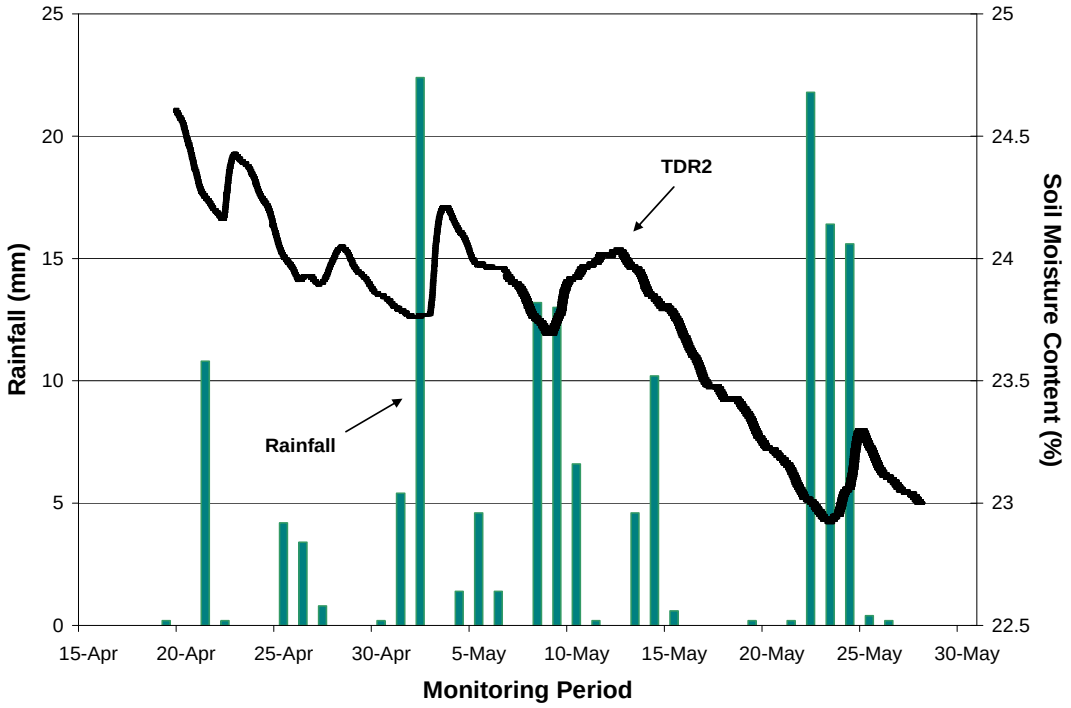

Figure 7-7: Rainfall Local Effect on Moisture Content Variation- Zone I

Seasonal Zone II occurs during the fall season when the soil moisture content shows an increasing trend. In Figure 7-6 Seasonal Zone II occurs from October to December 2004 when the soil moisture content increases from approximately 21 to 22 percent. In Seasonal Zone II the average monthly air and ground temperature show a decreasing trend. At the end of this period the average monthly air temperature is -4°C and the average monthly T-2 ground temperature is 0°C. Thus, the end of Seasonal Zone II and the beginning of Seasonal Zone III represent the onset of freezing ground temperatures.

Seasonal Zone III is defined as the period during which freezing ground conditions occur. In Figure 7-6 Seasonal Zone III occurs from December 2004 to March 2005. The soil moisture content in Seasonal Zone III initially decreased rapidly from 22 to 18 percent. This is followed

by rapid soil moisture content fluctuations and then by a period in which the moisture content is relatively constant (18.3 percent). Soil moisture content along with T-2 ground temperature from April 18 to May 28, 2004 is shown in Figure 7-8.

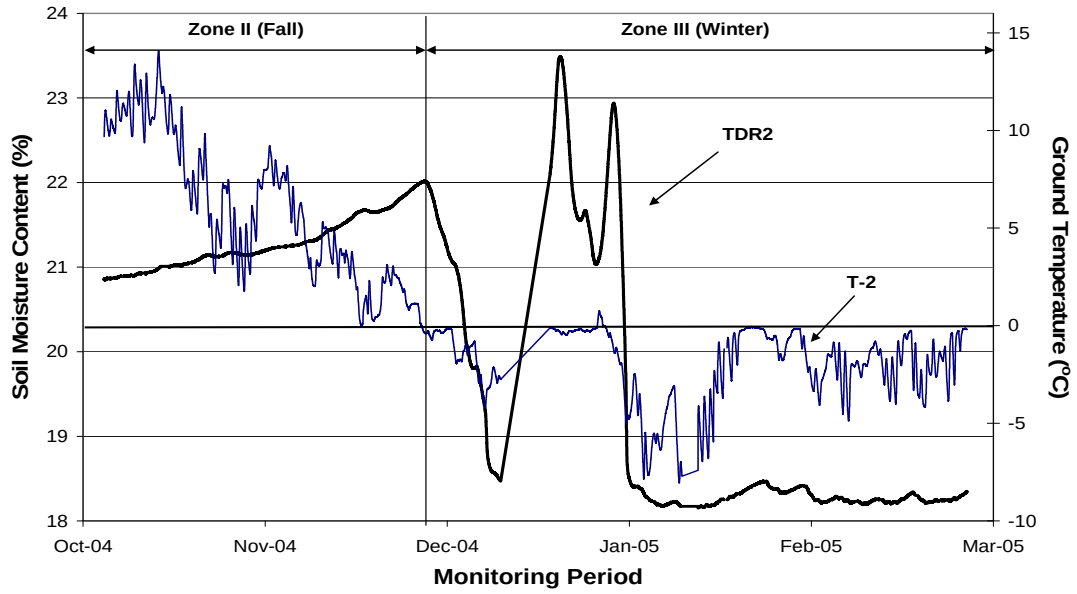

Figure 7-8: Temperature Correlation with Moisture Content (Zone II & III)

This figure shows that a rapid decrease in soil moisture content occurs when the temperature goes below zero degrees Celsius and rapid increases in soil moisture occur when the ground temperature is above zero degrees Celsius. Patterson and Smith (1981) found through laboratory testing of frozen soils that TDR probes provide an indication of unfrozen pore water since the dielectric constant of ice is similar to that of dry soil. Thus, it can be inferred that when the ground freezes the TDR probe will show a rapid decrease in soil moisture content and a rapid increase in soil moisture content when the ground thaws. The TDR rapid response is due to the changes in the volume of unfrozen pore water.

7.8 Moisture and Pavement Performance Variation over Monitoring Period

Subgrade resilient modulus, back-calculated from FWD data performed in the vicinity of the instrumented section, along with TDR1 soil moisture content from April 2004 to February 2005 are shown in Figure 7-9.

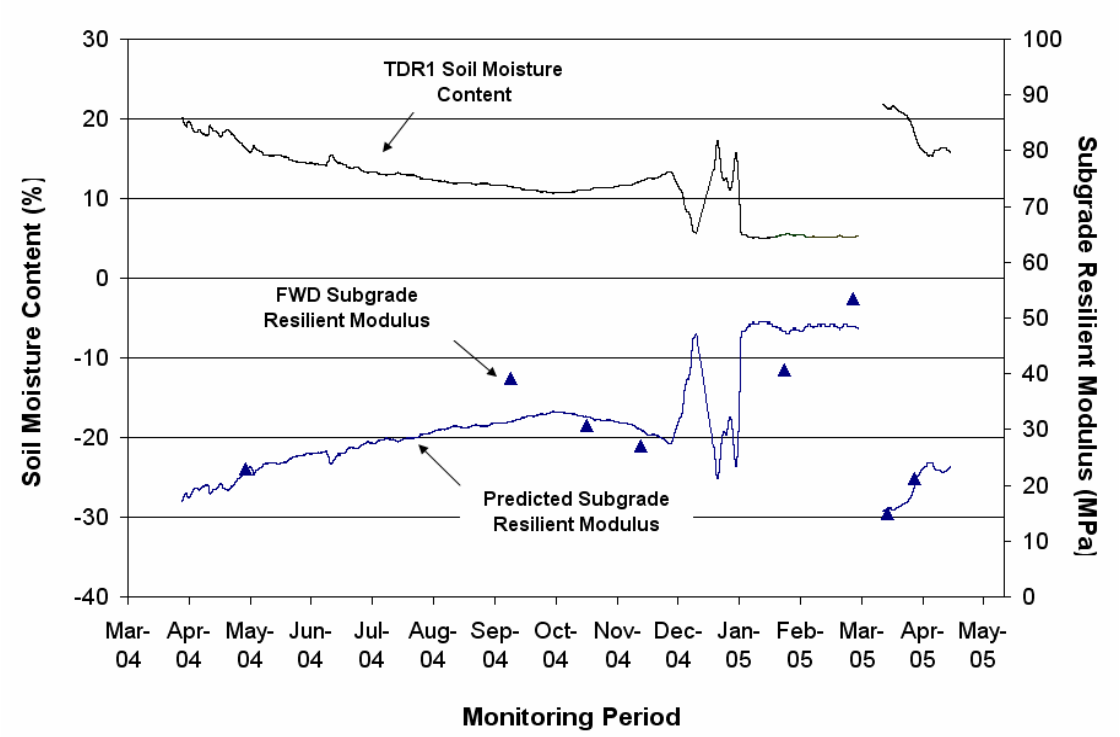

Figure 7-9: Correlation of FWD Deflection with Subgrade Resilient Modulus

This figure shows that the resilient modulus and moisture content are inversely correlated. For this site, a non-liner regression correlation, with a R^2 of 0.91, was found to fit the data.

$$M_R = 211.17.e^{-0.0694 \cdot \omega} \qquad (7\text{-}1)$$

where M_R is the subgrade resilient modulus (MPa), e is natural logarithm, and ω is soil moisture content in percentage.

Equation 7-1 and TDR 1 soil moisture content was used to predict the subgrade resilient modulus for the monitoring period shown in Figure 7-9. Predicted and FWD resilient modulus indicate that subgrade resilient modulus increases linearly in Seasonal Zone I, decreases linearly in Seasonal Zone II, and fluctuates dramatically during freeze-thaw events in Seasonal Zone III. The lowest subgrade resilient modulus (15 MPa) occurs at the beginning of Seasonal Zone I - 2005 when the ground rebounds from freezing. The highest subgrade resilient modulus (50 MPa) occurs when the ground is frozen. The highest unfrozen subgrade resilient modulus (34 MPa) occurs at the end of Seasonal Zone I-2004. The subgrade resilient modulus M_R at any time can be expressed using Equation 7-2 (NCHRP 2004):

$$M_R = F_{ENV} \cdot M_{Ropt} \qquad (7\text{-}2)$$

where F_{ENV} is an adjustment factor and M_{Ropt} is the subgrade resilient modulus at optimum condition.

Using the highest unfrozen subgrade resilient modulus as M_{Ropt}, F_{ENV} were determined for each Seasonal Zone and are presented in Table 7-1.

Table 7-1: Maximum and Minimum F_{ENV} for Each Seasonal Zone

Seasonal Zone	**F_{env}**	
	Max	**Min**
I-2004	1.0	0.6
II-2004	1.0	0.8
III-2004	1.5	0.6
I-2005	0.7	0.5

Table 7-1 indicates that the environmental adjustment factor increases in Seasonal Zone I from 0.5 to 1.0, decreases in Seasonal Zone II from 1.0 to 0.8, and fluctuates between 0.6 to 1.5 in Seasonal Zone III.

The environmental adjustment factor can be compared with the seasonal factors developed in Alberta, which is considered a seasonal frost area, and shown in Table 7-2 . This study was conducted in 1989 to 1994 by Alberta Transportation and Utilities to investigate the seasonal variation of subgrade strength (AT and U. 1997). FWD tests were performed on several pavement sections and the subgrade resilient modulus was back-calculated using the ELMOD computer program.

Table 7-2: Seasonal Factors in Alberta

Month	Jan	Feb	Mar	Apr	May	Jun	Jul	Aug	Sep	Oct	Nov	Dec
Seasonal Factor	5.00	5.00	2.75	0.63	0.88	1.00	1.00	1.00	1.00	1.00	2.00	4.00

7.9 Summary and Conclusions

This paper presented and discussed soil moisture and ground temperature data, recorded at five minute intervals over a two year monitoring period at the CPATT test track facility, located in Waterloo, Ontario, Canada. Rainfall precipitation, air temperature and FWD data were also presented and discussed.

Based on the data and information presented the following conclusions are drawn.

1. Soil moisture content and subgrade resilient modulus changes in the pavement structure can be divided into three distinct Seasonal Zones. Zone I consists of a period of decreasing soil moisture that occurs during the summer months, Zone II consists of a period of increasing soil moisture that occurs during the fall season, and Zone III consists of a period of low and high moisture contents when the ground freezes and thaws during the winter months.

2. In Zone I only significant rainfall event appeared to create a short-term and temporary increase in soil moisture. During the winter month the ground froze to a depth of at least 120cm.

3. Seasonal Zones can be used to estimate changes in resilient subgrade modulus for pavement response predictions. Although EICM provides environmental data on an hourly basis, it is obviously impractical to perform the linear elastic or the finite element analysis on an hourly basis. Therefore, the less number of analyses can be performed using the similarities inside each Seasonal Zone.

4. The EICM model in the M-E Deign method predicts changes in soil moisture content over time using climatic data. Currently, the climatic data required to input into the EICM model is not available for the CPATT test track site. Should climatic data for the site become available, EICM predications can be validated and/or calibrated for southern Ontario conditions using the above noted field data.

7.10 Acknowledgement

The authors would like to thank Professor Ralph Hass for his support during this research. Thanks are also for Natural Science and Engineering Research Council of Canada (NSERC) and CPATT due to funding this research project. Thanks are also due to Asphalt Research Associate Inc. (ARA) help in providing FWD data. The authors also appreciate Ken Bowman and Terry Ridgway, University of Waterloo technical staf, for their contribution during instrumentation and data collection.

Chapter 8: Measurement and Analysis of Flexible Pavement Thermal-Induced Strains

8.1 Overview

The focus of this study was to quantify the asphalt strain amplitude that occurs in flexible pavements as a result of thermal loading. A state-of-the-art field monitoring program was developed at the Centre for Pavement and Transportation Technology (CPATT) test facility to measure flexible pavement response to thermal loads. Asphalt temperature and longitudinal strain collected over a two years monitoring program were analyzed to interpret pavement response to thermal loads. Daily strain fluctuations as high as 650μm/m, and the irrecoverable strain as high as 2500μm/m per year were observed during 2004-2005 and 2005-2006.

8.2 Introduction

The trend to move toward a more mechanistic approach in flexible pavement design has emphasized the need to more accurately characterize pavement response and performance to environmental factors and vehicle loads. Temperature, one of the main environmental factors, affects the performance of the pavement materials (Mahoney and Vinson 1983). Low-temperature cracking and thermal fatigue cracking are two major distresses in flexible pavement as a result of thermal loads (Vinson et al. 1989).

Low-temperature cracking is a serious distress found in asphalt pavements that manifests itself through a uniform, often equally spaced, pattern of cracks perpendicular to the direction of traffic (Jackson and Vinson 1996; Shen and Kirkner 1999; Timm et al. 2003; Vinson et al. 1989; Zubeck and Vinson 1996). As the temperature drops the restrained pavement tries to contract and the tensile stress increases until it exceeds the tensile strength of Hot Mix Asphalt (HMA) and pavement cracks (Vinson et al. 1989). The current Superpave binder specification specifies a limiting low temperature for the asphalt binder to limit the occurrence of low-temperature cracking.

Unlike the low-temperature cracking, thermal fatigue cracking does not require a very low level of temperature to occur (Al-Qadi et al. 2005; Vinson et al. 1989). Similar to load-associated fatigue cracking, thermal fatigue cracking is the result of repetitive thermal cycles that cause cyclic stresses and strains in the material and a buildup of irrecoverable deformations (Al-Qadi et al. 2005).

Although significant advancements have been achieved in understanding the mechanisms of thermal fatigue cracking, there have not been enough field measurements that address the criticality of the associated strain amplitude in real pavements (Al-Qadi et al. 2005). Al-Qadi et al. (2005) carried out a field experimental program to measure thermal-induced strain in Virginia Smart Road. The result of the study indicates that the pavement response to thermal loading was associated with a high strain range, reaching a maximum recorded value of 350μm/m. The study confirms that unlike the wheel load- associated fatigue cracking, the criticality of thermal fatigue arises from the high stress-strain level exhibited in each cycle rather than its frequency. To date, no measurements have been performed to investigate the criticality of thermal-induced strains for pavements subjected to climates with freeze-thaw cycles (such as southern Canada).

A field investigation program was developed at the University of Waterloo to investigate the measured thermal-induced strain associated with thermal fatigue cracking in a climate subjected to freeze-thaw cycles. This paper provides an overview of the Centre for Pavement and Transportation Technology (CPATT) field test facility and presents the findings from a two year monitoring period.

8.3 CPATT Field Test Facility

8.3.1 Site Information

In this study, pavement temperature and asphalt longitudinal strain were measured at the CPATT test track (709m long and eight meters wide) located in Waterloo, Ontario, Canada. The instrumented test track section consists of 223 and 185mm of Hot-Laid 3 (HL3) mix, consisting of 40 percent crushed gravel, 45% asphalt sand, 15% screenings, and 5.3% PG 58-28 asphalt

cement, on west and east lane respectively. Below the HL3 are 200mm of Granular A base aggregate and 300mm of Granular B subbase aggregate. Compacted Granular A, 900mm in depth, is located below the subbase aggregate. Below the compacted Granular A is site subgrade that consists of compacted fill and well compacted clayey silt with some gravel. Granular A, as defined in the Ontario Provincial Standard Specification (OPSS) 1010, consists of crushed rock composed of hard, uncoated, fractured fragments, reduced from rock formations or boulders of uniform quality while Granular B consists of clean, hard, durable uncoated particles from deposits of gravel or sand (MTO 2003).

Based on historical weather data from the University of Waterloo weather station, the site average monthly mean air temperature typically varies from -10°C during the winter months to 26 °C during the summer months. Further details about the test track facility including its construction and pavement performance, can be found in Tighe et al. (2003).

8.3.2 Instrumentation

A state-of-the-art field instrumentation system was developed and installed to measure temperature of the asphalt, base, and subgrade materials, and asphalt longitudinal strain. Pavement temperatures were measured and recorded using a Campbell CRX10 data logger with four Campbell Scientific T107B thermistors (T-1 to T-4) installed 223, 800, 1350, and 1950mm below the asphalt surface respectively (Figure 8-1). Asphalt longitudinal strain was measured and recorded using five ASG-152 H-type asphalt strain gauges. As shown in Figure 8-1, ASG3 was placed on the road centerline, while ASG1 and ASG2 were placed 690 and 2700mm from the west pavement edge respectively. ASG5 and ASG 4 were placed 1380 and 3200mm from

the east pavement edge respectively. Asphalt strain gauge data was collected using a Somat eDAQ-plus®, data logger with the sampling rate set at 0.01 Hz (1 reading every 1.67 minutes).

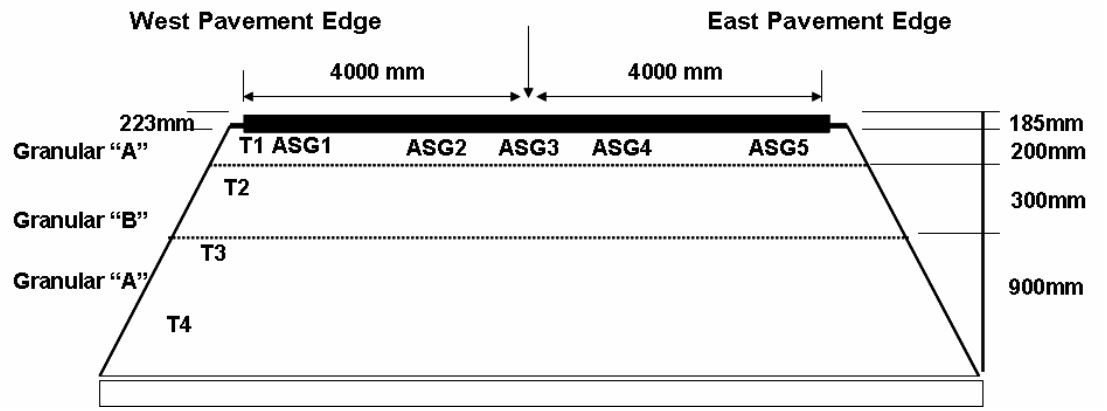

Figure 8-1: Instrumented Section Profile and Sensor Distribution Layout

Thermistor and asphalt strain gauge data was collected at a rate of 1 reading every 5 minutes (0.0033Hz). This sampling rate was deemed sufficient to record daily changes in probe readings.

Power was supplied to the data logger and probes using two 12V deep cycle batteries that were recharged using a solar panel. To conserve battery power during the winter time - when the duration of solar recharge was limited - a programmable timer was used to automatically turn the system off and on at predefined intervals. A power regulator was also used to prevent batteries from overcharging and discharging, and to prevent power flow from the batteries to the solar panel. Further details about the field monitoring program can be found in Adedapo (2007).

8.3.3 Thermal-Induced Strain-2004

Figure 8-2 shows the measured asphalt longitudinal strain (ASG5) at the bottom of the asphalt layer and the ambient air temperature for forty days period from August 21 to October 10, 2004.

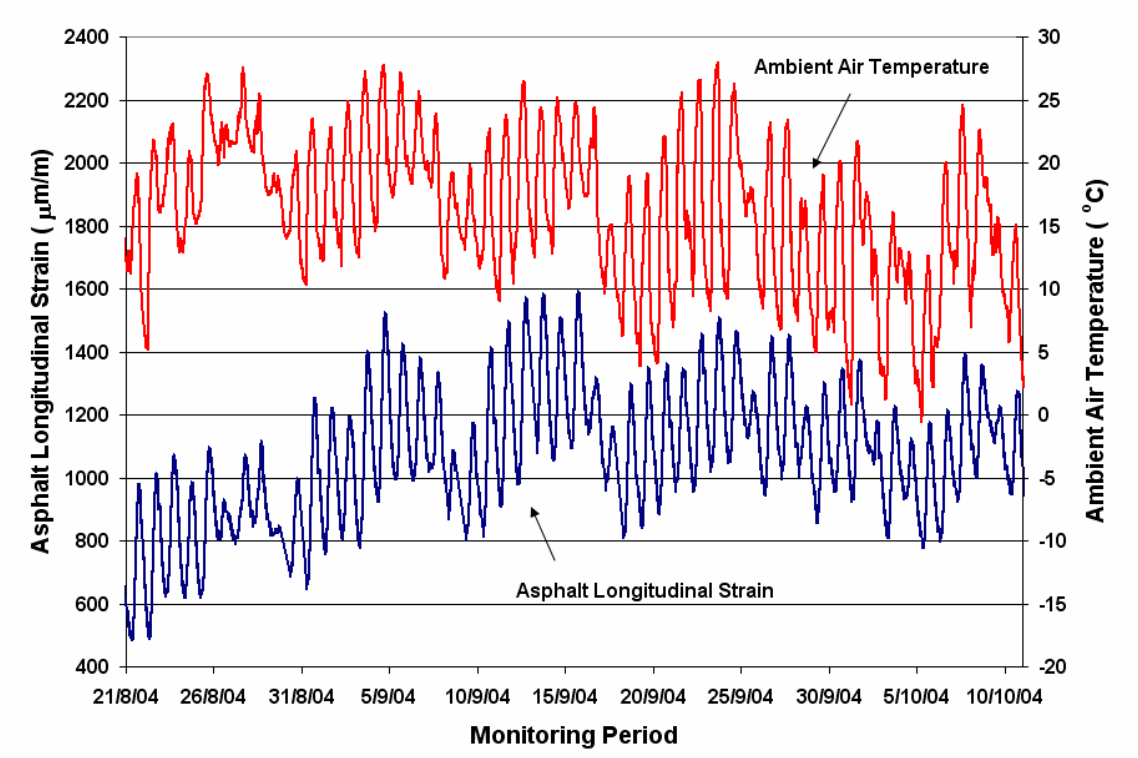

Figure 8-2: August 21 to October 10, 2004 Ambient Air Temperature and ASG5 Asphalt Longitudinal Strain Readings

The measured strain was solely in response to thermal loading, and the traffic data was collected in a separate channel in the data acquisition system. As expected, the ambient air temperature and ASG5 showed a similar cyclic response with a frequency of one cycle per day. As Figure 8-2 shows, the accumulation of strain was observed from August 21 to September 15, 2004. The ambient air temperature varied from -0.5 to 27.7°C and the maximum ambient air daily fluctuation was observed to be 20.2°C. ASG5 asphalt longitudinal strain varied from 504 to 1593μm/m, and the maximum ASG5 asphalt longitudinal strain daily fluctuation was observed to be 621μm/m.

Figure 8-3 shows the temperature at the bottom of the asphalt layer (T-1) and the measured asphalt longitudinal strain (ASG5) for the same monitoring period shown in Figure 8-2. Similar to ambient air, T-1 showed the cyclic response that varied from 12.1 to 27.8 ^{o}C. The maximum T-1 daily fluctuation was observed to be 5.96 ^{o}C.

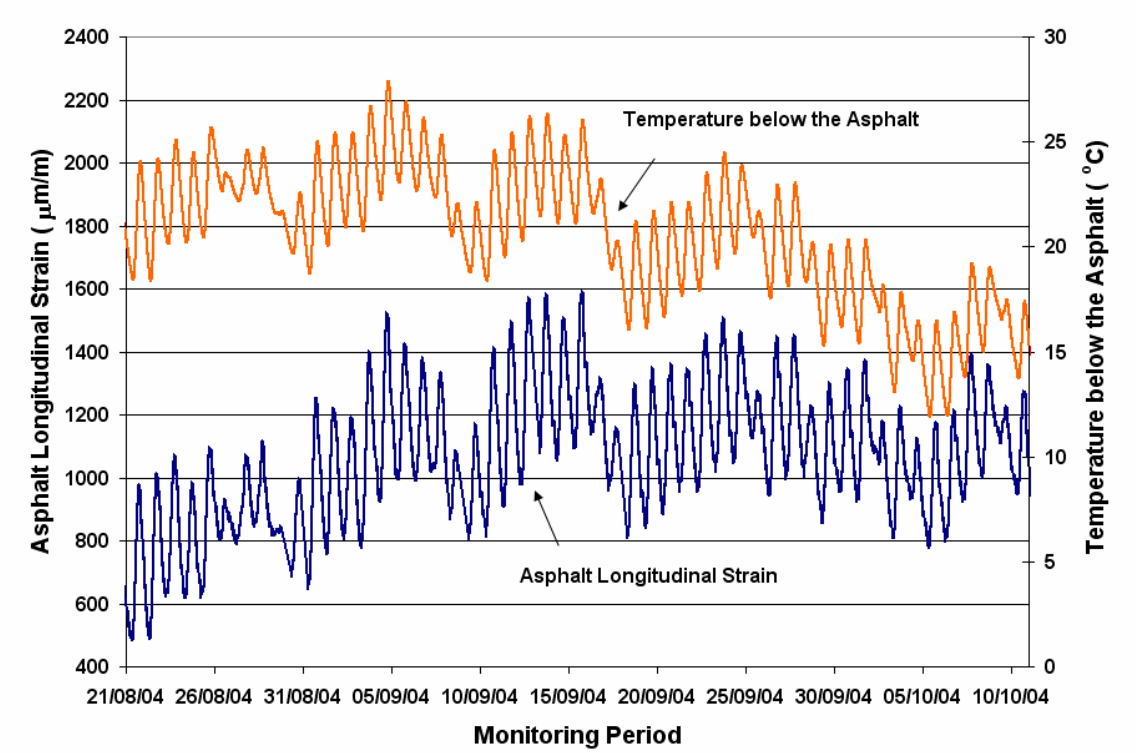

Figure 8-3: August 21 to October 10, 2004 Temperature below the Asphalt (T-1) and ASG5 Asphalt Longitudinal Strain Readings

Similar cyclic behavior was observed in the other asphalt strain gauges. Figure 8-4 shows the ASG3 asphalt longitudinal strain and the ambient air temperature for the same monitoring period shown in Figure 8-2. ASG3 asphalt longitudinal strain varied from 574 to 1685µm/m. The maximum ASG3 daily strain fluctuation was observed to be 610µm/m.

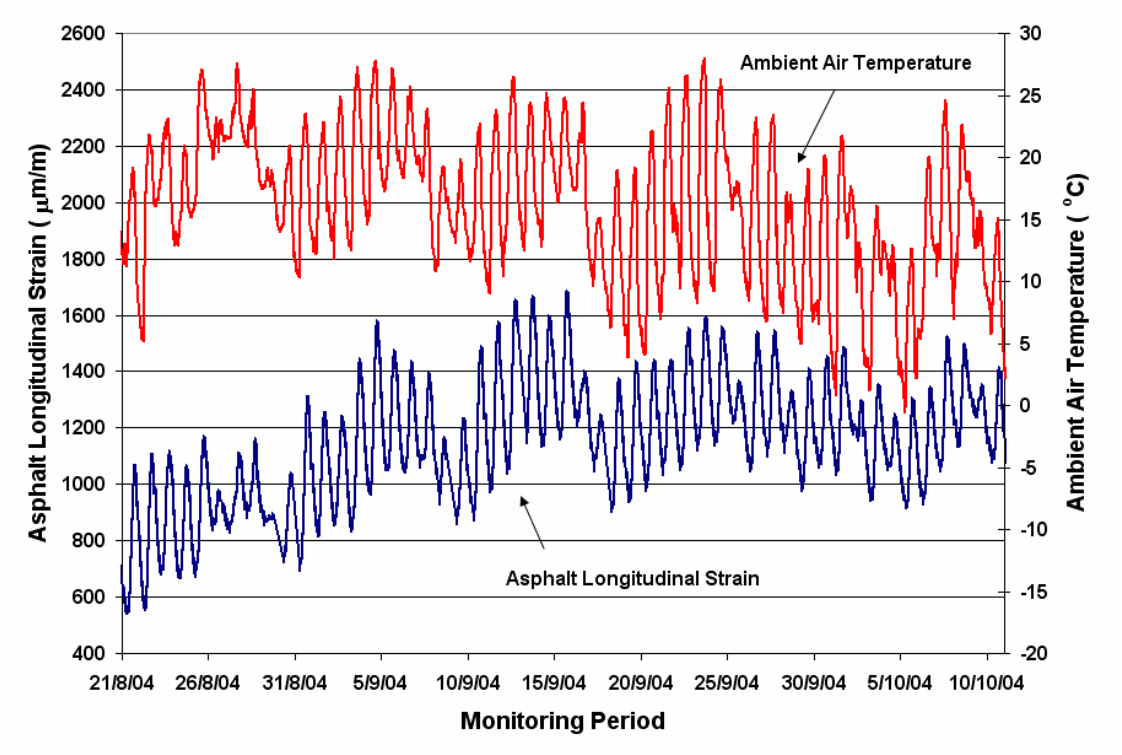

Figure 8-4: August 21 to October 10, 2004 Ambient Air Temperature and ASG3 Asphalt Longitudinal Strain Readings

8.3.4 Daily Thermal-Induced Strain Fluctuation

The daily thermal-induced strain fluctuation was calculated using Equation 8-1 (Norman 1999):

$$\Delta\varepsilon = \varepsilon_{max} - \varepsilon_{min} \qquad (8\text{-}1)$$

where:

$\Delta\varepsilon$ =Daily Thermal-Induced Asphalt Longitudinal Strain Fluctuation (μm/m)

ε_{max} =Daily Maximum Asphalt Longitudinal Strain (μm/m)

ε_{min} =Daily Minimum Asphalt Longitudinal Strain (μm/m)

Figure 8-5 shows the measured ASG5 daily thermal-induced strain fluctuation from January 2004 to January 2005. All strain gauges showed a similar trend.

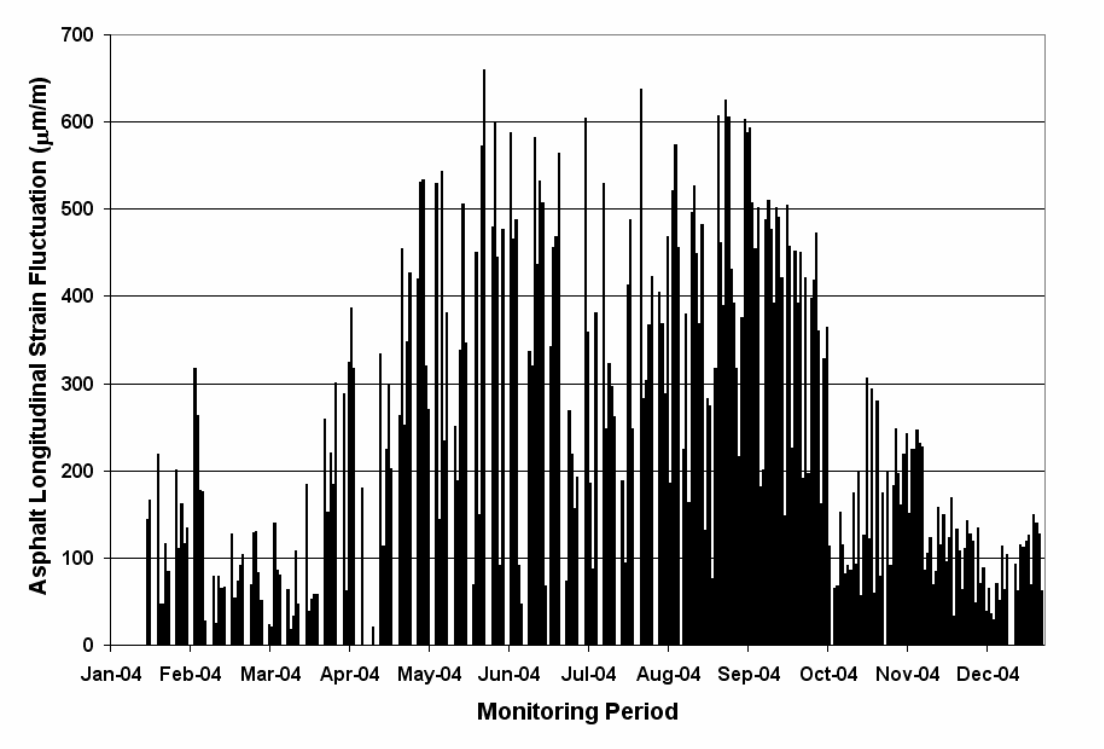

Figure 8-5: 2004 Thermal-Induced ASG5 Asphalt Longitudinal Strain Fluctuations

Small gaps at the measurements correspond to the periods when the data logger was inactive in the site. Figure 8-5 shows that daily strain fluctuation between 600 and 650μm/m can occur due to daily temperature changes.

Figure 8-6 shows the average ASG5 daily thermal-induced strain fluctuation from January to December 2004 and the average temperature fluctuation below the asphalt layer (T-1) from May to December 2004. The temperature data was not available from January to April 2004.

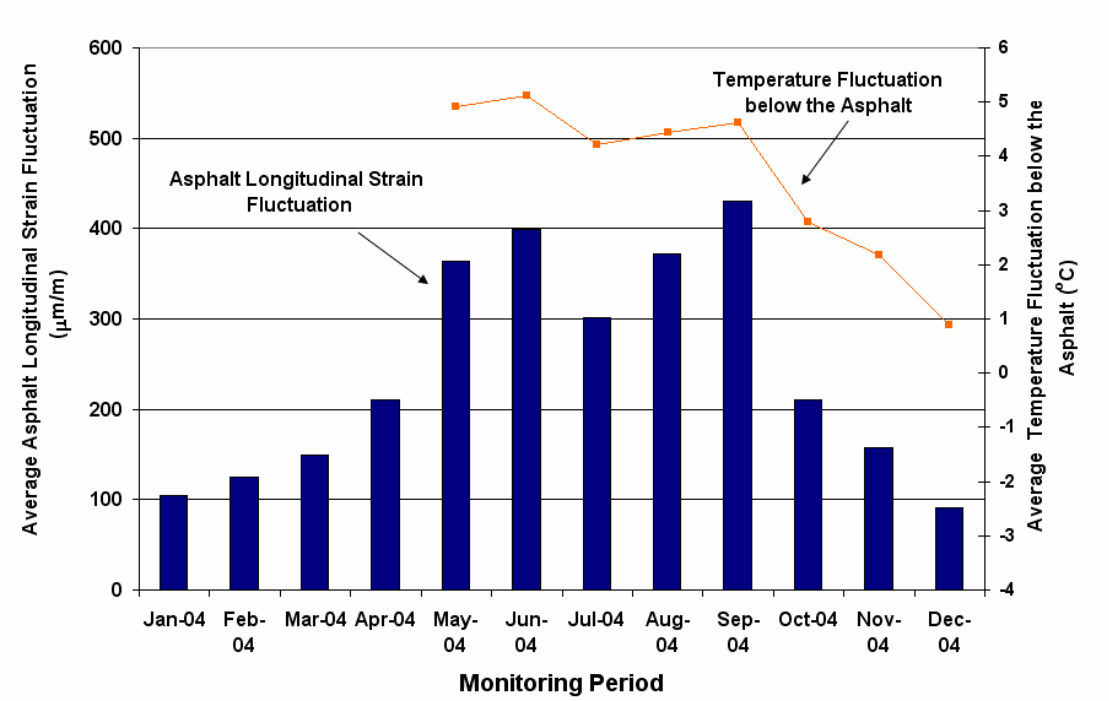

Figure 8-6: 2004 Average T-1 Temperature Fluctuations and Average ASG5 Daily Thermal-Induced Asphalt Longitudinal Strain Fluctuations

Figure 8-6 shows that the higher strain fluctuation occurs from May to September (spring and summer). It is evident from Figure 8-6 that the average daily strain fluctuation correlates to the average temperature fluctuation below the asphalt layer.

8.3.5 Thermal-Induced Strain and Temperature below the Asphalt

The least squared regression method was used to study the correlation between the ASG5 daily strain fluctuation and the temperature fluctuation below the asphalt layer. A linear relationship was found to fit the data with R^2 of 0.91 (Figure 8-7).

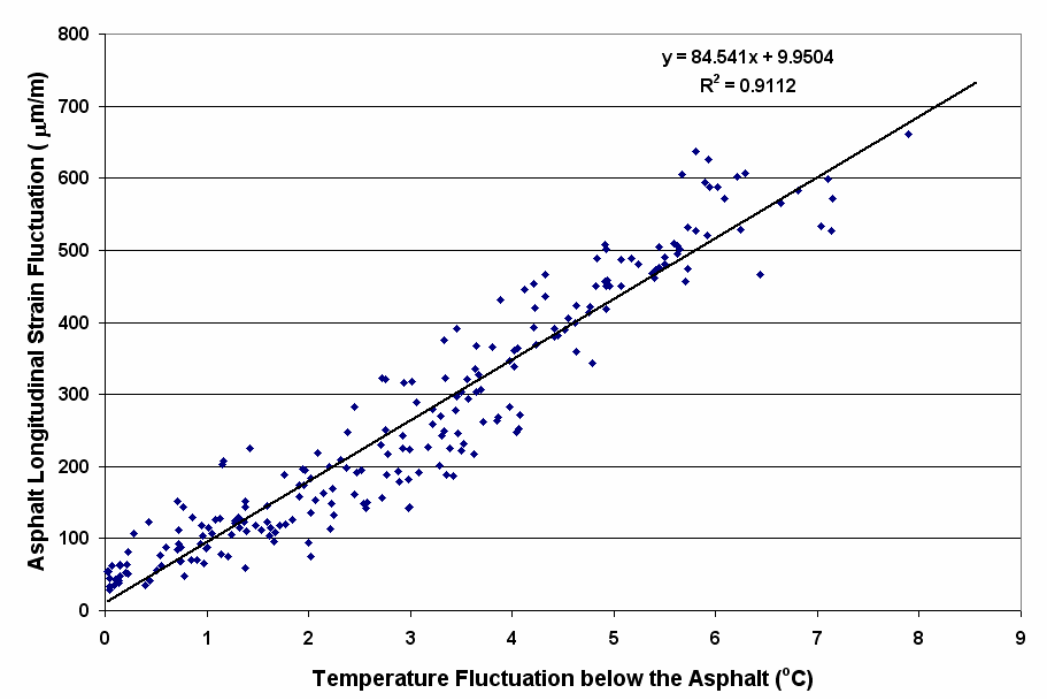

Figure 8-7: 2004 Daily ASG5 Thermal-Induced Asphalt Longitudinal Strain Fluctuations versus T-1 Temperature Fluctuation below the Asphalt Layer

8.3.6 Thermal Induced Strain- 2005

Figure 8-8 shows the measured ASG5 asphalt longitudinal strain and ambient air temperature from September 10-25, 2005. During this period, the ambient air temperature varied from 6 to 30°C, while the measured asphalt longitudinal strain level varied from 2059 to 3051µm/m.

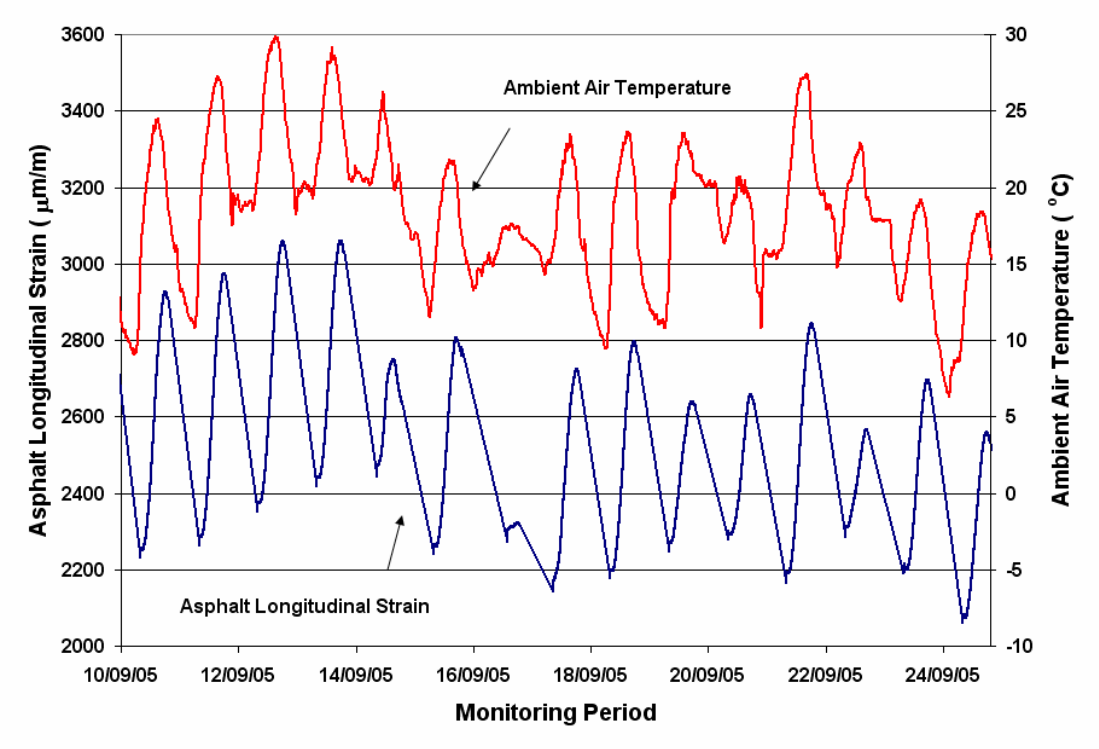

Figure 8-8: September 10 to 24, 2004 Ambient Air Temperature and ASG5 Asphalt Longitudinal Strain Readings

It is evident from Figure 8-8 that the strain level in September 2005 (2059 to 3051μm/m) increased compared to the measurements shown in Figure 8-2 from September 2004 (850 to 1593μm/m). Similar increases in strain were observed in the other strain gauges.

8.3.7 2004-2006 Asphalt Strain Gauge

Figure 8-9 shows the measured ASG5 asphalt longitudinal strain, T-1 temperature below the asphalt layer, and the ambient air temperature for the monitoring period of 2004-2006. Small gaps in the measurements correspond to the periods when the data logger was inactive at the site.

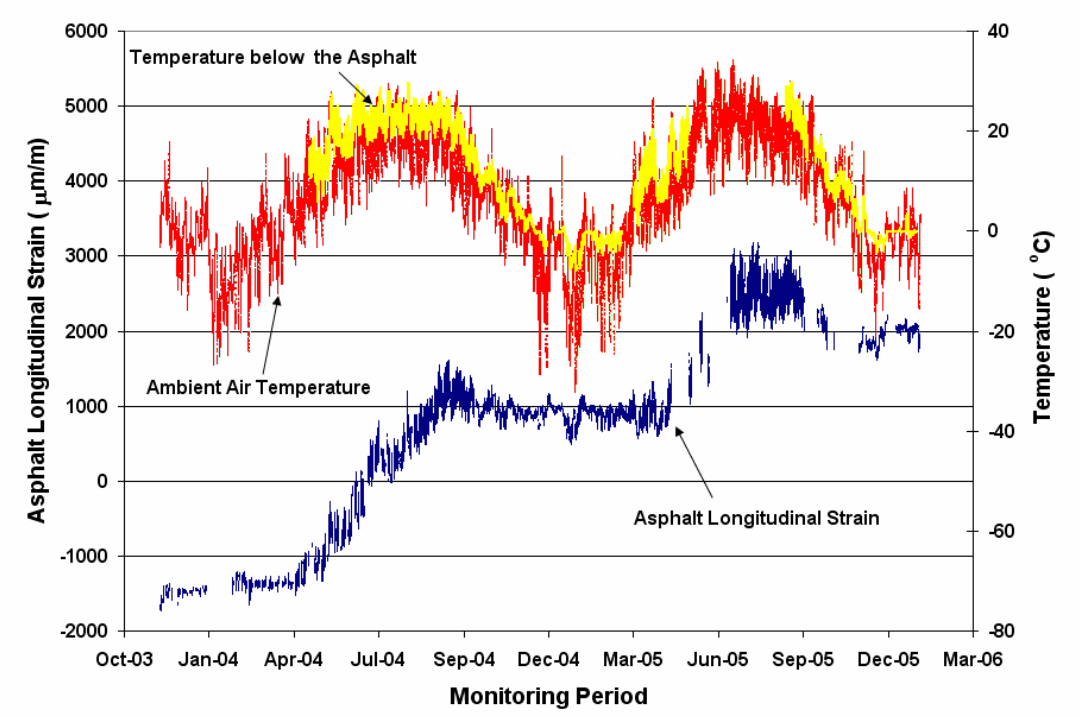

Figure 8-9: 2004-2006 Ambient Air Temperature, Temperature below the Asphalt (T-1), and ASG5Asphalt Longitudinal Strain

Figure 8-9 shows that an accumulation of irrecoverable strain was observed from April to September, 2004 and 2005. Similar trends were observed in the other strain gauges. Figure 8-10 shows the measured ASG3 asphalt longitudinal strain, T-1 temperature below the asphalt layer, and the ambient air temperature for the monitoring period of 2004-2006.

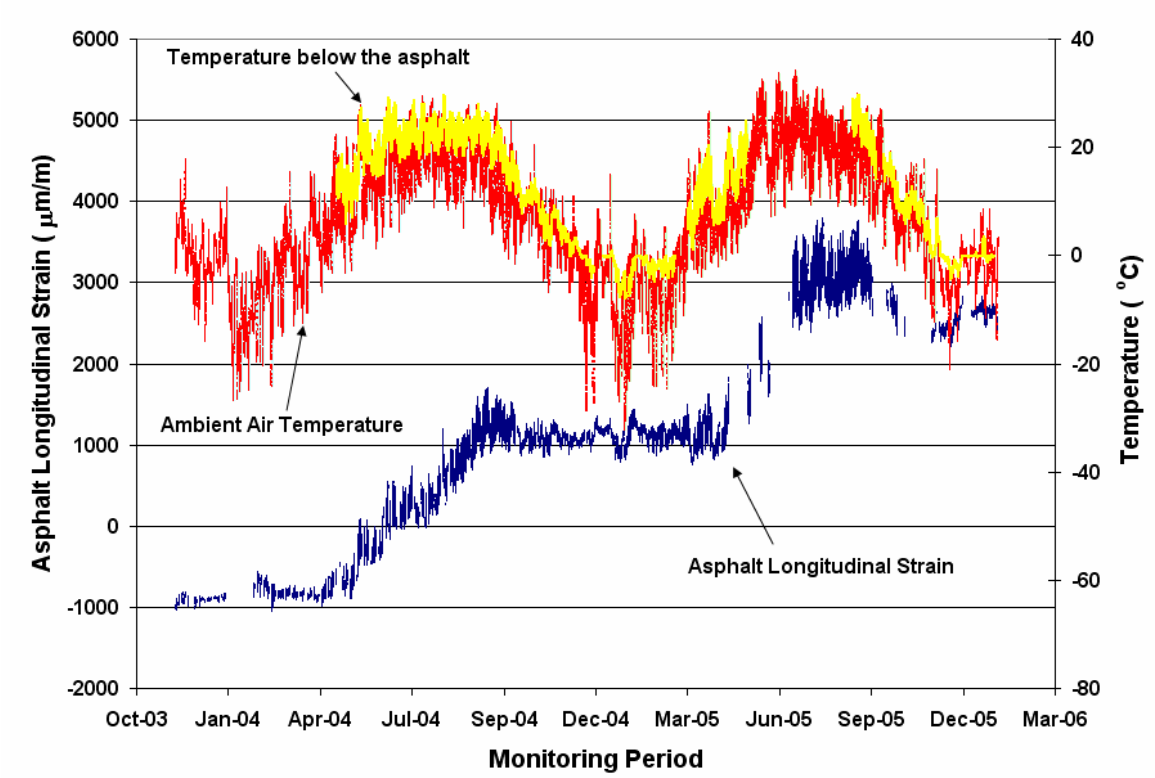

Figure 8-10: 2004-2006 Ambient Air Temperature, Temperature below the Asphalt (T-1), and ASG3 Asphalt Longitudinal Strain

Using the ASG5 strain measurements, shown in Figure 8-9, the average monthly asphalt longitudinal strain level was calculated for 2004-2005 and 2005-2006 (Figure 8-11 and Figure 8-12).

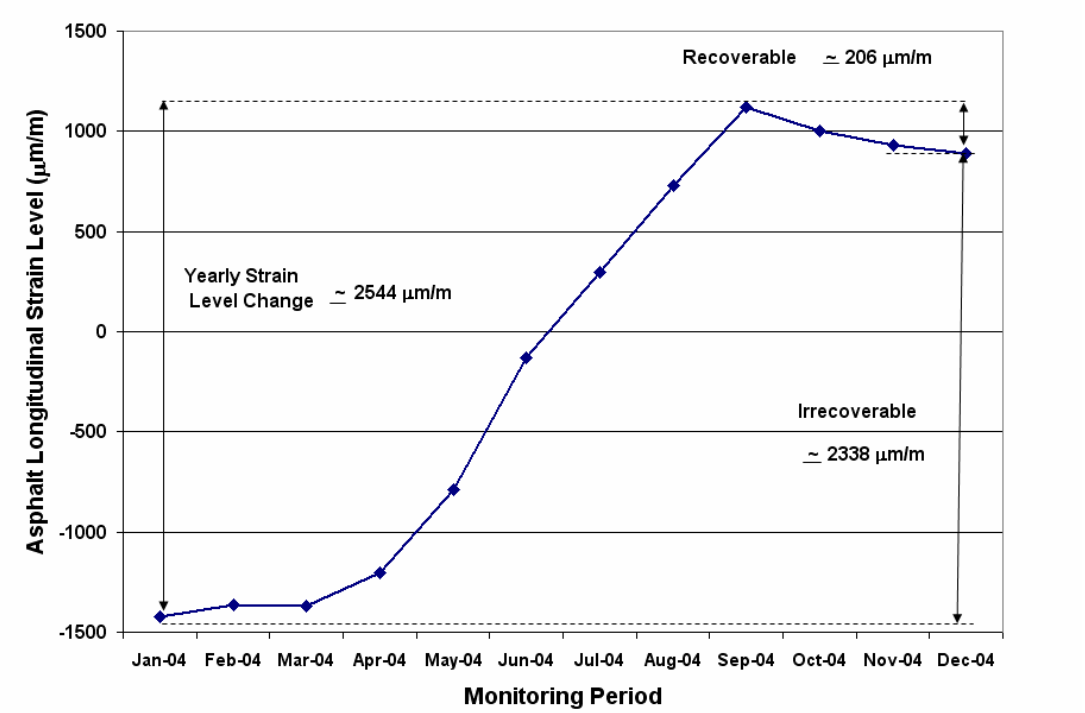

Figure 8-11: 2004-2005 Average Monthly ASG5 Longitudinal Strain Level

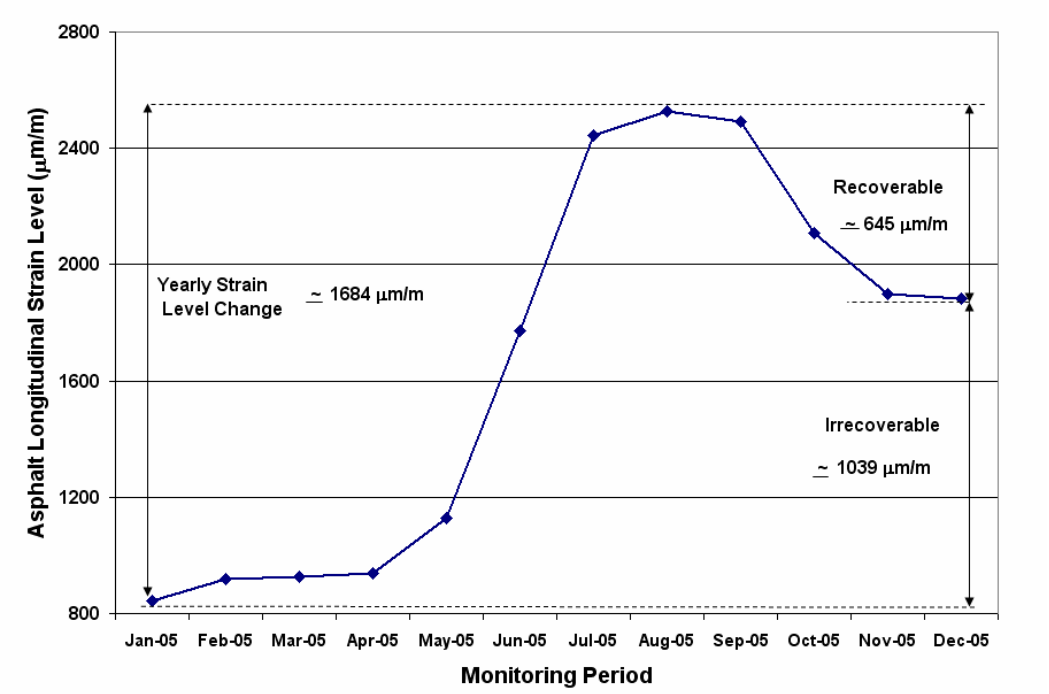

Figure 8-12: 2005-2006 Average Monthly ASG5 Longitudinal Strain Level

The 2004-2005 strain level fluctuation was observed to be 2544μm/m comprising of 206μm/m recoverable and 2338μm/m irrecoverable. The 2005-2006 strain level fluctuation was observed to be 1684μm/m comprising of 645μm/m recoverable and 1039μm/m irrecoverable.

8.4 Summary and Conclusions

The objective of this study was to quantify the asphalt strain amplitude associated with thermal loading in flexible pavements. A state-of-the-art field monitoring program was implemented to measure temperature of the asphalt, base, and subgrade materials, and asphalt longitudinal strain. Results of the experimental program indicate that pavement response to thermal loading is associated with a very high strain range with a maximum recorded value of 680μm/m. The accumulation of irrecoverable strain was observed during spring and summer during both the monitoring years. The irrecoverable strain was 2338μm/m during 2004-2005 and 1039μm/m during 2005-2006. The results strongly suggest that the strain associated with thermal loads are extremely critical for accurate pavement performance prediction.

8.5 Acknowledgements

The authors acknowledge the Natural Sciences and Engineering Research Council of Canada (NSERC), Canada Foundation for Innovation (CFI), Ontario Innovation Trust (OIT), Ontario Research and Development Challenge Fund (ORDCF), along with the Center for Pavement and Transportation Technologies (CPATT) private and public sector partners for providing research funding. The authors also acknowledge the University of Waterloo technical staff, Ken Bowman, Terry Ridgway, and Doug Hirst, for their guidance, help, and assistance with the field instrumentation.

Chapter 9: Conclusions and Recommendations

9.1 General Summary

The focus of this study was to investigate the impact of traffic loads and environmental conditions at the CPATT test facility in Waterloo, Ontario, Canada. Pavement responses were measured under a variety of wheel loads by utilizing a state-of-the-art field instrumentation and data acquisition system. A detailed controlled wheel load test was performed to verify pavement responses under a variety of traffic loading and environmental conditions. A three-step procedure was implemented to identify the dynamic modulus of the HL3 material. A finite element model was developed using MichPave program to predict the asphalt longitudinal strain for a variety of loading conditions. The predicted responses were compared to the measured field responses. The daily and seasonal changes in environmental parameters that affect flexible pavement response and performance was monitored and measured using the instrumentation system. FWD and direct strain measurement were used to quantify the impact of environmental parameters on pavement response and performance.

A number of contributions to the understanding of the influence of traffic and environmental loads on flexible pavement response and performance have been presented in this dissertation. The conclusions from the various investigations are provided at the end of each chapter Key findings of this research are summarized and presented below. Suggestions for further work are also provided.

9.2 Conclusions

- CPATT Field data is a unique and represents response of flexible pavements under freeze/thaw environments.

- The CPATT instrumentation system, which includes remote access and control capabilities, has worked exceptionally well for over six years. The remote monitoring system provides real-time access to the instrumentation system that reduces required site visits, ensures continuous data collection, and enables to detect any form of abnormalities within the instrumentation system.

- Two data acquisition systems were implemented at the CPATT test facility. Low frequency data acquisition system is used to record daily temperature and soil moisture content changes and high frequency to record pavement stresses and strains due to passing wheel loads.

- A detailed wheel controlled test was performed to determine the impacts of wheel wander, vehicle speed, and changes in asphalt temperature on sensor readings. The following findings were observed:

    - Asphalt Longitudinal strain showed that the pavement fully recovers after each wheel pass.

    - Wheel wander was found to make significant change on asphalt longitudinal strain. Wheel wander of 16 cm reduced asphalt longitudinal strains by 36 percent.

- An exponential relationship was found between asphalt longitudinal strains and asphalt mid-depth temperature when the truck speed and wheel loading was constant. The daily temperature fluctuations can double the asphalt longitudinal strain.

- The measured asphalt longitudinal strain was found to decrease with increasing truck speed.

- Using the stress pulse recorded at pressure cells, the loading time was found to be a function of truck speed and depth below the pavement surface.

- The laboratory determined dynamic modulus for HL3 was found to be:

  - An exponential function of the test temperature when loading frequency was constant.

  - A non-linear function of the loading frequency when the test temperature was constant.

- The comparison of laboratory dynamic modulus and field measured asphalt longitudinal strain showed that the laboratory determined dynamic modulus was inversely proportional to the field measured asphalt longitudinal strain.

- A simplified method was proposed to characterize HMA properties using the laboratory dynamic modulus test, pressure cell data, and asphalt temperature. Pavement response obtained with the field representative dynamic modulus correlated with field measured asphalt longitudinal strains.

- Two years of environmental monitoring showed that :
    - For long-term field studies, when large volume of data are collected, careful consideration must be given to the development of efficient and effective data collection, processing, and analysis.
    - Somat eDAQ-plus® data logger and TCE software were found to be ideal for programming sensors and for long-term data collection at high and low frequencies.
- TDR probes and FWD data showed that Soil moisture content and subgrade resilient modulus changes in the pavement structure can be divided into three distinct Seasonal Zones. Zone I consists of a period of decreasing soil moisture that occurs during the summer months, Zone II consists of a period of increasing soil moisture that occurs during the fall season, and Zone III consists of a period of low and high moisture contents when the ground freezes and thaws during the winter months.
- Temperature data showed that during the winter months the ground froze to a depth between 1134 and 1734mm below the asphalt surface. It also showed that the pavement went through several freeze-thaw cycles during the winter months.
- Daily asphalt longitudinal strain fluctuations were found to be correlated with daily temperature changes with a maximum recorded value of 680μm/m.

- The cumulative irrecoverable pavement strains were observed during spring and summer in both monitoring years. The irrecoverable strain was 2338μm/m during 2004-2005 and 1039μm/m during 2005-2006.

9.3 Recommendations and Future Work

The trend to move toward M-E pavement design methods emphasizes the need to identify the impact of traffic and environmental loads on pavement response and to develop realistic and accurate models to compute and predict critical pavement responses. This study provided insight into traffic and environmental parameters affecting pavement dynamic load responses. It also validated the chosen model for asphalt longitudinal strain.

The following recommendations are suggested for future studies:

- Although various conditions in finite element analyses and the material behavior of HMA were considered and data from a multitude of controlled vehicle runs were examined, exploration of other wheel load configurations and pavement sections are recommended to expand the predictive capability of the proposed method.
- Comparison of the field measured pavement response with prediction of other finite element programs.
- Validation of the proposed finite element model for vertical stresses at the top of base, subbase, and subgrade.
- Validation of the proposed finite element model for soil strain gauge data.

- Numerical simulation of pavement subjected to temperature variation.

- Evaluation of nonlinear elastic models for unbound granular materials

- Continue monitoring environmental parameters and pavement performance to investigate to establish seasonal shift factors that can reflect the variation of the temperature and moisture content.

References

AASHO (1962). The AASHO Road Test., National Research Council, Washington, D.C., USA.

AASHTO. (1993). Guide for Design of Pavement Structures, American Association of State Highway and Transportation Officials, Washington, D.C., USA.

AASHTO (2003). Standard Test Method for Determining Dynamic Modulus of Hot-Mix Asphalt Concrete Mixtures., American Association of State Highway and Transportation Officials.

Acum, W. E. A., and Fox, L. (1951). "Computation of Load Stresses in a Three-Layer Elastic System." Geotechnique, 2, 293-300.

Adedapo, A. A. (2007). Pavement Deterioration and PE Pipe Behavior Resulting from Open-Cut and HDD Pipeline Installation Techniques., PhD Thesis, University of Waterloo, Ontario, Canada.

Akhter, G. F., and Witczak, M. W. (1985). "Sensitivity of Flexible Pavement Performance to Bituminous Mix Properties." Transp. Res. Rec., 70-79.

Al-Qadi, I. L., Loulizi, A., Elseifi, M., Lahouar, S. (2004). "The Virginia Smart Road: The Impact of Pavement Instrumentation on Understanding Pavement Performance." Proc., Association of Asphalt Paving Technologist, White Bear Lake, MN, United States, 427-465.

Al-Qadi, I. L., Loulizi, A., Janajreh, I., Freeman, T. E. (2002). "Pavement Response to Dual Tires and New Wide-Base Tires at Same Tire Pressure." Trans. Res. Rec., (1806), 38-47.

Al-Qadi, I. L., Hassan, M. M., Elseifi, M. A. (2005). "Field and Theoretical Evaluation of Thermal Fatigue Cracking in Flexible Pavements." Trans. Res. Rec., 1919, 87-95.

AMADEUS. (2000). AMADEUS: Advanced Models for Analytical Design of European Pavement Structures, Belgian Road Research Centre, Belgian.

AT and U. (1997). Pavement Design Manual., Alberta Infrastructure and Transportation, Edition 1.

Baker, H. B., Buth, M. R., Van Deusen, D. A. (1994). Minnesota Road Research Project: Load Response Instrumentation Installation and Testing Procedures, Minnesota Dept. of Transportation, Maplewood.

Bari, J., and Witczak, M. (2005). "Evaluation of the Effect of Lime Modification on the Dynamic Modulus Stiffness of HMA: Use with the New RR 1929 M-E Pavement Design Guide." Trans. Res. Rec., (1929), 10-19.

Boussinesq, J. (1885). Application Des Potentiels à l'Étude De l'Équilibre Et Du Mouvement Des Solides Élastiques. Paris: Lille, 57–75.

Brown, E. R. (2006). NCAT Test Track Findings, Better Roads, 76(11), 82-87.

Burmister, D. M. (1945). "The General Theory of Stresses and Displacements in Layered Soil Systems." Journal of Applied Physics, 16, Paris, France.

Chatti, K., Mahoney,P., Monismith, C. L., Tom, M.(1995). Field Response and Dynamic lodeling of an Asphalt Concrete Pavement Section under Moving Heavy Trucks., University of Michigan Transportation Research Institute, Ann Arbor, MI.

Chisholm, R. A., Phang, W. A. (1983). “Measurement and Prediction of Frost Penetration in Highway”. Trans. Res. Rec., No 918, Washington D.C., 1-10.

Christison, J. T., Anderson, K. O., Shields, B. P. (1978). "In Situ Measurements of Strains and Deflection in a Full-Depth Asphaltic Concrete Pavement.”, Proc., Assoaciation of Asphalt Pavement Technologies, 47, Minneapolis, Minn., 398-433.

COST 333. (1997.) Development of New Bituminous Pavement Design Method., European Commission, Office for Official Publications of the European Communities, Luxembourg.

Doré, G., and Duplain, G. (2002). “Monitoring Pavement Response during Spring Thaw using Fiber-Optic Sensors24." Proc., 6th International Conference on the Bearing Capacity of Roads and Airfields, Lisbon, Portugal.

Drumm, E. C., Reeves, J. S., Madgett, M. R., Trolinger, W. D. (1997). "Subgrade Resilient Modulus Correction for Saturation Effects." J. Geotech. Geoenviron. Eng., 123(7), 663-670.

Elseifi, M. A., Al-Qadi, I. L., Yoo, P. J. (2006). “Viscoelastic Modeling and Field Validation of Flexible Pavements." ASCE Journal of Engineering Mechanics, 132(2), 172-178.

Fernando, E. G., Musani, D., Park, D., Liu, W. (2006). Evaluation of Effects of Tire Size and Inflation Pressure on Tire Contact Stresses and Pavement Response, Texas Transportation Institute, Texas A&M University System, College Station, Texas.

Haas, R.C.G (1968). “Low Temperature Performance of Flexible Pavements" .Proc., Canadian Technical Asphalt Association, Ottawa, Ontario, Canada.

Hadi, M., and Bodhinayake, B. C. (2003). “Non-Linear Finite Element Analysis of Flexible Pavements.", Advances in Engineering Software, 34, 657-662.

Hamad, A. (2007). Effect of Axle Load and Seasonality on Thin Membrane Pavements., M.Sc Thesis, University of Calgary, Canada.

Harichandran, R. S., Yeh, M. S., Baladi, G. Y. (1990). “MichPave: A Nonlinear Finite Element Program for Analysis of Flexible Pavements." Trans. Res. Rec., (1286), 123-131.

Hildebrand, G. (2002). Verification of Flexible Pavement Response from a Field Test., Ph.D Thesis, Cornell University, USA.

Huang, Y. H. (1993). Pavement Analysis and Design, Prentice Hall, Englewood Cliffs, New Jersey, USA.

Huang, B., Mohammad, L. N., Rasoulian, M., Roberts, F. L., Qin, H. (2002). " Numerical Validation of Pavement Performance at the Louisiana Accelerated Loading Facility (ALF)." Proc., Ninth International Conference on Asphalt Pavements, Copenhagen, Denmark.

Huhtala, M., Pihlajamaki, J., Pienimaki, M. (1989). “Effects of Tires and Tire Pressures on Road Pavements.", Trans. Res. Rec., (1227), 107-114.

Immanuel, S., and Timm, D. H. (2006). "Measured and Theoretical Pressures in Base and Subgrade Layers under Dynamic Truck Loading." Proc., 2006 Airfield and Highway Pavement Specialty Conference, American Society of Civil Engineers, 155-166.

Jackson, N. M., and Vinson, T. S. (1996). "Analysis of Thermal Fatigue Distress of Asphalt Concrete Pavements." Transp. Res. Rec., (1545), 43-49.

Knight, M. A., Tighe, S. T., Adedapo, A. (2004). "Trenchless Installation Preserves Pavement Integrity." Proc., Annual Conference of the Transportation Association of Canada, Quebec City.

Li, D., and Selig, E. T. (1994). "Resilient Modulus for Fine-Grained Subgrade Soils." J. Geotech. Eng., 120(6), 939-957.

Liao, Y. (2007). Viscoelastic FE Modeling of Asphalt Pavements and its Application to U.S. 30 Perpetual Pavements, PhD Thesis, Ohio University.

Loulizi, A., Al-Qadi, I. L., Flintsch, G. W., Freeman, T. E. (2002). "Using Field Measured Stresses and Strains to Quantify Flexible Pavement Responses to Loading." Proc., Ninth International Conference on Asphalt Pavements, International Society for Asphalt Pavements, Copenhagen, Denmark.

Loulizi, A., Al-Qadi, I. L., Lahouar, S., Freeman, T. E. (2001). "Data Collection and Management of Instrumented Smart Road Flexible Pavement Sections." Transp. Res. Rec., (1769), 142-151.

Loulizi, A., Al-Qadi, I. L., Elseifi, M. (2006). "Difference between in Situ Flexible Pavement Measured and Calculated Stresses and Strains." J. Transp. Eng., 132(7), 574-579.

Loulizi, A., Flintsch, G., Al-Qadi, I., Mokarem, D. (2006). "Comparing Resilient Modulus and Dynamic Modulus of Hot-Mix Asphalt as Material Properties for Flexible Pavement Design." Transp. Res. Rec., (1970), 161-170.

Loulizi, A., Al-Qadi, I., Lahouar, S., Freeman, T. E. (2002). "Measurement of Vertical Compressive Stress Pulse in Flexible Pavements: Representation for Dynamic Loading Tests." Transp. Res. Rec., (1816), 125-136.

Mahoney, J. P., and Vinson, T. S. (1983). "Mechanistic Approach to Pavement Design in Cold Regions", Proc., Permafrost 4th International Conference, Washington, DC, USA, 779-782.

Mamlouk, M. S., and Mikhail, M. Y. (1998). "Concept for Mechanistic-Based Performance Model for Flexible Pavements." Trans. Res. Rec., (1629), 149-158.

Metcalf, J. B. (1996). NCHRP Synthesis of Highway Practice 325: Application of Full-Scale Accelerated Pavement Testing. Transportation Research Board, National Research Council, Washington, D.C.

Monismith, C. L. (2004). "Evolution of Long Lasting Asphalt Design Methodology: A Perspective", Distinguished Lecture, Proc., International Symposium on Design and Construction of Long Lasting Asphalt Pavements, Auburn University, Alabama.

Monismith, C. L., Marker, V., Anderson, K. O., Shields, B. P., Dacyszyn, J. M., Schmidt, R. J., Zube, E., Kelly, J. E. (1966). "Symposium - Non-Traffic Load Associated Cracking of Asphalt Pavements." Association of Asphalt Paving Technologists, 239-357.

MTO. (2003). Ontario Provincial Standard Specification for Aggregates-Base, Subbase, Select Subgrade, and Backfill Material, Ministry of Transportation Ontario, Ontario, Canada.

NCHRP (2004). Guide for Mechanistic-Empirical Design of New and Rehabilitated Pavement Structures, National Cooperative Highway Research Program.

Newmark, N. (1947). "Influence Charts for Computation of Vertical Displacements in Elastic Foundations", University of Illinois Experiment Station Bulletin, 367.

Norman, D. (1999). Mechanical Behavior of Materials: Engineering Methods for Deformation, Fracture, and Fatigue, Prentice Hall, Upper Saddle River, N.J.

Park, D., Buch, N., Chatti, K. (2001). "Effective Layer Temperature Prediction Model and Temperature Correction via Falling Weight Deflectometer Deflections." Transp. Res. Rec., 1764, 97-111.

Park, H. M., Kim, Y. R., Park, S. W. (2005). "Assessment of Pavement Layer Condition with use of Multiload-Level Falling Weight Deflectometer." Trans. Res. Rec., (1905), 107-116.

Patterson, D.E., Smith, M. W. (1981). 'The Measurement of Unfrozen Water Content by the Time Domain Reflectometry: Results from Laboratory Tests". Canadian Geotechnical Journal, Vol. 18, 131-144

Popik, M., and Tighe, S. T. (2006). "The Effect of Subgrade Modulus Sensitivity on Pavement Design." Proc., 10th International Conference on Asphalt Pavements, Quebec City.

Priest, A. L., Timm, D. H., Solaimanian, M., Gibson, N., Marasteanu, M. (2005). "A Full-Scale Pavement Structural Study for Mechanistic-Empirical Pavement Design." Proc., Association of Asphalt Paving Technologists, White Bear Lake, USA, 519-556.

Raad, L., and Figueroaand, J. L. (1980). "Load Response of Transportation Support Systems", Journal of Transportation Engineering, ASCE, 106, 111-128.

Rainwater, R.N., Yoder, R.E., Drumm, E.C., Wilson, V., (1999),"Comprehensive Monitoring System for Measuring Subgrade Moisture Condition", Journal of Transportation Engineering, v 125, n 5, Sep-Oct, 1999, 439-448

Salem, H. M. A. (2004). Quantification of Environmental Impacts on the Performance of Asphalt Pavements., Ph.D Thesis, University of Idaho, USA.

Sanborn, J. L., and Yoder, E. J. (1967). "Stress and Displacements in an Elastic Mass under Semi-Ellipsoidal Loads.", Proc., Second International Conference on the Structural, Ann Arbor, Michigan.

Sargand, S. M., Green, R., Khoury, I. (1997). "Instrumentation Ohio Test Pavement." Transp. Res. Rec., 1596, 23-30.

Sargand, S. M., and Beegle, D. (2002). "Three Dimensional Modeling of Flexible Pavements." Proc., International Conference on Highway Pavement Data, Analysis and Mechanistic Design Applications, Ohio University, Ohio.

Sargand, S. M., Khoury, I. S., Figueroa, J. L. (2007). "Forensic Investigation of Sections 390103, 390108, 390109, and 390110 of the Ohio SHRP U.S. 23 Test Pavement." Proc., Forensic Engineering, 286-301.

Schiffman, R. L. (1962). “General Solution of Stresses and Displacements in Layered Elastic systems." Proc., International Conference on the Structural Design of Asphalt Pavement, University of Michigan.

Sebaaly, P. E., and Mamlouk, M. (1987). “Prediction of Pavement Response to Actual Traffic Loading." Transp. Res. Rec., Washington, DC.

Sebaaly, P. E., Tabatabee, N., Kulakowski, B., Scullion, T. (1991). Instrumentation for Flexible Pavements – Field Performance of Selected Sensors., Federal Highway Administration, Washington, DC.

Selig, E.T. (1988). "Soil Parameters for Design of Buried Pipelines, Pipeline Infrastructure". Proc., American Society of Civil Engineers, New York, NY, 99-116.

Selvaraj, S. I. (2007). Development of Flexible Pavement Rut Prediction Models from the NCAT Test Track Structural Study Sections Data., Ph.D Thesis, Auburn University, USA.

Shen, W., and Kirkner, D. J. (1999). "Distributed Thermal Cracking of AC Pavement with Frictional Constraint." J. Eng. Mech., 125(5), 554-560.

Siddharthan, R. V., Krishnamenon, N., El-Mously, M., Sebaaly, P. E. (2002). "Validation of a Pavement Response Model Using Full-Scale Field Tests", International Journal of Pavement Engineering, 3(2).

Solaimanian, M., Stoffels, S., Yin, H. (2006). "Seasonal Effects on Roadways Asphalt Layers Strain Response to Loading." Proc., 10th International Conference on Asphalt Pavements, Quebec, Canada.

Sousa, J. B., Craus, J., Monismith, C. L. (1991)."Summary Report on Permanent Deformation in Asphalt Concrete", Transportation Research Board, National Research Council, Washington, D. C.

Stoffels, S. M., Solaimanian, M., Morian, D., Soltani, A. (2006). "Field Instrumentation and Testing Data from Pennsylvania's Superpave In-Situ Stress/Strain Investigation." Proc., Airfield and Highway Pavement Specialty Conference, American Society of Civil Engineers, Reston, VA, United States, , 107-118.

Tighe, s., Jeffray, A., Kennepohl, G., Haas, R., Matheson, M. (2003). "Field Experiments in CPATT's Long-Term Program of Pavement Research." Proc., Transportation Association of Canada Annual Conference, St. John's, NF.

Timm, D. H., Guzina, B. B., Voller, V. R. (2003). "Prediction of Thermal Crack Spacing." Int. J. Solids Structures, 40(1), 125-142.

Timm, D. H., and Newcomb, D. E. (2003). "Calibration of Flexible Pavement Performance Equations for Minnesota Road Research Project.", Transp. Res. Rec., (1853), 134-142.

Timm, H. D., Priest, A. L., McEven, T. V. (2004). Design and Instrumentation of the Structural Pavement Experiment at the NCAT Test Track., National Center for Asphalt Technology, AL, USA.

Tompkins, D. M., Lev Khazanovich, M., Johnson, D. M. (2007). "Overview of the First Ten Years of the Minnesota Road Research Project.", J. Transp. Eng., 133(11), 599-609.

Tran, H., and Hall, K. D. (2003). Investigation of the Simple Performance Test for Measuring Hot Mix Asphalt Dynamic Modulus., University of Arkansas, Fayetteville, Arkansas.

Tu, W. (2007). Response Modeling of Pavement Subjected to Dynamic Surface Loading Based on Stress-Based Multi-Layered Plate Theory., Ph.D Thesis, The Ohio State University, USA.

Ullidtz, P., and Stubstad, R. N. (1985)."Analytical-Empirical Pavement Evaluation Using The Falling Weight Deflectometer", Transp. Res. Rec., 36-44.

Ullidtz, P., Krarup, J., Wahlman, T. (1994). "Verification of Pavement Response Models." Proc., The Symposium on Nondestructive Testing of Pavements and Backcalculation of Moduli, ASTM, Philadelphia, PA, USA, 143-158.

Ullidtz, P. (1998). Modeling Flexible Pavement Response and Performance, Narayana Press, Denmark.

Uzan, J. (1985.). "Characterization of Granular Materials." Transp. Res. Rec., 1022.

Uzarowsky, L. (2006). The Development of Asphalt Mix Creep Parameters and Finite Element Modeling of Asphalt Rutting., Ph.D Thesis, University of Waterloo.

Vinson, T. S., Janoo, V. C., Haas, R. C. G. (1989). Low Temperature and Thermal Fatigue Cracking., National Research Council, Washington, D.C., USA.

Watson, D. K., Rajapakse, R.K.N.D. (2000), “Seasonal Variation in Material Properties of a Flexible Pavement”, Canadian Journal of Civil Engineering, V. 27, n.1, 44-54

Worel, B. J., Clyne, T. R., Burnham, T. R., Johnson, D. M., Tompkins, D. M. (2007). "Low-Volume-Road Lessons Learned Minnesota Road Research Project." Transp. Res. Rec., 1(1989), 198-207.

Wu, Z., and Hussain, M. (2003). Pilot Instrumentation of A Superpave Test Section at the Kansas Accelerated Testing Laboratory., Department of Civil Engineering, Kansas State University, Manhattan, KS.

Wu, Z., Zhang, Z., King, B., Raghavendra, A., Martinez, M. (2006). "Instrumentation and Accelerated Testing on Louisiana Flexible Pavements." Proc., 2006 Airfield and Highway Pavement Specialty Conference, American Society of Civil Engineers, 119-130.

Xu, B., Ranjithan, S. R., Kim, Y. R. (2002). “New Relationships between FWD Deflections and Asphalt Pavement Layer Condition Indicators." Transp. Res. Rec., (1806), 48-56.

Yoder, E. J., and Witczak, M. W. (1975). Principles of Pavement Design, Second Edition, John Wiley and Sons, New York, NY.

Zubeck, H. K., and Vinson, T. S. (1996). "Prediction of Low-Temperature Cracking of Asphalt Concrete Mixtures with Thermal Stress Restrained Specimen Test Results." Transp. Res. Rec., (1545), 50-58.

Zuo, G. (2003), Impacts of Environmental Factors on Flexible Pavements, PhD Thesis, University of Tennessee, United States, Tennessee.